Cancer Cell International

REVIEW

Open Access

# A state-of-the-art review of the recent advances of theranostic liposome hybrid nanoparticles in cancer treatment and diagnosis

Hannaneh Azimizonuzi[1], Arman Ghayourvahdat[1], Mareb Hamed Ahmed[2], Radhwan Abdul Kareem[3], Athmar Jaber Zrzor[4], Aseel Salah Mansoor[5], Zainab H. Athab[6] and Shaylan Kalavi[7*]

## Abstract

Theranostics is a way of treating illness that blends medicine with testing. Specific characteristics should be present in the best theranostic agents for cancer: (1) the drugs should be safe and non-toxic; (2) they should be able to treat cancer selectively; and (3) they should be able to build up only in the cancerous tissue. Liposomes (LPs) are one of the most efficient drug delivery methods based on nanotechnology. Stealth LPs and commercial LPs have recently had an impact on cancer treatment. Using the valuable information from each imaging technique, along with the multimodality imaging functionality of liposomal therapeutic agents, makes them very appealing for personalized monitoring of how well therapeutic drugs are working against cancer in vivo and for predicting how well therapies will work. On the other hand, their use as nanoparticle delivery systems is currently in the research and development phase. Nanoscale delivery system innovation has made LP-nanoparticle hybrid structures very useful for combining therapeutic and imaging methods. LP-hybrid nanoparticles are better at killing cancer cells than their LP counterparts, making them excellent options for in vivo and in vitro drug delivery applications. Hybrid liposomes (HLs) could be used in the future as theranostic carriers to find and treat cancer targets. This would combine the best features of synthetic and biological drug delivery systems. Overarchingly, this article provided a comprehensive overview of the many LP types used in cancer detection, therapy, and theranostic analysis. An evaluation of the pros and cons of the many HLs types used in cancer detection and treatment has also been conducted. The study also included recent and significant research on HLs for cancer theranostic applications. We conclude by outlining the potential benefits and drawbacks of this theranostic approach to the concurrent detection and treatment of different malignancies, as well as its prospects.

**Keywords** Liposome hybrids, Cancer, Theranostic, Detection, Treatment

*Correspondence:
Shaylan Kalavi
shaylankalavi@gmail.com
Full list of author information is available at the end of the article

**Graphical Abstract**

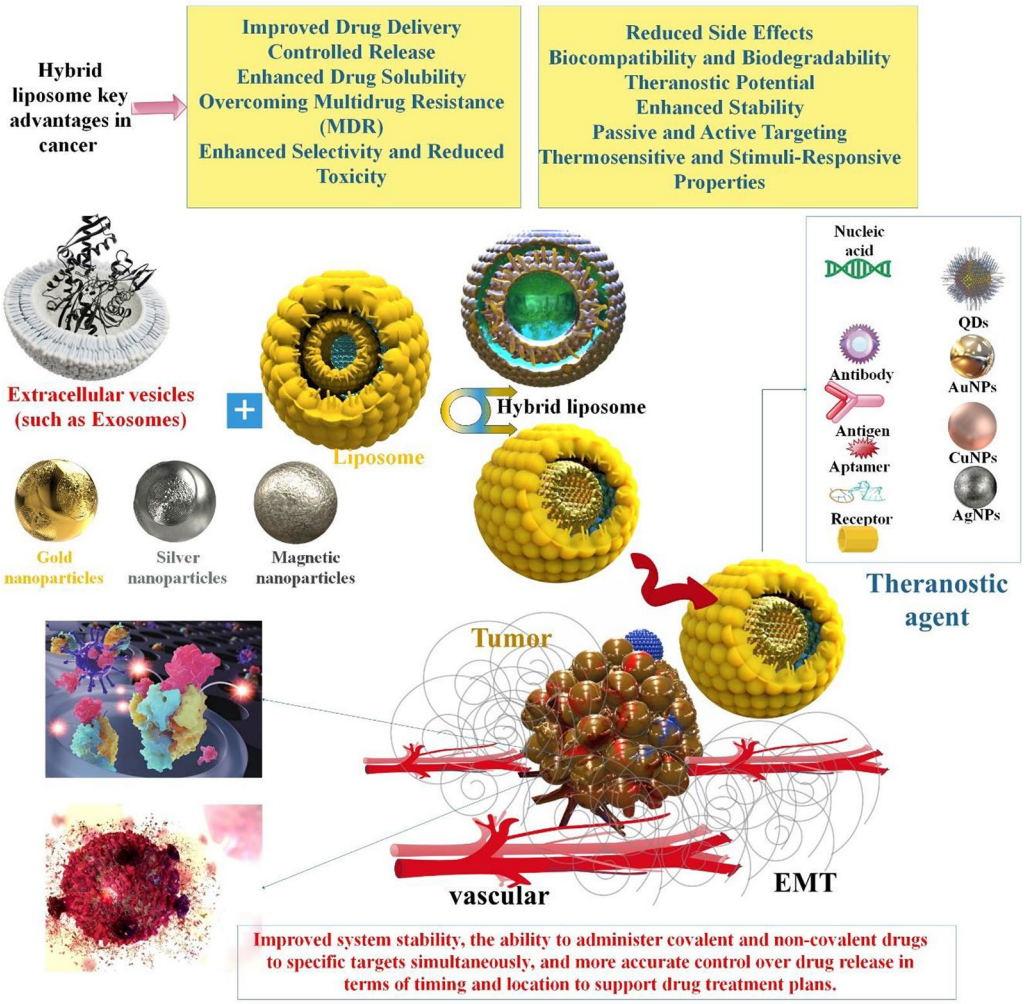


## Introduction

Cancer is a severe medical condition with often poor prognoses. In the world, cancer comes in third place after infectious illnesses and cardiovascular disorders as the primary causes of death [1]. As the hunt for successful anti-cancer treatments goes on, it's becoming more and more evident that creating treatment regimens that work requires an accurate and educational depiction of anti-cancer medicines after they've been administered [2, 3]. A new age in cancer detection and therapy is dawning, propelled by remarkable developments in nanotechnology [4]. Modern cancer therapies, including chemotherapy, radiation, gene therapy, and immunotherapy, have helped many people go into complete remission, yet cancer is still a leading cause of death worldwide [5]. Therapeutic resistance, toxic side effects (i.e., in healthy tissues), and a lack of therapeutic specificity are the significant causes of the low response rates for many malignancies [6]. To overcome the constraints of traditional cancer therapies, nanotechnology has emerged as a crucial domain for developing nanoparticles (NPs) capable of eradicating cancerous cells [7].

NPs can transport substantial quantities of cancer medications to tumors owing to their small size. Additionally, they may be equipped with specific molecules (such as folate or peptides) to selectively target certain kinds of cancer cells, achieved by receptor-mediated endocytosis [8]. Nanotechnology has facilitated the use of NPs that may passively aggregate at tumor locations,

making them an ideal substitute for traditional methods in cancer therapy. The NPs were analyzed for several therapeutic applications, such as drug delivery, gene delivery to malignancies, and imaging agents with high selectivity and extensive measurement capabilities. NPs may be used in targeted drug delivery, offering benefits such as biocompatibility and less toxicity. NPs exhibit diverse properties, including a significant surface-to-volume ratio, which facilitates their ability to bind, absorb, and transport small biomolecules, such as DNA, RNA drugs, and protein molecules, to specific locations. This, in turn, enhances the efficacy of therapeutic agents. The benefits above render them significantly distinct and productive when compared to conventional methods in the treatment of cancer [9]. They may be grouped into many categories based on their characteristics, shapes, or dimensions. To name a few, there are fullerenes, metal NPs, ceramic NPs, and polymeric NPs. Due to their very high surface area and minimal size on the nanoscale, NPs display unique physical and chemical properties. Their size is believed to affect their optical properties, which in turn cause them to absorb light of different colors. Because of their unique structure, size, and form, they are reactive and tough, among other things [10]. Nanotheranostics have shown the creation of sophisticated platforms capable of early-stage diagnosis, initiation of primary therapy, monitoring, and prompt initiation of additional treatments for brain cancer [11].

Nanotheranostics refers to cutting-edge advancement in the field of localized imaging and cancer treatment. Currently, many conjugated nanohybrids have been suggested for noninvasive diagnostics and treatments; however, their progress in practical application could be better. However, it is essential to address the early detection of tumors in their initial stages and the effective delivery of nanosized systems to the tumor environment in nanomedicine. Conventional theranostics systems that have been used in the past are currently encountering various obstacles, including limited image clarity, significant toxicity, quick elimination from the body, inadequate and non-specific distribution within the body, instability, rapid clumping, slow breakdown, non-specific distribution within the body, lack of multifunctional capabilities, and limited ability to penetrate tissues. Therefore, these constraints impede the preclinical examinations of nanobiomaterials in the field of nanomedicine. Hence, there have been suggestions for the development of targeted theranostics agents, which include a combination of integrated imaging, therapeutics, and targeting agents within a unified platform, to achieve improved results. Nevertheless, the integration of a comprehensive platform at the nanoscale may diminish its effectiveness in diagnosis and treatment, as it may result in the untimely release of diagnostic and therapeutic chemicals that have been loaded onto it. The presence of these prematurely released cargo molecules may result in a multitude of adverse consequences on healthy cells and tissues. In addition, the consolidation of all agents into a single system might lead to intricate synthesis pathways with diminished product yield and limited repeatability [12–15].

Liposomes (LPs), being the fundamental artificial biological cells, have a broad spectrum of potential applications in molecular imaging, gene therapy, medicine administration, and vaccine delivery [16]. Nano LPs are LPs that typically have a size of 200 nm or less [17]. As specialized delivery vehicles, LPs—which consist of phospholipids around an aqueous core—can transport a variety of cancer treatment agents, including drugs, photosensitizers, and even genetic material [18].

Additionally, it should be noted that the NPs can incorporate imaging agents, including radioisotopes, fluorophores, and magnetic resonance imaging (MRI) contrast material. This enables their utilization in monitoring and evaluating the progress of therapeutic interventions [19, 20]. A multitude of cancer therapies have been devised since the introduction of the nanomedicine concept, using medication compositions mediated by nanostructures [21]. When it comes to (i) solid tumor cancer theranostics, (ii) image-guided treatments, and (iii) combined therapeutic applications, nanosized LPs are known to be a clinically proven way to deliver a variety of imaging and therapeutic agents to specific locations [22]. In 1995, the FDA approved Doxil®, a PEGylated LP containing doxorubicin (DOX), for the treatment of Kaposi's sarcoma associated with AIDS. This was nanomedicine's first approval. Consequently, several diseases have been approved for the treatment of LP-based medications, and additional clinical trials are still being carried out. The LP-based treatments were successful because of the following: (1) they were easy to synthesize; (2) they were compatible with living things; (3) they could hold both water-soluble and water-insoluble substances; and (4) they had persistent circulation properties following the application of polyethylene glycol (PEG). Numerous new features have recently been added to the LP platform. This includes (1) the incorporation of temperature- and pH-sensitive lipid components; (2) the integration of in vivo imaging probes for optical imaging, MRI, positron emission tomography (PET), and single-photon emission computed tomography (SPECT); and (3) the creation of innovative agents for photodynamic and photothermal therapies (PDT, PTT). The LP is a particularly appealing nanoplatforms for theranostics

because of its mix of well-established advantages and recent experimental achievements [23].

However, researchers encounter challenges in developing LPs for clinical drug delivery systems (DDS), including rapid clearance by the immune system, development of immunosuppression, and buildup in organs responsible for clearance [24]. Furthermore, the findings of current clinical trials suggest that these kinds of medication compositions only slightly increase the antitumor effectiveness [25]. Biological obstacles, including poor circulation stability, low extravasation efficiency in tumors, limited tumor penetration capacity, and the development of multidrug resistance, are primarily responsible for the shortcomings of these formulations [26].

LP structures categorize bilayers into four classifications based on their size and quantity: small unilamellar vesicles (SUV), large unilamellar vesicles (LUV), multilamellar vesicles (MLV), and multivesicular vesicles (MVV) [27]. Unique properties distinguish engineered liposomal NPs as cargo carriers in cancer therapy and care [28]. Liposomal theranostics have made great strides in the last few years, showing promising results in animal and human cancer models. Liposomal hybrid systems have obtained Food and Drug Administration (FDA) approval and have successfully entered the market [29].

New information suggests that hybrid nanocarriers have made strides, especially in the area of imaging capability integration. To accomplish this, imaging components may be either surface-attached to these hybrids or integrated into their core domains [1]. To diagnose tumors before or after surgery or to aid in the study of how drugs are absorbed, distributed, metabolized, and eliminated in the body to reduce the harmful effects of drugs on healthy tissues [30].

To summarize, these hybrid nanocarriers have great promise for addressing the drawbacks of conventional chemotherapy, such as its fast clearance, high toxicity, and non-specific distribution to cells and tissues [31]. Platelet exosome (EXO) hybrid liposomes (HLs) combine the advantageous characteristics of LPs and platelet EXOs. They have a high drug-loading capacity similar to LPs and possess the ability to specifically target tumors, which is a desirable trait of platelet EXOs. Platelet EXO HLs have significant promise for clinical use as drug carriers [22]. The vesicular and micellar molecules that makeup HLs may be synthesized by sonicating them in a buffer solution, provided that no organic solvents are present to prevent contamination. Furthermore, HL structures may be easily generated by subjecting a combination of vesicular and micellar molecules to ultrasonic waves in a buffered solution. Researchers used a mouse model of colorectal cancer (CRC) using HCT116 cells to study the therapeutic benefits and diagnostic capacities of HLs in detecting cancer. The researchers' goal was to determine if HLs may be used as theranostic agents. HLs demonstrated therapeutic activity in vitro by impeding the proliferation of HCT116 CRC cells, perhaps via the promotion of apoptosis, in the absence of a chemotherapeutic agent. HLs delivered intravenously also significantly decreased the relative weight of the cecum in a rat model of CRC with orthotopic grafting. Researchers' histological study indicated that hematoxylin and eosin (H&E) staining stated a reduction in tumor size in the cecal sections. The TUNEL labeling revealed the activation of apoptosis in HCT116 cells inside the orthotopic transplant animal model of CRC. To diagnose CRC using hyperspectral imaging, researchers observed the buildup of hyperspectral images, including a fluorescent probe [indocyanine green (ICG)] in HCT116 cells inside an in vivo model of CRC after intravenous injection. The findings suggest that HLs may build up in tumor cells in the cecum of the orthotopic transplant mice model of CRC for an extended duration and impede the proliferation of HCT116 cells [32]. Membrane fusion-based hybrid exosomes (MFHE) are a novel kind of NPs used for drug delivery, which combines the advantages of both LPs and EXOs. MFHE is formed by the fusion of EXOs and LPs utilizing a range of membrane fusion procedures. MFHEs provide notable characteristics such as a high drug loading capacity, excellent stability, and straightforward surface modification. Furthermore, they have exceptional biocompatibility and little immunogenicity, akin to EXOs. This provides innovative viewpoints on NP DDS [24, 33].

Various vesicular carriers, including metallic hybrid nano-vesicle systems, lipid peptides, and lipopolymersomes, have shown potential in nanomedicine. Nevertheless, the existing cancer treatments discussed by researchers, together with other significant constraints such as poor productivity, high energy consumption, costly setup, lengthy process durations, and so on, make it challenging to use these systems in clinical settings commercially. These restrictions may be lessened with the use of combinatorial hybrid systems. Because they combine the best features of many carriers into one, hybrid nanovesicular systems have the potential to increase the therapeutic index and enhance clinical outcomes. Cell-based DDSs have been particularly effective in cancer therapy because of their distinct characteristics. Erythrocytes and platelets are long-circulating cells that may greatly benefit nanoparticles (NPs) due to their characteristics. Nanomaterials are crucial in cell-based drug delivery because of their one-of-a-kind physicochemical characteristics. When several nanomaterials and cell types are combined, the resultant delivery systems have a multitude of desired features. A lipid shell encases a polymer core in NPs,

making them core–shell nanostructures of the next generation. Recent years have seen a dramatic change in the method for producing lipid-polymer hybrid NPs, with the two-step process giving way to a one-step method that relies on the self-assembly of lipids and polymers. Due to its dual purpose, this approach has piqued the attention of oncologists as a combinatorial drug delivery platform [34].

To overcome these practical restrictions, a new approach called EXO fusion with LPs has been developed recently. These methods guarantee a large amount of medication, are very stable and biocompatible, and do not elicit an immune response. The physicochemical characteristics of hybrid vesicle liposomes (HVs)—which mix EXOs and LPs—can vary according to the manufacturing process used. For instance, even if they contain a lot of medicinal drugs, HVs made via the freeze–thaw method might have some of those compounds leaked out. Another method for preparing HVs is via natural incubation; however, although this technique is straightforward, the resulting HVs have poor fusion efficiency. Hybrid vesicles that were manufactured via polyethylene glycol-mediated fusion had an increase in blood circulation time. On the other hand, stealthy HVs show less absorption by cells. Although shear stress during the extrusion process is possible, HVs manufactured using the membrane extrusion method nevertheless showed benefits such as homogeneity, a quick building process, and manageable size controllability. The hybrid vesicles outperformed LPs in terms of physical qualities and reduced cell viability to a greater extent, albeit this effect likely varied by cell type. Researchers shed light on the kinds of Extracellular Vesicles (EVs) that can be used to make hybrid vesicles, which might lead to the development of a more effective DDS, and it also suggested that fusion-based hybrid vesicles give a new way to deliver therapeutic drugs. Finally, stable HVs, including EVs and LPs, were successfully manufactured and showed enhanced cellular absorption of DOX by cancer cells. The HVs' internalization methods were somewhat in line with ATP-dependent endocytosis, depending on the HVs' composition and various cell types. Researchers offered a proof of concept for HV preparation via the fusion process, which may inspire future generations of drug delivery carriers [35].

Furthermore, NPs that combine LPs and polymers were developed and evaluated for use in nasal vaccination administration. To increase biocompatibility, colloidal stability, and consistent antigen release, researchers added hyaluronic acid (HA) to cationic DOTAP LPs and then PEGylated them. When compared to soluble vaccine formulations, these NPs co-loaded with adjuvant compounds and protein antigens improved dendritic cell (DC) maturation and induced higher humoral and cellular immune responses [36]. The use of gene silencing in cancer therapy has great promise. Nevertheless, creating carrier systems that are both safe and highly targeted is essential for improving its efficiency. Their immunogenicity is usually the limiting factor for cationic carriers. Because epithelial malignancies have an overabundance of the protein epithelial cell adhesion molecule (EpCAM), scientists have developed HLs that encapsulate a Poly (L-lysine)-siRNA complex in an effort to silence it. Researchers showed that for the HLs LL1 (Egg PC: DSPE-PEG, 10:0) and hybrid immunoliposomes LL2 (Egg PC: DSPE-PEG, 8:2) linked to the EpCAM antibody as the targeted ligand, the encapsulation efficiency (EE) was 70% and 86%, respectively. With a zeta (ζ)-potential of −26 mV, LL2 LPs demonstrated exceptional colloidal stability at 37 °C in phosphate-buffered saline (PBS), which included fetal bovine serum and bovine serum albumin. Research on cell absorption revealed that LL2 LPs were more efficiently absorbed than LL1 LPs. Researchers lastly tested the hybrid immunoliposomes' ability to reduce tumor volume in SCID mice. Every one of the eight animals received a dosage of 0.15 mg/kg of siRNA, one of the lowest quantities ever recorded. Compared to the positive control and LL1 treatment groups, the LL2-treated animals reduced tumor volume by around 45% after 28 days. Researchers demonstrated that the 'nano-in-nano' concept of encapsulating poly (l-Lysine) complexed EpCAM siRNA in immunoliposomes would be a workable way to treat EpCAM-positive epithelial cancers, especially as an adjuvant therapy [37].

This article generally discussed the kinds of LPs used in cancer detection, treatment, and therapy. Additionally, the types of HLs that are useful for cancer detection and treatment have been examined, along with their benefits and drawbacks. Essential and recent research on the use of HLs in cancer therapy was also discussed. Lastly, the advantages and disadvantages of this theranostic approach to the concurrent detection and treatment of many malignancies were examined.

## Typical features of liposomes

LPs, which are vesicles with a spherical form and composed of one or more layers of phospholipids, were first documented in the mid-1960s [38]. LPs are vesicles composed of phospholipids that may be either uni or multilamellar in structure. These LPs can be derived from natural or synthetic sources and possess the advantageous properties of being non-toxic, biodegradable, and

readily producible in large quantities [39]. Soybean, egg yolk, artificial, and hydrogenated phosphatidylcholine are among the most often used types of phospholipids in a range of formulations [40]. At present, they function as highly valuable replicas, chemical reaction substances, instruments, and components in numerous scientific disciplines, such as biology, mathematics, theoretical physics, biophysics, chemistry, colloid science, and biochemistry [41]. Subsequently, LPs have become available for purchase. LPs, one of several innovative new DDSs, represent a cutting-edge method for transporting active molecules to the site of action; several formulations are currently in clinical use [42]. LPs are natural, non-toxic phospholipids and cholesterol that can be utilized in their production. Phosphoric and hydrophilic properties, in addition to biocompatibility, render LPs auspicious DDS [43]. LPs, because of their many manifestations, need more investigation. These structures can transport both hydrophilic and hydrophobic pharmaceuticals for various purposes, such as cancer treatment, antibiotic and antifungal therapies, immunomodulation, diagnostics, ophthalmic applications, vaccines, enzymes, and genetic elements [44]. The formulation of LPs influences the properties of these systems. Bangham and colleagues defined LPs as products that can be produced from phospholipids, cholesterols, non-toxic surfactants, and membrane proteins approximately forty years ago. As a consequence of this group's investigations, LPs have been classified as delivery systems, with the central section transporting a diverse array of compounds [45]. These structures are capable of encapsulating and harmfully delivering both hydrophilic and hydrophobic substances [46, 47]. Primarily composed of phospholipids (e.g., soybean phosphatidylcholine, synthetic dialkyl, or trialkyl lipids), LPs are synthesized [48]. Cholesterol is an essential component of LPs because it regulates the permeability of membranes, alters their fluidity, and makes bilayer membranes more stable when exposed to biological fluids like blood and plasma [49]. To enhance the efficacy of the encapsulated drug, prolong the circulation half-life, and improve the biodistribution profile, liposomal formulations may additionally incorporate membrane proteins and polymers. Furthermore, it has been demonstrated that incorporating phospholipids-attached polyethyleneglycol (PEG) into the infrastructure of stealth-stabilized LPs is an effective technique for modulating the pharmacokinetic properties and biodistribution profiles of LPs [50, 51].

In addition, the kinds of LPs may be classified as unilamellar, multilamellar, or gigantic unilamellar varieties according to the production procedures [52]. Based on the size and number of bilayers, LP structures are categorized into four groups: SUV, LUV, MLV, and MVV. Concentric phospholipid spheres assemble into a multilamellar structure known as MVV, which is composed of numerous unilamellar vesicles generated within larger LPs [53]. When it comes to hydrophilic chemicals, the efficacy of LP encapsulation decreases with the number of bilayers, but it rises with the size of the LP. When it comes to controlling the circulation half-life of LPs, one of the most crucial factors is the size of the vesicles. The quantity of the medicine that is encapsulated is affected by both the size of the bilayers and the number of them [27].

LPs are vulnerable to various influences, including light-induced, thermal, ionic, and acid–base effects, as well as free radicals. As a result, their practical applications are constrained by the external environment; therefore, stability enhancement of LPs is a crucial prerequisite. Surface modifiers, such as proteins (polysaccharides), have been employed by scientists to address the issues above. These modifiers establish a barrier of contact between phospholipids and the external environment, thereby enhancing the stability of LPs. Using layer-by-layer self-assembly, these LPs not only maintained their fundamental characteristics—surface hydrophilicity, a lipid bilayer, and a hydrophilic inner lumen—but also enhanced their stability and resistance to phospholipid oxidation, as well as their biocompatibility [54].

Furthermore, as carriers for medications, LPs have notable characteristics like specific targeting, excellent compatibility with living organisms, capacity to break down naturally, simplicity of modification, little harmful effects, and low likelihood of triggering immune responses. These traits significantly enhance the controlled release of drugs and improve their therapeutic effectiveness. Nevertheless, LPs are rapidly eliminated from the bloodstream. Consequently, to enhance their durability inside a living organism, several investigations have been conducted on the specific alteration of the surfaces of LPs. An example of this is the process of attaching the hydrophilic polymer PEG to the surface of LPs. This prevents the adsorption of opsonins, which in turn reduces the absorption of the mononuclear phagocyte system (MPS) and allows for extended circulation. Presently, typical functionalized LPs include long-circulating PEGylated LPs, ligand functionalized LPs, stimuli-sensitive LPs for highly efficient targeted treatment, and sophisticated cell membrane-coated biomimetic nanocarriers. Additionally, the safety of nanoLPs is influenced by several factors, such as their dimensions, composition, surface charge, stability, incorporation into tissues, and interactions with cells [55, 56] (Fig. 1).

## Liposomes in cancer detection

The early identification or thorough visualization of cancer-related biomarkers is significant for cancer treatment [57]. Traditional histological imaging methods sometimes exhibit limited sensitivity in detecting cancer during its first stages [58]. The area of in vivo biomarkers and illness detection has significantly progressed thanks to the capacity to alter the surface characteristics of different recognition agents and change the composition of LPs [28].A significant worry in cancer diagnostics is the toxicity of detecting agents. These chemicals are often injected into the body for imaging or to track the growth of tumors. Despite their importance for accurate cancer diagnosis, their compatibility with the body and lack of side effects must be prioritized. When it comes to diagnosing patients, characterizing diseases, and planning treatments, anatomical and physiological imaging using CT and MRI is crucial. It is becoming more common for procedures that use CT and MRI to ask for the injection of contrast media, including iodinated CT and gadolinium (Gd) for MRI. Although iodinated and, to a lesser degree, Gd-based contrast media are often employed in clinical practice, they can have adverse effects: MRI contrast chemicals may cause nephrogenic systemic fibrosis (NSF) and potentially fatal contrast-induced nephropathy (CIN) in the kidneys. Any sudden decrease in renal function after the injection of iodinated contrast media (a rise in serum creatinine of more than 0.5 mg/dl) is called CIN. It is believed that the most vulnerable population to get CIN consists of patients with moderate to severe chronic renal impairment. When it comes to ionic high-osmolar contrast CT medium, CIN has more incredible experience. Skin and systemic connective tissue production are hallmarks of the uncommon disorder known as NSF. Patients prone to NSF include those with chronic kidney disease (stages 4–5), acute kidney injury, or end-stage renal disease. There is a higher likelihood of NSF when using nonionic linear Gd-chelates [59]. The use of NPs as cancer theranostics is hindered by their high toxicity, off-target effects, and poor biocompatibility, all of which pose severe risks to cancer patients and even jeopardize their lives. When NPs aggregate within cells to create a protein corona, they disrupt the biomolecules' normal function; as a result, the formulation loses its ability to regulate the proliferation of cancer cells. Dangerous toxicities may result from NPs interacting negatively with living things. The accumulation of small NPs (< 100 nm) in organs and tissues that are not intended for their use, including the liver, spleen, or lungs, might cause harm to these organs [60, 61].

The significance of molecular and diagnostic imaging has significantly risen in recent years, particularly in cancer therapy and the planning of treatment for other illnesses. Nanomedicine offers intriguing prospects for integrating imaging and treatment. Tumor-targeting engineered LPs can specifically accumulate in tumor tissue and may effectively deliver both therapeutic medications and imaging agents. This enables a theranostic strategy that holds significant promise in the field of personalized medicine. The process of attaching radioactive labels to LPs has been a common practice in preclinical research to assess the behavior of LPs in living organisms. This technique has played a crucial role in the advancement of liposomal medication development. Nevertheless, modern imaging methods now provide novel opportunities for the non-invasive tracking of LP biodistribution in human subjects. Advancements in imaging technology and LP radiolabeling methods have opened up new possibilities for using imaging to identify patients and monitor therapy when using nanocarrier-based medications. Nanocarrier imaging agents may possess intriguing characteristics that might be valuable for disease diagnosis and staging [62]. Numerous well-established and frequently employed medical imaging modalities, including fluorescence, magnetic resonance, ultrasound, and nuclear imaging, have utilized LPs as nanocarriers [63].

LPs serve as exceptionally efficient carriers for molecular imaging instruments and medications intended for use within living organisms. LPs, characterized by a diameter below 200 nm, exhibit considerable promise in terms of facilitating blood flow and promoting cargo accumulation in particular tumor or inflamed tissues through the enhanced penetration and retention (EPR) mechanism of passive targeting. Moreover, active targeting can be achieved through the modification of the vesicle surface via the application of antibodies or other suitable targeting ligands. Additionally, LPs can be infused with NPs of various compositions and sizes, thereby expanding the potential applications of this class of materials, which have garnered considerable research attention in recent decades due to their remarkable properties and attributes. These materials demonstrate unprecedented physical and chemical characteristics as a result of the confinement effects of quantum mechanics and their substantial surface area. NPs find utility across a vast array of domains, including but not limited to medicine, energy-based research, sensing, imaging, and environmental applications. The feasibility of these applications stems from the capacity to modify the characteristics of NPs—such as their optical, magnetic, and catalytic properties—via their size, shape, and the inherent properties of the elements comprising them. Although a universally accepted definition of nanomaterials is still elusive, they are frequently defined as substances containing at least one

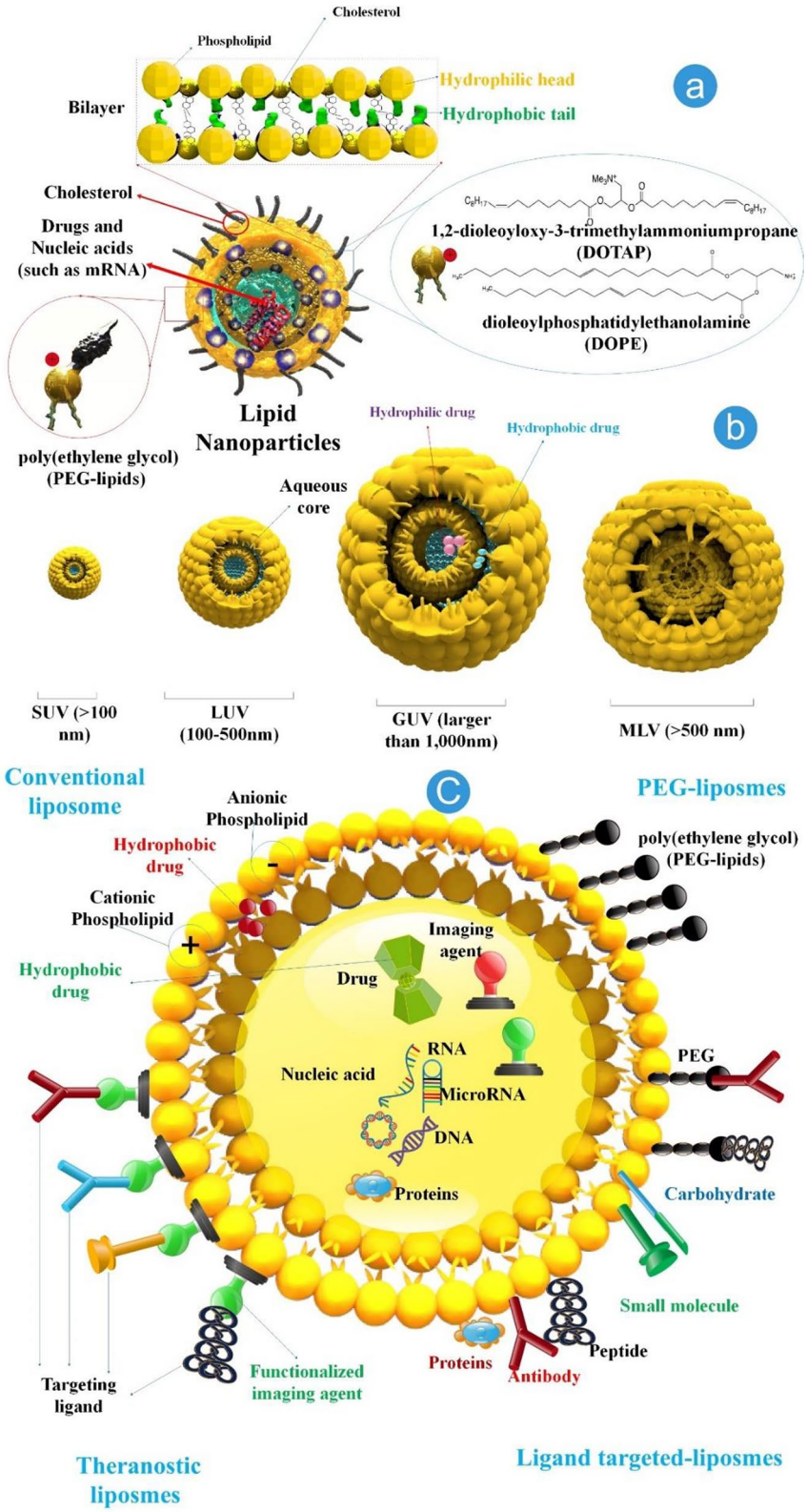


**Fig. 1** **A** Diagram showing the liposome (LP)'s structural makeup. **B** LPs may be classified as GULV, LUV, SUV, multilamellar LP, and multivesicular LP, depending on their size and lipid-bilayer structure. **C** There are many liposomal drug delivery systems available, including PEGylated LPs, Theranostic LPs, Ligand-targeted LPs, and Conventional LPs

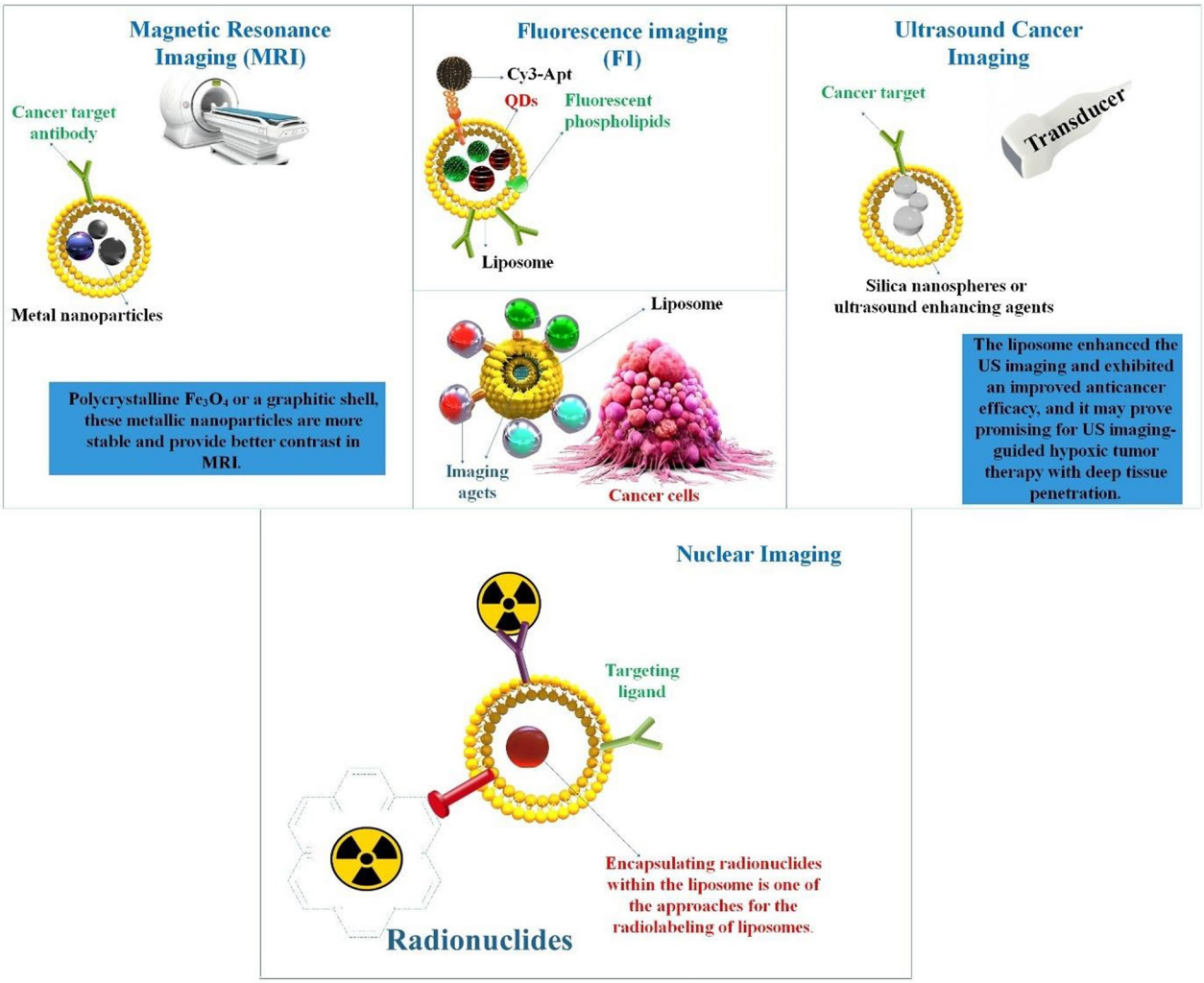


**Fig. 2** Fluorescence imaging, magnetic resonance imaging, ultrasound cancer imaging, and nuclear imaging are all approaches used to image LPs

dimension ranging from one to 100 nm. The European Commission formally established a definition for nanomaterials in 2011. Nanomaterials, as per this definition, can be observed either in an unconstrained state or in the form of aggregates or agglomerates. Furthermore, one or more external dimensions of a minimum of 50% of the particles in the number size distribution must be contained within the range of 1–100 nm [64] (Fig. 2).

#### Liposome in fluorescence imaging of cancer

Fluorescence is crucial in the detection of cancer. The examination of tissue emission spectra forms the basis of this method, which is often shown as a graph showing the relationship between intensity and wavelength [65]. To perform fluorescence spectroscopy, either steady-state or time-resolved methods may be utilized. External labeling of fluorescent proteins and the utilization of single or multiple-wavelength excitations are examples of such techniques [66]. The approach most often used for analyzing emission spectra is steady-state fluorescence. Autofluorescence is achieved by not using external fluorescence markers, allowing for in vivo detection without the need to prepare tissue samples [67]. Imaging by fluorescence is the most prevalent diagnostic method. It enables the examination of the biological functions of biomolecules by visualizing their location, gene expression, and enzyme activity in living cells or tissues [68].

Mucin 1 (MUC1) is a significant biomarker that is involved in the spread and infiltration of different forms of cancer. Early cancer detection and disease progression monitoring depend on effective methods for identifying MUC1 in liquid samples and imaging MUC1 at the cellular level. Researchers used a polydiacetylene (PDA) LP-based sensing technology to develop a nanosensor for MUC1 detection. A Cy3-labeled MUC1 binding aptamer (Cy3-Apt) was used to functionalize the device, and it

functioned via a fluorescence "turn-on" mechanism. Energy transfer between the fluorogenic and PDA-conjugated backbones instantly quenches the fluorescence of Cy3-Apt in the sensor device. When MUC1 is present, the aptamer (Apt) binds to it and causes both the PDA LPs and the Apt to undergo a structural change, resulting in the restoration of red fluorescence. With a detection limit of around 0.8 nM, MUC1 may be detected explicitly in water-based solutions. Accurately measuring the spatial expression of MUC1 in cancer cells demonstrated the nanosensor's remarkable sensitivity and further validated its usefulness [69].

Imaging and fluorescence microscopy methods are often used to track the migration of LP tumors. To investigate the possible relationship between the fluorescent label type and the accumulation of LPs, researchers created PEGylated LPs that were labeled with two types of fluorescent phospholipids (Cy3-DSPE or Cy5-DSPE) and indocarbocyanine lipids (ICLs: DiD or DiI). Although the LPs had comparable cyanine headgroups, they had different spectra. Scientists used ex vivo confocal microscopy and imaging methods to directly examine the accumulation and extravasation of FPLs and ICLs originating from malignancies. In a mouse model of 4T1 breast cancer (BC) that is genetically identical to the host, immune cells known as ICLs and FPLs were shown to first gather in the blood vessels of the tumor and the surrounding region after being injected systemically. ICLs gathered in tumor macrophages and spread throughout a much wider area of the cancer at subsequent time points. In contrast, FPLs were mainly restricted to the blood vessels and showed negligible signals outside of them. This effect was confirmed in LY2 models of head and neck cancer and was not influenced by the makeup of LPs or the kind of ICL/FPL. Researchers also observed this phenomenon in syngeneic cerebral GL261 glioma. When tagged with two distinct dyes, the LPs were stable in plasma and were able to deliver both dyes to tumors in their early stages. Significantly, whereas the concentration of ICLs rose with time, FPLs eventually vanished from tumors and other organs in a living organism, most likely owing to the breakdown of the phospholipid. Researchers' findings suggest that the label's mobility and persistence are essential considerations when using fluorescence microscopy and imaging to assess the leakage and accumulation of nanocarriers in malignancies and other organs [70].

As semiconductor nanocrystals, quantum dots (QDs) are among the most auspicious nanostructures in terms of potential in vitro diagnostic applications. For long-term imaging purposes, such as tracking intracellular biomolecules or entire cells, they are regarded as optimal candidates as fluorescent probes due to their intense fluorescence, narrow emission, broad excitation, and high photostability. Utilizing LPs to enhance the performance of QDs has been an extremely fruitful endeavor. The utilization of LPs as carriers for hydrophobic QDs can effectively address the issue of biocompatibility, whereas encapsulating hydrophilic QDs within LPs can mitigate cytotoxicity. Additionally, an active targeting agent, such as anti-HER protein, epidermal growth factor (EGF) ligand, folate, or platelet-derived growth factor (PDGF), that is linked with the lipid compounds can significantly enhance the ability of LPs to target tumor cells. By incorporating QDs into LPs, the absorption of living cells can be substantially enhanced. The LPs that are laden with QDs are distributed predominantly in the liver, spleen, and tumor. The MPS is capable of clearing them. The development of multifunctional LPs laden with QDs, including multi-fluorescent LPs, fluorescent paramagnetic LPs, and theranostic LPs, has significantly accelerated the progress toward personalized medications [71]. Using LPs with enhanced pharmacokinetic properties, fluorescence imaging substances can be delivered to the target area. For instance, Kostarelos et al. devised functionalized-QD-liposome (f-QD-L) hybrid NPs for cancer imaging by encapsulating PEG-coated QDs within the aqueous phase of DOPC-supported LPs [72].

The use of QDs to detect and monitor malignancies is auspicious. Nevertheless, their diminutive dimensions enable them to amass in significant quantities within healthy cells as well as tumor cells, thereby augmenting their cytotoxicity. In an investigation, stealth LPs encapsulating hydrophilic graphene QDs (GQDs) were synthesized and their release was induced via ultrasound. The objective was to establish a method for delivering fluorescent markers to tumors that is both secure and precisely regulated. The outcomes of the researchers' investigation validated the effective encapsulation of the QDs within the central region of the LPs. In contrast, the size and stability of the synthesized LPs remained unaffected. Additionally, their findings demonstrated that low-frequency ultrasound is a proficient technique for delivering QDs encapsulated within LPs in a controlled manner for space and time. This controlled release guarantees the efficient transportation of QDs to tumors while mitigating their systemic toxicity [73].

#### Liposome in magnetic resonance imaging (MRI)

The ability to monitor medical treatments in real-time and the patient's reaction to therapy is made possible by non-invasive in vivo imaging. Radiofrequency pulses detect the nuclear spins of hydrogen atoms in water in MRI, a widely used non-invasive medical imaging method that allows for non-invasive imaging of the body's structure and physiological functions. [74]. The advancement of magnetic contrast agents has been instrumental

in the expansion of MRI's functional capabilities. These agents are utilized to investigate particular structures or to monitor local environmental changes. Comparable to fluorophores, LPs can encapsulate a wide range of contrast agents for MRI. This facilitates the controlled and effective administration of these instruments, leading to enhanced imaging capabilities [75]. Currently, transrectal ultrasound (TRUS) is primarily used for biopsy guidance rather than for identifying the precise location and size of prostate cancer. However, more advanced imaging techniques like endorectal coil MRI and magnetic resonance spectroscopic imaging (MRSI) have the potential to detect prostate cancers [76].

Most clinically authorized iron oxide nanoparticles (IO NPs) used as MRI contrast agents have been taken off the market due to safety concerns or lack of profitability. To overcome this challenge, LPs have been used to create IO-based T2 contrast agents. Researchers examined how different phospholipids affected the relaxivity (r2) values of magneto-liposomes (MLs) that included magnetic NPs in the bilayer. Investigators have shown that the fluidity of the bilayer and r2 are significantly correlated. The relaxivity of lipid bilayers is enhanced considerably by embedding 5-nm IO NPs; r2 values for DPPC/cholesterol/DSPE-PEG (96/50/4) to DOPC/DSPE-PEG (96/4), ranging from $153 \pm 5$ $s^{-1}$ $mM^{-1}$, surpass the value of $673 \pm 12$ $s^{-1}$ $mM^{-1}$. In contrast, "free" IO NPs have a r2 value of $16 \pm 1$ $mM^{-1}$, as measured at a 9.4 T MRI scanner. In conjunction with the ICP-MS analysis, in vitro MRI measurements and ICP-MS measurements demonstrated that MLs functioned as remarkably selective contrast agents, being preferentially internalized by malignant T24 cells. This enhanced contrast resulted in a more distinct differentiation between healthy and malignant cells. Effective MRI contrast agents could be produced from MLs via meticulous lipid bilayer selection, even at deficient IO NPs concentrations [77].

Metastasis is the leading cause of death in cancer patients in clinical settings. Hence, it is essential to precisely monitor the spread of cancer to secondary sites, efficiently eliminate cancerous cells, and subsequently enhance the prognosis of individuals with advanced disease. Consequently, scholars devised an LP-based targeted system that employs targeting peptides and single-stranded DNA. Sequential administration of this system, followed by its assembly within the body, facilitates a pre-targeted synergistic treatment utilizing multimodal imaging for metastatic BC. Dual LPs comprise the pretargeted system. The initial LP comprises downconversion nanoprobes (DCNP) for near-infrared (NIR) fluorescence imaging (NIR-II) and SPIO (L1/C-Lipo/DS), an MRI contrast agent. This LP is utilized for MRI/NIR-II dual-modal imaging of primary and metastatic malignancies. As the therapeutic component, the second LP contains glucose oxidase (GOx) and DOX (L2/C-Lipo/GD). The L1/C-Lipo/DS formulation contains superparamagnetic iron oxide (SPIO), which accumulates in the tumor tissue and provides vital iron ions to the therapeutic LP (L2/C-Lipo/GD), enabling it to execute the targeted ferroptosis treatment on cancer cells efficiently. Based on multimodal imaging, researchers provide evidence that the DNA-mediated pretargeting method may facilitate a synergistically enhanced anticancer effect between the two LPs. Clinical application of this novel method of pretargeted and synergistic in vivo assembly nanomedicine holds promise for the diagnostic and therapeutic management of cancer [78].

The primary objective of the researchers' endeavor was to evaluate the theranostic capabilities of nanomedicine, which could produce MRI contrast in response to the localized exposure of pulsed low-intensity non-focused ultrasounds (pLINFU)-induced release of the antitumor drug DOX from LPs. Gadoteridol served as an outstanding imaging agent for assessing the release of DOX after pLINFU activation, as shown by in vitro tests. The theranostic system was later examined in vivo using a syngeneic mouse model of TS/A BC. MRI offered outstanding insight for tracking the drug's release triggered by pLINFU. Furthermore, it furnished the following: i) an in vivo demonstration of the liposomal content's efficacy in release and ii) confirmation that the overall protocol conferred therapeutic advantages. *Ex* vivo fluorescence imaging indicates that the positive treatment effect was due to improved drug diffusion into the tumor after the administration of the pLINFU stimulation. Remarkably, the LPs seemed to enable considerable drug diffusion throughout the tumor stroma. Scientists have highlighted either the huge therapeutic benefit of using stimuli originating in the United States to securely start the release of medicine from its nanocarrier or the enormous potential of such stimuli. Ultimately, MRI proved to be a beneficial modality in assisting chemotherapy and monitoring its efficacy. Moreover, the MRI agent used in this specific case has previously been approved for human use, indicating a high degree of clinical translatability for the theranostic agent [79].

It is still difficult to treat glioblastoma and to assess the treatment's efficacy without intrusive procedures. Using a brain-compatible drug-loaded liposomal hydrogel, researchers were able to effectively monitor early tumor response using Chemical Exchange Saturation Transfer (CEST) MRI, and they also created a robust technique. The development of this CEST-detectable liposomal hydrogel began with the goal of creating a DDS that could withstand the brain tumor's unique environment, which is hostile to the growth of tumor cells. After injecting the

hydrogel near the tumor using three distinct CEST contrasts, researchers were able to follow the tumor response and drug release longitudinally at 3 T. In comparison to the control group, the treatment group consistently showed a decrease in tumor volume. Researchers also observed a substantial reduction in CEST contrasts associated with the tumor response at 3.5 ppm (Amide Proton Transfer; APT) and − 3.5 ppm (relayed Nuclear Overhauser Effect; rNOE). Curiously, the 3.5 ppm molecular alteration on day 3 was discovered before the substantial reduction in tumor volume on day 5. There was a robust relationship between the amount of tumor-initiating cells and an APT signal. This indicates that prior to the morphological alteration in tumors, APT detected a significant decrease in tumor-associated mobile proteins and peptides. The APT signal, which was associated with either growing or dying cells, showed a regional response to the therapy, allowing for a thorough evaluation and prediction of the tumor treatment response. In order to meet clinical demands employing CEST MRI for image-guided brain tumor therapy, researchers have proposed a newly created liposomal hydrogel [80].

#### Liposome in ultrasound cancer imaging

Medical ultrasonography is a prevalent non-invasive imaging modality that operates by utilizing sound waves possessing frequencies exceeding 20,000 Hz. Ultrasound imaging consists of the emission of ultrasound pulses in the direction of tissue and the subsequent measurement of the echoes generated by the tissue at different angles of reflection [81]. Similar to MRI, contrast agents utilized in ultrasound possess the capability to designate specific categories of tissue or lesions selectively. As acoustic liposomes (ALs), LPs containing perfluoropropane gas can function as probes for ultrasound imaging. ALs ranging in diameter from 100 to 200 nm have the potential to function as DDS by passively localizing to tumor tissue via the enhanced permeability and retention (EPR) effect [82].

The possibility of using ultrasound contrast agents to make cell membranes more permeable to an ultrasonic pulse has shown promising strategies to enable the delivery of a larger intracellular payload to specific target sites. Given the above, scientists report the development of submicron nanobubble-paclitaxel (PTX) LP (NB-PTXLp) complexes that allow drugs to be delivered to cancer cells in response to ultrasound and ultrasound imaging. The LPs measuring 200 nm in size formed conjugates with the nanobubbles with an efficient tethering process using PTX entrapment with an accuracy of 85.4 ± 4.39%. The cellular permeability of MiaPaCa-2 cells was significantly improved by sonoporation with nanobubbles and ultrasound, leading to a 2.5-fold increase in the uptake of LPs compared to treatment with LPs alone. The anticancer activity of NB-PTXLps was observed to be over 300-fold more significant than that of the commercial formulation ABRAXANE when tested in the presence of ultrasound on the MiaPaCa-2, Panc-1, MDA-MB-231, and AW-8507 cell lines. Furthermore, the echogenicity of the NB-PTXLp conjugates was shown to be comparable to that of SonoVue, a commercial ultrasound contrast agent. Compared to the six-hour stability demonstrated by the commercially available ultrasound contrast agent SonoVue, the generated nanobubbles' echogenic stability was found to be larger than one week. Consequently, the NB-PTXLps might be used as a less invasive and perhaps successful theranostic platform for cancer treatments in the future [83].

The discipline of drug delivery is becoming increasingly intrigued by targeted drug delivery utilizing image guidance. The use of microbubbles as contrast agents in diagnostic ultrasonography creates new opportunities for noninvasive image-guided medication administration. Researchers evaluated the innovative DOX LP-loaded microbubbles' imaging and therapeutic qualities. The microbubbles may be followed in vivo and photographed in real time because they scatter enough signal at scanning settings (1.7 MHz and 0.2 mechanical indexes) to allow for nonlinear ultrasound imaging. In contrast to treatments using free DOX or DOX LP-loaded microbubbles alone, an in vitro therapeutic evaluation demonstrated that the application of ultrasound at a frequency of 1 MHz and pressures up to 600 kPa in combination with microbubbles loaded with DOX led to a fourfold decrease in cell viability. Increased glioblastoma cell uptake of the unbound DOX and ultrasound-induced DOX release from the LPs are linked to therapeutic effectiveness. Researchers indicated that the utilization of microbubbles laden with DOX LPs in conjunction with ultrasound can offer a novel approach to image-guided drug delivery that is noninvasive [84].

This challenge was overcome by the newly discovered ultrasound-switchable fluorescence (USF) imaging, which allowed for the in vivo imaging of a mouse utilizing the contrast agent ICG dye encapsulated in poly(N-isopropylacrylamide) (ICG-PNIPAM). However, there are several drawbacks to the ICG-PNIPAM, such as concerns about cytotoxicity and blue-shifted emission and excitation spectra. To address the above-described issues and broaden the range of contrast agents available for USF imaging, this work introduces a novel ICG-encapsulated LP. The USF imaging capabilities and biostability of the ICG-LP are exceptional, with an emission peak of 836 nm. The test for cell viability also confirms the trait of low cytotoxicity. After that, successful ex vivo and in vivo USF imaging is achieved, leading to the capture of 3D

USF pictures. The ex vivo results confirm that the ICG-LP continues to conduct USF imaging and maintains its thermoresponsive characteristics in the liver's right lobe. Further in vivo USF imaging shows that while the liver as a whole showed fluorescence emission, the functioning ICG-LP is only seen in the liver's right lobe [85].

Despite their excellent efficacy in solid tumor imaging, small organic dye-based fluorescent agents encounter obstacles such as weak tumor binding, limited circulation, nonspecific dispersion, and poor photostability. These problems are remedied by nanocarriers, which exhibit superior physicochemical and biological performance, especially in the field of cancer imaging. Lipid formulations are one kind of nanosized carrier that has received clinical approval; nevertheless, they have not yet been developed into a brilliant nano-contrast agent that can be used to diagnose solid tumors without harming neighboring tissues. For solid tumor imaging and biodistribution, researchers have created and evaluated 698 ICG encapsulated targetable lipid nanoparticles (LNPs) as safe contrast agents (~200 nm). Scientists have discovered that ICG-LNPs with distinct assemblies are created by nanoprecipitation. This assembly is responsible for their excellent brightness and enhanced quantum yield (3.5%) in a water-based medium. The biophotonic agents are visible, optically stable for 30 days, and show fast accumulation (in 1 h) and extended retention (up to 168 h) at the primary tumor site. After a single dosage ($17.7 \times 10^1$ LNP), the signal intensity is improved. The inclusion of folic acid (735 folic acid/LNPs) aids in the targeted binding of tumors and the dispersion of intravenously administered NPs to particular sites, all while avoiding harm to healthy tissues. In comparison to the targetable ICG-liposomal nanoparticles (532 MESF), the engineered targetable ICG-LNP (634 MESF) exhibits high-contrast fluorescence and tumor area resolution. A number of in vitro and in vivo studies have shown that engineered bright LNPs had cancer diagnostic effectiveness on par with that of reported clinically recognized imaging agents. This led the researchers to conclude that these LNPs could be helpful in the early detection of cancer in the future [86].

#### Liposome in nuclear imaging

There are two distinct techniques available for the imaging of radionuclides: SPECT and PET. By utilizing radiolabelling, which involves the 'labeling' or 'labeling' of compounds with radionuclides, it is possible to trace small molecules, macromolecules, and cells within the body non-invasively and gain real-time insight into biological processes occurring within living organisms. By their ability to detect high-energy photons emitted by radionuclides, PET and SPECT exhibit superior sensitivity ($10^{-10}$–$10^{-12''}$M) in comparison to alternative imaging modalities like MRI ($10^{-3}$–$10^{-5''}$M) and have no depth penetration limitations in tissue. Critically, as alluded to briefly previously, the combination of these properties enables imaging to be conducted on animals and humans with the use of minute quantities of compounds that do not disrupt the observed biological process [87, 88]. Several LPs capable of encapsulating radionuclide tracers within their aqueous compartments or chemically engineered lipid bilayers have been documented. Utilizing a combination of PET and fluorescence imaging, Ferrara and colleagues investigated the design of stable, temperature-sensitive LPs. LP formulations containing lipids labeled with either 18F or $_{64}$Cu (Copper) were employed to encapsulate the hydrophilic model drug, the fluorophore Alexa Fluor 750 [89].

In addition, owing to their inherent high sensitivity, nuclear imaging techniques such as PET and single-photon computed tomography have attained considerable success in clinical contexts [90]. Radionuclide imaging is the predominant modality used for molecular imaging in the field of cancer [91]. Radionuclide-based molecular imaging has used many molecules, but there is significant interest in creating nanomaterials that are more suited for therapeutic use, especially in the detection and treatment of cancer. Many types of cancer have already integrated imaging technology into their procedures for detecting, diagnosing, and determining the stage of the disease [92]. Among these methods, MRI has gained popularity as a valuable tool for tumor diagnosis due to its exceptional ability to penetrate deep into the body, its high level of spatial resolution, and its ability to provide clear contrast between different types of soft tissues [93]. Technetium-99 m ($^{99m}$Tc) is the most often used radioisotope for labeling LPs. This is mostly because of its abundant availability, affordability, favorable imaging characteristics, and a half-life that permits imaging for a duration of up to 24 h. It is the second most used radionuclide, preceded by radioisotopes of iodine. In recent times, there has been a rising use of positron-emitting radionuclides, including 18F, 52Mn, 89Zr, and notably $_{64}$Cu. This trend is a result of the expanding interest in PET imaging and the greater accessibility to preclinical and clinical PET scanners [88].

Fluorodeoxyglucose-PET (18F-FDG-PET) is an effective method for detecting, staging, and monitoring cancer. Nevertheless, 18F-FDG-PET imaging exhibits a significant number of false positives due to its inability to differentiate between tumor and inflammatory areas, both of which exhibit heightened glucose metabolic activity. Researchers developed LPs that were covered with glucose and the chelator dodecane tetraacetic acid (DOTA) complexed with Cu. These LPs were designed

to be used as a diagnostic tool to distinguish between cancer and inflammation. The LP technique used in this context relies on materials that the FDA has authorized. It allows for the formation of complexes with metal cations and radionuclides. The researchers discovered that cancer cell types with high metabolic activity selectively absorbed these LPs, facilitated by glucose transporter-1. Within living organisms, these LPs were readily absorbed by tumors, in contrast to LPs without a glucose coating. Furthermore, in a mouse model where tumors and inflammation were present together, these LPs gathered specifically in the tumor tissue rather than the area affected by inflammation. Therefore, this technique has a strong ability to target tumors specifically while avoiding inflammation. It also has the potential to be quickly implemented in clinical settings and integrated with current PET imaging systems. This would significantly improve the accuracy of cancer detection by reducing false positive results [94].

The use of surface-modified LPs has shown to be a very efficient delivery approach, characterized by a substantial encapsulation efficacy and an extended half-life for LPs. Applying hydrophilic materials to the surface of LPs, such as silica acid, polymer PEG, or monosialogangioside (GM1), may improve blood vessel permeability and decrease LP absorption of protein opsonins. The enhanced hydrophilicity of the LP surfaces causes LPs to accumulate more in tumors. "Long-circulating LPs" is another term for these modified LPs. The size and lipid makeup of the LPs are two critical considerations that must be made in order to produce a LP with extended circulation. The FDA-approved LP formulation Pegylated liposomal DOX, which is sold under the brand name Doxil®, has a size of less than 100 nm. It is used to treat ovarian cancer and multiple myeloma. The use of this pegylated liposomal formulation as a carrier resulted in a notable enhancement in both pharmacological and therapeutic indices. Multiple liposomal formulations have received clinical approval, including DaunoXome®, which encapsulates daunorubicin and is used for treating Kaposi's sarcoma, DepoCyt®, which encapsulates cytarabine and is used for treating lymphomatous meningitis, and Marqibo®, which encapsulates vincristine and is used for treating acute lymphoblastic leukemia. Additionally, numerous other liposomal formulations are currently undergoing preclinical or clinical studies. However, functional group molecules, including proteins, antibodies, antibody fragments, carbohydrates, and other tiny molecules, must be attached to the LPs to achieve exact distribution. LPS must be able to recognize cells that express the appropriate receptors after surface alterations. Researchers call this mechanism "active transport." [95–97] (Table 1).

## Liposome in cancer treatment

In pancreatic cancer (PC) therapy, nano-sized DDS, including LPs, have been utilized extensively. They may evade the reticuloendothelial system (RES) and create lipoplexes with small interfering RNAs (siRNAs) to prolong circulation. At the same time, they can also encapsulate amphiphilic medicines. They are effective in chemotherapy due to the ease with which they can be functionalized on the surface, administered selectively, and stabilized drugs in vivo. Many anticancer drugs (such as nucleoside analogs, mitotic inhibitors, and enzyme modulators) and gene/nucleic acids (such as TR3 siRNA and siRNA of nerve growth factor (NGF)) have so far been administered via LPs in PC, either by themselves or in conjunction with other targeting strategies. The utilization of liposomal surface functionalization, such as antibody fragment conjugates, has been implemented to facilitate the targeted delivery of multiple medications, including insulin and chemotherapeutics. Utilizing physicochemical and biological cues, including photodynamic sensitivity, temperature, pH, magnetic field, and redox potential, nucleic acids, and chemotherapeutic medications can be targeted in a regulated manner. Primarily, the most favorable results have been achieved through the combination of the techniques mentioned above with anticancer drugs [98–100]. LPs that possess enhanced drug delivery capabilities and prolonged circulation properties have gained recognition as viable clinical carriers. Additionally, LPs facilitate the targeting of cell-type-specific responses in cancer through the use of functionalized agents [101]. Reduced toxicity and enhanced therapeutic efficacy are the results of liposomal compositions. They have an essential role in structural and signaling processes, among many others, in living organisms [102].

Therefore, the similarities between LPs and the components of the cell membrane, as well as their small size (less than 400 nm), which allows them to enter and interact with cells via the EPR effect, contribute to their success in delivering cancer treatment [103]. The appealing biological characteristics of LPs, including their capacity to degrade naturally, lack of toxicity, and excellent compatibility with living organisms, together with their advantageous size, charge, and surface features that enable easy adjustment of production techniques, suggest that they have great potential as cancer therapies. LPs function as vehicles for pharmacologically active compounds in medical environments and are non-toxic to humans [104]. Particular DDS, such as those using LP carriers or as excipients in formulations, may be used to enhance the therapeutic index of anticancer medicines that have significant adverse effects [105].

**Table 1** Liposome in cancer detection

| Liposomes carrier | Detection method | Cancer | Characteristics of liposomes | Explains | References |
|---|---|---|---|---|---|
| ICG-liposome (LPs) | Ultrasound-switchable fluorescence (USF) | Liver cancer | LPs derived from 1,2-dipalmitoyl-sn-glycero-3-phosphocholine (DPPC), measuring between 136 nm and 10.11 µm in size | The ex vivo findings attest to the ICG-LP's sustained ability to perform USF imaging and preserve its thermoresponsive properties throughout the right lobe of the liver | [85] |
| Fluorodeoxyglucose-PET (18F-FDG-PET) | PET imaging | SCC (A431) tumors | Researchers made 120 nm LPs using DSPE-PEG-COOH, cholesterol, and HSPC. 129.0 ± 2.20 nm was the size of $Cu^{2+}$-labeled LPs coated with glucose and having a ζ-potential of − 16.53 ± 1.30 mV | To produce LPs, researchers coated the chelator dodecane tetraacetic acid (DOTA) complexed with Cu with glucose. However, since 18F-FDG-PET imaging cannot distinguish between tumor and inflammatory regions, both of which have elevated glucose metabolic activity, it presents a high proportion of false positives | [94] |
| polydiacetylene (PDA) LP-based | Mucin 1 (MUC1) | Human epithelial cancers | Uniform spherical shapes were noted for PDA-Apt LPs. The morphological modifications were followed by a shift in the size distribution from 97.8 ± 0.5 nm to 66.9 ± 1.0 nm. The ζ-potential of the unaltered PDA LPs were observed to be −50.9 ± 2.0 mV before polymerization and −487.7 ± 0.3 mV after the process. Nevertheless, the negatively charged oligonucleotides caused these values to drop to − 58.3 ± 3.3 and − 53.5 ± 0.5 mV for PDA-Apt LPs | Researchers used a PDA LP-based sensing technology to construct a nanosensor for MUC1 detection. Utilizing a Cy3-labeled MUC1 binding aptamer (Cy3-Apt) to functionalize it, the apparatus functioned via a fluorescence "turn-on" process. The remarkable sensitivity of the nanosensor was shown by its exact mapping of MUC1 spatial expression in cancer cells, which further validated its usefulness | [69] |
| PEGylated LPs | Fluorescence microscopy and imaging | Breast cancer (BC) | A 130 nm negatively charged EPC/DSPE-PEG2000 LP containing 0.2 mol% DiI and 0.2 mol%, the research team synthesized Cy5-DSPE. Size = 150, polydispersity index (PDI) = 0.188, and ζ-potential = − 22.7 mV for the HSPC/Chol/DSPE-PEG2000/DiI/Cy5-DSPE 0.2%/0.2% | In PEGylated LPs, two kinds of fluorescent phospholipids (Cy3-DSPE or Cy5-DSPE) and indocarbocyanine lipids (ICLs: DiD or DiI) were tagged to examine any potential correlation between the fluorescent label type and the accumulation of LPs<br>Researchers directly examined the buildup and extravasation of FPLs and ICLs arising from malignancies using ex vivo confocal microscopy and imaging techniques | [70] |

**Table 1** (continued)

| Liposomes carrier | Detection method | Cancer | Characteristics of liposomes | Explains | References |
|---|---|---|---|---|---|
| Functionalized-quantum dot-liposome (f-QD-L) | QDs | Colorectal cancer | The LPs were produced using a process known as thin-film hydration. Their average radius was 86 ± 1.35 nm before incubation and 85 ± 0.32 nm after 24 h of incubation, indicating their size. When QDs were loaded, the stealth LPs' ζ-potential value dropped from 12.14 ± 0.143 mV to a more modest 6.98 ± 0.323 mV | Researchers have shown low-frequency ultrasound to be a successful technique for systematically distributing QDs contained in LPs over time and location. This regulated release ensures that QDs are transported to tumors effectively while reducing systemic toxicity | [73] |
| DNA-Functionalized LPs | NIR-II/MRI | Metastatic BC | The DCNP was produced using a thermal breakdown approach. Compared to L1/C-Lipo/DS or L2/C-Lipo/GD alone, the combined solution had a significantly greater particle size distribution (150–300 nm) and an average particle size change (189.76 ± 1.75 nm). The fact that L1/C-Lipo/DS and L2/C-Lipo/GD were successfully prepared was further supported by their ζ-potential values, which were − 38.05 ± 0.85 mV and − 29.73 ± 0.58 mV, respectively | Based on multimodality imaging, researchers provide evidence that the DNA-mediated pretargeting approach may offer a synergistically enhanced anticancer effect between the two LPs | [78] |
| LPs of the antitumor drug Doxorubicin (DOX) | MRI | BC | The lipid components include DPPC, DSPC, ethanol, and DSPE-PEG2000 in a proportion of 10:5:4:1. The hydrodynamic diameter of the LPs was 150 nm (PDI ≤ 0.1). Typical concentrations of Gadoteridol and DOX in LP suspensions were around 20 mM and 1.8 mM, respectively, or about 1 mg/mL. Encapsulated Gadoteridol and DOX had a molar ratio of around 11:1 | Analyze the theranostic effectiveness of nanomedicine that could provide MRI contrast in reaction to the local exposure to pulsed low-intensity non-focused ultrasounds (pLINFU) that cause the anticancer drug DOX to be released from LPs | [79] |

**Table 1** (continued)

| Liposomes carrier | Detection method | Cancer | Characteristics of liposomes | Explains | References |
|---|---|---|---|---|---|
| NB-PTXLps | Ultrasound imaging | Human BC and head and neck cancer | Producing nanobubble-paclitaxel LP (NB-PTXLp) complexes, measuring 528.7 ± 31.7 nm, for application in drug delivery and ultrasound-responsive cancer cell imaging. With a conjugation efficiency of around 98.7 ± 0.14% and an entrapment efficiency of 85.4 ± 4.39%, the 200 nm-sized LPs successfully produced conjugates with the nanobubbles. The physicochemical analysis of the NBs revealed that their hydrodynamic size, ζ-potential, and PDI were 320 ± 30.2 nm, 9.3 ± 1.47 mV, and 0.261 ± 0.07, respectively | When tested against the Mia-PaCa-2, Panc-1, MDA-MB-231, and AW-8507 cell lines under ultrasonic circumstances, NB-PTXLps demonstrated anticancer activity that was more than 300 times greater than that of the commercial formulation ABRAXANE. For the treatment of cancer, the NB-PTXLps may prove to be a useful and less invasive theranostic platform | [83] |

Further LP structures are now being created for the transportation of alternative medications. Liposomal anthracyclines have successfully achieved a high level of drug encapsulation, leading to notable anticancer effects while minimizing damage to the heart. This category includes liposomal daunorubicin and pegylated liposomal DOX, which have significantly extended circulation throughout the body. DOX has shown significant effectiveness in the treatment of BC, both when used alone and when combined with other chemotherapy drugs [106].

In addition to reduced severe adverse effects, novel LPs that have been modified with PEG, cationic lipids, and highly selective molecules exhibit enhanced stability, half-life, and selectivity. Nevertheless, novel LPs remain innocuous [107]. PEG deposited on the surface of LPs impedes drug-cancer cell interaction. Normal tissues are susceptible to oxidative injury and cytotoxicity caused by cationic LPs. To enhance the safety profile of liposomal pharmaceuticals, they must exhibit a high degree of selectivity towards cancerous tissues and cells, while simultaneously minimizing harm to healthy cells [108, 109] (Fig. 3).

Among gynecological malignancies, ovarian cancer has the second-highest death rate, according to one research. Researchers developed a new estrogen-targeted PEGylated LP loaded with PTX and oxaliplatin (ES-SSL-OXA/PTX). The SKOV-3 cell surface expresses the estrogen receptor (ER) in large quantities, and the LP was engineered to attach to this receptor specifically. The goal was to reduce side effects and increase the efficacy of SKOV-3 tumor treatment. ES-SSL-OXA/PTX was produced via thin-film hydration and seemed to have a stable spherical shape. The EE was determined using the HPLC technique, and the results showed that PTX had an EE of 65.85% and OXA of 44.10%. The mean particle size was 168.46 nm, and the polydispersity index (PDI) was 0.145 respectively. In vitro and in vivo targeting tests were used to confirm the optimum specific targeting capabilities of ES-SSL-OXA/PTX. On the other hand, ES-SSL-OXA/PTX showed improved anticancer effectiveness in both in vitro and in vivo environments, preventing SKOV-3 cell proliferation and tumor formation with an 85.24% tumor inhibition rate. ES-SSL-OXA/PTX's pharmacokinetic properties showed a longer half-life and a slower rate of elimination. A reduced toxicity profile was found in the preliminary safety evaluation of ES-SSL-OXA/PTX's acute and long-term toxicity. Based on the findings shown above, ES-SSL-OXA/PTX may offer a potentially innovative formulation for the treatment of ovarian cancer in future clinical studies [110].

Hypoxia constitutes a salient attribute of solid tumors and a significant contributor to radiotherapeutic resistance. Investigators demonstrated that hypoxic cell radiosensitizers may enhance the efficacy of radiotherapy; however, their limited dosing restricts their application in clinical settings. Researchers' approach involved encapsulating hypoxic cell radiosensitizers within temperature-sensitive liposomes (TSL). This will enable precise localization of the radiosensitizers within tumors while preventing their undesired accumulation in healthy tissues. The primary aim of this research is to fabricate and analyze TSL that has been infused with the radiosensitizer pimonidazole (PMZ). Researchers evaluated the in vitro efficacy of PMZ encapsulated in TSL and free PMZ when combined with radiation and hyperthermia (HT). The TSL–PMZ, which was created by actively loading PMZ into TSL at different drug/lipid ratios, was evaluated for its stability and physicochemical characteristics. PMZ release was assessed in fetal bovine serum at 42 °C and in HEPES buffered saline at 37 °C. FaDu cells were treated to different PMZ concentrations in a hypoxic environment before being subjected to ionizing radiation in order to ascertain the concentration-dependent radiosensitizing impact of PMZ. The clonogenic test for cell survival and histone H2AX phosphorylation for DNA damage were used to assess the efficacy of TSL–PMZ in combination with HT and radiation in vitro. At 4 °C and 20 °C, all TSL–PMZ formulations demonstrated excellent encapsulation efficiencies and sustained stability for 30 days. Rapid PMZ release was seen at 42 °C, regardless of the drug-to-lipid ratio. The effects of ionizing radiation were significantly enhanced as PMZ concentration rose. Compared to irradiation alone, cell mortality rose 14.3 times when preheated TSL–PMZ was applied in addition to radiation. According to the researchers' results, radiotherapy may be more effective in hypoxic situations when TSL–PMZ and HT are combined [111].

The objective is to develop an LP that is sensitive to NIR Light and contains DOX and hollow gold nanospheres (HAuNS). Researchers assessed how well this LP enhances anticancer activity and regulates medication release. The TSL formulation served as the basis for the creation of the LPs (DOX&HAuNS-TSL), which have hydrophobically modified HAuNS affixed to their membrane. The quick and repeated release of DOX is made possible by exposing the LPs (DOX&HAuNS-TSL) to an NIR laser. The combination of DOX&HAuNS-TSL and NIR laser irradiation demonstrated considerably better cytotoxicity against tumor cells when compared to treatments such as DOX&HAuNS-TSL alone (chemotherapy alone), DOX-TSL alone (chemotherapy alone), and HAuNS-TSL plus NIR laser irradiation (photothermal ablation, PTA, alone). Due to the simultaneous photothermal and chemotherapeutic action, an in vivo anticancer analysis revealed that the combination of

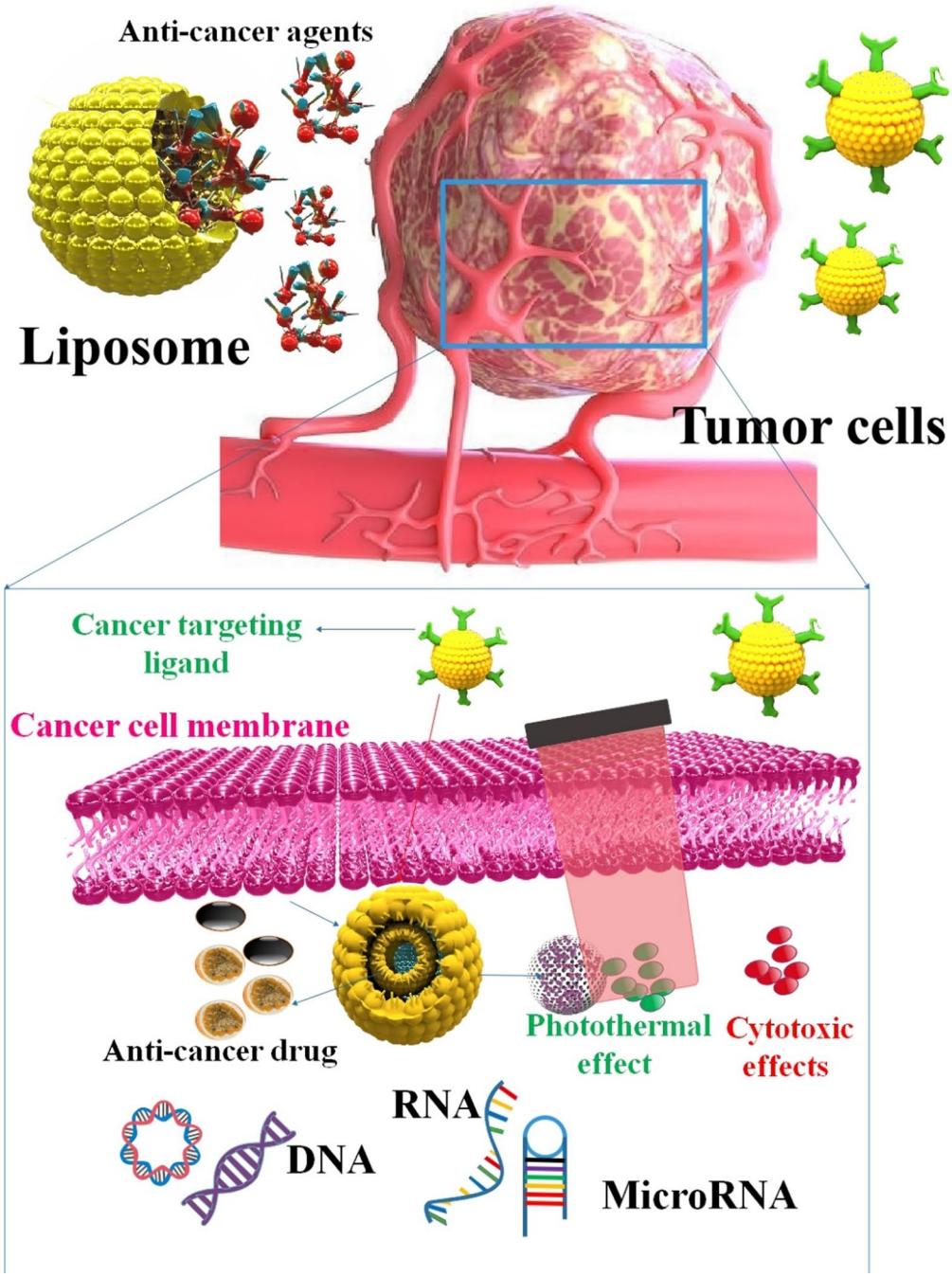


**Fig. 3** Liposomes have many advantages, such as improved encapsulated pharmaceutical pharmacokinetics, extended circulation times, and passive targeting and disposal in inflammatory and tumorous areas due to the enhanced permeability and retention (EPR) mechanism

DOX&HAuNS-TSL and NIR laser produced significantly better antitumor effectiveness when compared to the usage of HAuNS-TSL and NIR laser alone [112].

Using NIR laser irradiation, it would be easy to trigger the LPs' fast and repeated release of DOX (DOX&HAuNS-TSL). As compared to DOX-TSL alone (chemotherapy alone), HAuNS-TSL plus NIR laser irradiation (photothermal ablation, PTA, alone), and DOX-TSL alone (photothermal ablation, alone), the cytotoxicity of tumor cells treated with DOX&HAuNS-TSL followed by NIR laser irradiation was significantly higher. Research on tumors in living organisms has shown that

a combination of photothermal and chemotherapeutic effects produced by DOX&HAuNS-TSL with NIR laser irradiation is much more successful in killing tumors than each method alone. Create multi-functional nanoplatforms with a core-interlayer-shell architecture using MSNs@CaP@PEGylated LPs. In addition to improving NPs cellular absorption and pH-triggered controlled drug release, in vitro studies showed that calcium phosphate (CaP) might promote cell death by creating high osmotic pressure in endo/lysosomes. Additionally, the photosensitizer ZnPc aided the chemotherapy with DOX and PDT. In addition, the MSNs@CaP@PEGylated LPs showed incredible tumor-targeting capacity via the EPR effect [113].

Natural killer (NK) cells are an appealing therapeutic target for stopping the illness from spreading to the lymph nodes since their activity is a strong predictor of a favorable outcome in cancer patients. Researchers created LPs that include the apoptotic ligand TRAIL to cause cancer cell death and are connected to anti-CD335 antibodies to target NK cells precisely. In order to produce LPs with a diameter of around 100 nm, a thin film hydration process was used, followed by extrusion. The thiol-maleimide click chemistry was then used to conjugate the proteins to the LPs. The segregated NK cells successfully bind to the TRAIL/anti-CD335 LPs. Compared to NK cells alone, these "Super Natural Killer Cells" were more effective in killing metastatic COLO205 CRC cells and oxaliplatin-resistant SW620 cells by TRAIL-mediated apoptosis when adhered to the surface of NK cells. Importantly, when exposed to the typical levels of fluid shear stress seen in the lymphatics, Super NK cells demonstrated increased effectiveness. The distribution of LPs inside the body was investigated after intravenous administration. For at least four days, LPs were shown to be present in the spleen and tumor-draining mesenteric lymph nodes. Investigators indicated that NK cells equipped with liposomal TRAIL have increased apoptotic effects on CRC cells that are clinically significant. This lays the foundation for further research on the therapy of CRC in mice models [114] (Table 2).

LP biocompatibility, adjustable characteristics, and the ability to load hydrophilic and hydrophobic chemicals are just a few of the many benefits that make them ideal drug delivery vehicles. Despite their clinical relevance and therapeutic potential, there is currently a lack of information on the risks of LP administration. The fact that cationic LPs, which are often used for the transport of nucleic acids, have the potential to be harmful to macrophages and decrease the production of crucial immunomodulators is a significant cause for toxicological worry. Furthermore, after being injected intravenously, LPs are captured in the MPS organs, including the liver and spleen. This leads to toxicity in these organs, which in turn depletes cells that are essential for the immune system to function correctly. LPs can activate the immune system by triggering an inflammatory response. This reaction is marked by the secretion of cytokines that are pro-inflammatory and produced by monocytes. It has also been shown that LPs activate the complement system; however, the extent to which this occurs depends on many parameters, including size, charge, and mol% of cholesterol, among others. When pegylated liposomal formulations stimulate B cells to produce PEG antibodies, another significant immune activation mechanism happens: the anti-PEG response. Because of this, the immune system is able to identify and eliminate the threat. Actually, the stealthiness of pegylated LPs is rendered useless after many doses due to their faster blood clearance. This further supports the notion that avoiding early clearance and maximizing the therapeutic advantages of each injection requires meticulous optimization of the dosage of liposomal drugs. LPs have the potential to cause hypersensitive responses, such as cardiac distress, depending on the rate of injection. When it comes to therapeutic uses of liposomal formulations, the mode of distribution and time of administration are crucial factors to consider. Concerns about LPs originate from their potential to activate the immune system and cause harm to healthy tissues. LPs have the potential to bring about novel, as-yet-unknown toxicities, but they are also an appealing tool for reducing the dose-limiting adverse effects of treatments in patients [115].

## Liposomes as a theranostic agent in cancer

Therapeutic and diagnostic agents are essential for the early diagnosis and treatment of illnesses. Another effective tactic is to combine the diagnostic and therapeutic chemicals into one system so that treatment and detection may happen simultaneously [116]. To achieve these goals, it is critical to develop theranostic systems characterized by exceptional stability and targeting capabilities while also guaranteeing the absence of interference between different therapeutic and diagnostic agents within the system [117]. Of all the nanocarrier types that have been studied so far, LPs continue to be one of the most promising systems for clinical use [118]. In clinical investigations, the pharmacokinetics and biodistribution of theranostic agents within LPs are superior to those of numerous alternative carriers due to the LPs' inherent advantages, which include biocompatibility, high stability in biological environments, and high agent-loading efficiency [119]. Consequently, LPs have emerged as one of the most effective delivery methods for the identification and management of several illnesses. There is a lot of interest in using LPs as nanocarriers for theranostic

**Table 2** Liposome in cancer treatment

| Liposomes | Treatment agents | Cancer type | Characteristics of liposomes | Explain | References |
|---|---|---|---|---|---|
| PEGylated LP | ES-SSL-OXA/PTX | Ovarian cancer (SKOV-3 tumor) | The thin film hydration approach was used to create ES-SSL-OXA/PTX, which displayed a homogeneous spherical shape. According to the HPLC technique, the EE for OXA was 44.10%, and for PTX, it was 65.85%. The average particle size was 168.46 nm, and the PDI was 0.145. Research on the targeting capabilities of ES-SSL-OXA/PTX in both living organisms and laboratory settings has shown that it is very effective | Researchers created a novel estrogen-targeted PEGylated LP (ES-SSL-OXA/PTX) loaded with PTX and oxaliplatin. With an 85.24% tumor inhibition rate, ES-SSL-OXA/PTX demonstrated enhanced anticancer efficacy in both in vitro and in vivo settings by inhibiting the growth of SKOV-3 cells and the development of tumors | [110] |
| TSL | Combination of DOX&HAuNS-TSL and NIR laser | Human liver carcinoma | When comparing OMP-HAuNS with OMP alone, the faint characteristic peak of the hydrosulfide group at 2500 $cm^{-1}$ ~ 2900 $cm^{-1}$ vanished entirely. This indicates that the -SH group in OMP converted to -S–Au. The charge on HAuNS was negative, measuring 49.6 mV. The OMP-HAuNS ζ-potential was almost neutral after the alteration. According to DLS, the average diameter of the blank TSL was 102.7 nm. The average diameter of DOX&HAuNS-TSL, as measured by DLS, grew dramatically to 154.8 nm as a result of the encapsulation of DOX and HAuNS | When the LPs (DOX&HAuNS-TSL) are exposed to an NIR laser, DOX may be released quickly and repeatedly. Due to the combined photothermal and chemotherapeutic activity, an in vivo anticancer evaluation revealed that resulted in considerably greater antitumor effectiveness compared to the use of HAuNS-TSL and NIR laser alone | [112] |
| Core-interlayer-shell MSNs@CaP@PEGylated LPs | Enhanced Synergetic Chemo-Photodynamic Therapy | HeLa cells | The core particles of the MSNs were synthesized using the standard base-catalyzed sol–gel process using a hexadecyl trimethyl ammonium bromide (CTAB) template. The size and ζ-potential of MSNs@CaP@PEGylated LPs are 122 ± 5 nm and 17.1 ± 2.7 mV, respectively | In vitro studies suggested that CaP may enhance NP cellular absorption and offer pH-triggered, regulated drug release. Still, it may also raise endo/lysosome osmotic pressure, which may lead to cell death. The photosensitizer ZnPc also facilitated the chemotherapy with DOX and PDT. Additionally, by the EPR effect, the MSNs@CaP@PEGylated LPs demonstrated exceptional tumor-targeting capabilities | [113] |
| TRAIL/anti-CD335 LPs | Natural killer (NK) cells | Colorectal cancer (CRC) | The LPs were made via a thin-film hydration method and then extruded to a diameter of around 100 nm. With no changes in polydispersity, the size increased from 109.3 ± 2.1 to 122.5 ± 2.9 nm, confirming the successful conjugation of anti-CD335 and TRAIL | These "Super Natural Killer Cells" adhered to the surface of NK cells and were more successful than NK cells alone in inducing TRAIL-mediated apoptosis in oxaliplatin-resistant SW620 cells and metastatic COLO205 CRC cells. NK cells provide a promising therapeutic target to prevent disease transmission to the lymph nodes | [114] |

applications because of their capacity to contain a broad range of therapeutic and diagnostic substances [89, 120].

For instance, the objective of the Muthu et al. study was to create a novel category of multifunctional (theranostic) LPs coated with d-alpha-tocopheryl PEG 1000 succinate mono-ester (TPGS). These LPs would comprise qDs and docetaxel and be utilized for cancer imaging and therapy. Utilizing the solvent injection method, both non-targeting and folate receptor-targeting theranostic LPs were fabricated. These LPs were then assessed for the following characteristics: drug EE, particle size, polydispersity, ζ-potential, and surface chemistry. As an in vitro model, folate receptor overexpressing MCF-7 BC cells were utilized to evaluate the cellular uptake and cytotoxicity of QDs-loaded LPs and the drug. It was determined that the mean particle sizes of the non-targeting and targeting LPs were 210 and 202 nm, respectively. FETEM, or field emission TEM, verified the existence of QDs in the hydrophobic membranes of the LPs' peripheries. Contrascal laser scanning microscopy was utilized to observe the qualitative internalization of multifunctional LPs by MCF-7 cells. The 50% inhibitory concentration (IC50) value, denoting the drug concentration required to induce 50% cell death within a specified time interval, was determined to be 9.54 ± 0.76 μg/ml for the commercial Taxotere®, 1.56 ± 0.19 μg/ml for the non-targeting LPs, and 0.23 ± 0.05 μg/ml for the targeting LPs, following a 24-h culture period with MCF-7 cells. The targeting of LPs in vitro drug release is different from the non-targeting LPs. One possible explanation for the increased percentage or rate of drug release from targeted LPs might be the effect of DSPE-mPEG-FA on their surface. Because the exposed PEG chains on the TPGS-coated and TPGS/DSPE-mPEG-FA LPs had different molecular weights, the drug release kinetics of the two types of LPs varied. While DSPE-mPEG-FA had a molecular weight of 2000, TPGS had a molecular weight of 1000 for its hydrophilic portion. The results demonstrated that the drug release rate was slower for DTX-QD LPs compared to DTX-QDFA because the former were more hydrophobic. The combination of DSPE-mPEG-FA and TPGS in DTX-QDFA LPs resulted in a more significant percentage and quicker rate of drug release compared to TPGS alone in DTX-QD LPs. This was owing to the hydrophilic component of DSPE-mPEG-FA having a more substantial solubilization impact. The efficacy of targeting multifunctional LPs was found to be superior to that of non-targeting LPs, indicating significant potential for enhancing cancer imaging and therapy [121].

Luminescence probes for live cell imaging were developed and used by researchers as new imaging agents. These agents were folate receptor (FR)-targeted LPs enclosing hydrophilic CdTe QDs. The FR-targeted QD LPs were created by wetting the lipid thin film with CdTe solution, and hydrophilic CdTe QDs were immediately generated in the water phase. Liposomal particle size, ζ-potential, fluorescence, and ultraviolet (UV)-visible tests were used to describe the formulations. Researchers used the HeLa human uterine cervix cancer cell line to study the targeting and imaging capabilities of FR-targeted LPs. Additionally, HeLa cells were used to assess the cytotoxicity of QD LPs by incubating them with FR-targeted, nontargeted, and free QDs. A spherical FR-targeted QD LP exhibited excellent photochemical stability, effective cancer targeting, little cytotoxicity, and high fluorescence production, as shown by the researchers. The size range of FR-targeted fluorescent LPs was relatively narrow, and their average size was about $10^5$ nm. There was no evidence of QD leakage or change in size after 11 months of storage at 4 °C for QD LPs. An appealing probe for tumor cells or tissue imaging for long-term monitoring might be FR-targeted CdTe QD LPs, which can target tumor cells via FR-mediated endocytosis [122].

According to different research, ruthenium coordination complexes may provide new cancer treatment options. Effective tumor accumulation, however, poses a significant obstacle to their clinical use. Researchers created a LP-based theranostic nano delivery system for (Ru(phen)2dppz)($ClO_4$)2 (Lipo-Ru). The dynamic light scattering (DLS) and Transmission Electron Microscopy (TEM)images showed that the NPs were bilayers with an average size of 82.53 ± 2.66 nm. Since the liposomal encapsulation maintained the metal-to-ligand charge transfer (MLCT) peak, absorption tests of Lipo-Ru did not reveal a wavelength change. The fluorescence intensity of the non-fluorescent Ru-complex reduced in a time-dependent way after incubating Lipo-Ru with Triton X-100, which breaks down the bilayer structure since the complex became fluorescent after being encased in the lipid bilayer. Past research on the rate of lipid bilayer solubilization after prolonged exposure to Triton X-100 in LPs has shown this to be possible. When integrated into the hydrophobic lipid bilayer of the delivery vehicle or the DNA helix, this ruthenium polypyridine complex generates a robust fluorescent signal that makes the therapeutic drug visible in tumor tissues. When Lipo-Ru is added to MDA-MB-231 BC cells, double-strand DNA breaks are produced, which in turn causes apoptosis. Lipo-Ru therapy significantly slowed the development of tumors in a mouse model of triple-negative BC. Studies on the biodistribution of Lipo-Ru showed that the tumor accumulated over 20% of the injected dosage. To determine whether Lipo-Ru may accumulate in tumor tissue after intravenous treatment, researchers used an orthotopic mouse model of MDA-MB-231 human BC. When comparing the Lipo-Ru group to the

Ru group in whole-body pictures taken with the IVIS-200 system, it was found that the tumor signal was significantly amplified in the former. Tumor tissue slices taken 2 h after Lipo-Ru injection showed distinct fluorescent patches. Additionally, two hours after injection, the IVIS-200 imaging equipment was used to observe the buildup of Lipo-Ru in the tumor, liver, kidneys, spleen, heart, and lungs. The liver and tumor were the primary sites of Lipo-Ru particle accumulation (34% and 30% of the injected dosage, respectively). The LP group showed a significant increase in intratumoral Ru deposition. The increased permeability and retention (EPR) effect, a result of the specific features of tumor vasculature, is probably responsible for the increased buildup of Lipo-Ru particles in tumor tissue. To be more specific, tumor blood vessels are very disordered, multiply quickly, and create a gaping hole, leading to the creation of openings smaller than 600 nm that allow NPs to get in. Also, LP buildup in the MPS is reduced because the PEG chains of Lipo-Ru decrease absorption by macrophages. These findings imply that Lipo-Ru may be a viable theranostic platform for cancer research [123].

According to different research, a potential approach to cancer treatment is the simultaneous integration of effective therapeutic medicines, adjustable drug delivery vehicles, and US imaging contrast ants into a single theranostic nanoplatform. Researchers created a 2,2′-azobis(2-(2-imidazolin-2-yl)propane)dihydrochloride (AIPH)-loaded LP (Lip-AIPH), when exposed to ultrasound (US) radiation, may simultaneously produce gas bubbles and a high concentration of reactive oxygen species (ROS). Results from in vivo experiments verified that the produced gas and alkyl radicals were not reliant on oxygen production and could be effectively used for SDT and synergistic gas treatment in a hypoxic tumor microenvironment. More significantly, the produced gas bubbles significantly improved the US contrast to direct cancer treatment when used as a potent US contrast agent. Furthermore, the Lip-AIPH displayed clear US contrast signals, with the echo strength progressively rising as the US irradiation duration increased. A substantial increase in contrast under US imaging was achieved because microbubbles created a significant acoustic impedance mismatch between the gas bubbles and the surrounding medium. As a result of the gas bubbles produced by Lip-AIPH, the average grey values of the US picture jumped from 12.7 to 53.0, a 4.2-fold increase compared to the PBS and blank LP groups, which exhibited no discernible change. Also, throughout the irradiation period, Lip-AIPHs exhibited fast signal amplification, as shown by the rate constant for signal amplification following US irradiation. The LP demonstrated increased US imaging and improved anticancer activity as a US-activated theranostic drug. It may hold promise for US imaging-guided hypoxic tumor treatment with deep tissue penetration [124].

The investigation of Kim et al. involved the practical synthesis of melanin@PFH@5-FU-LPs via thin-film hydration. The dimensions of the spherical shape were 209.6 ± 4.3 nm. In response to NIR irradiation, melanin@PFH@5-FU-LPs demonstrated efficient heat generation by the intrinsic photothermal properties of melanin. Due to the light-to-heat conversion of melanin in the LP, PFH vaporized significantly, resulting in the formation of bubbles. The rate at which 5-FU was released from the melanin@PFH@5-FU-LP increased immediately in a sequential fashion due to the photothermal effect. Researchers tested the drug release behavior of melanin@PFH@5-FU-LPs with and without NIR laser irradiation, which is caused by the photothermal effect of melanin and causes bubble production of PFH. For this experiment, the melanin@5-FU-LP and melanin@PFH@5-FU-LP were placed in disposable cuvettes and exposed to an 808 nm NIR laser with a power density of 1.5 W/cm2 for 10 min. Following that, a dialysis bag (MWCO 12,000 Da) was used to hold each solution. The bags were then submerged in 5 ml of PBS and put in a water bath that was set at 37°C. The drug's absorbance was measured at a wavelength of 265 nm using a UV-spectrophotometer (T60U, PG Instruments Limited, UK). Ultrasound imaging contrast was enhanced as a result of the formation of bubbles caused by NIR laser exposure. Furthermore, a CRC mouse model was developed by the researchers to validate the in vivo accumulation and temperature increase of melanin@PFH@5-FU-LP. Researchers were also able to obtain ultrasound images caused by bubble generation under laser irradiation following intravenous injection of melanin@PFH@5-FU-LP via the mouse tail vein. At 1, 4, and 12 h post-injection of melanin@PFH@5-FU-LPs, the contrast signal at the tumor location was markedly amplified by laser irradiation. Four hours after injection, the bubbles' contrast-enhancing effects at the tumor location were at their peak. The heat produced by the melanin@PFH@5-FU-LP, when exposed to NIR laser radiation, can effectively kill cancer cells, thus effectively impeding the development of tumors. The increased permeability and retention (EPR) effect is responsible for the accumulation of Melanin@PFH@5-FU-LPs in tumor tissues. The melanin@PFH@5-FU-LP was determined to be safe for future in vivo assessment based on cell cytotoxicity data obtained in vitro. Nano-sized compounds can concentrate at tumor locations using the EPR effect. By monitoring the local temperature increase at the injection site after laser irradiation, one may anticipate the successful accumulation of melanin@PFH@5-FU-LP in tumor tissues. After around 4 h,

the maximum accumulation of LPs in the lesion after intravenous injection occurs, albeit this is dependent on physicochemical properties, including surface charge and particle size. Researchers' findings indicated that the melanin@PFH@5-FU-LP has the potential to serve as an appealing agent in the context of photothermal tumor therapy and ultrasound imaging [125].

The difficult objective in an investigation is to design a nanotheranostic agent with higher concentration in solid tumor microenvironment and more excellent picture resolution. Researchers developed a light-mediated photo-triggered approach to improve nanohybrid tumor accumulation. NFGL is the name of a designed multifunctional LP-based nanotheranostics filled with emissive GQDs and AuNPs. To further demonstrate phototriggered chemotherapy, DOX hydrochloride was encapsulated in NFGL and functionalized with ligands that target folic acid. Because encapsulated drugs are emissive and have high contrast, they demonstrated imaging bimodality for in vivo tumor diagnosis. Due to heat and ROS produced, targeted NFGL nanohybrids showed tumor decrease mediated by NIR light (NIR, 750 nm). Furthermore, NFGL nanohybrids showed exceptional ROS scavenging capacity in comparison to GQD-loaded LPs, which was confirmed by anticancer research. Therefore, this strategy and designed system may provide a new path for cancer treatment and targeted imaging [13] (Table 3).

The presence of hypoxia in the tumor microenvironment is a significant barrier to employing PDT to treat cancer, and Liu and colleagues set out to address this issue in their work. In order to overcome this obstacle, the researchers use Synechococcus 7942 (Syne), a photosynthetic bacterium, to enhance PDT. This is achieved by creating a biomimetic system called S/HSA/ICG, in which the Syne surface is stably linked to HSA/ICG NPs, which are NPs that encapsulate ICG inside human serum albumin (HSA). Using Syne's photosynthetic capacity in conjunction with HSA/ICG's medicinal properties is a novel strategy. When subjected to laser irradiation, S/HSA/ICG builds up within tumors in tumor-bearing mice and continually creates oxygen via photosynthesis, resulting in a substantial quantity of oxygen and the generation of ROS with photodynamic features. This oxygen production relieved the hypoxic conditions within the tumor while also reversing the immunosuppressive microenvironment. Enhancing tumor hypoxia increased ICG's efficacy in PDT and activated immunogenic cell death (ICD), which in turn generated an immunological response against the tumor. Researchers showed that the administration of HSA/ICG NP-coated Syne (S/HSA/ICG) led to synergistic suppression of both local and metastatic tumors in a mouse model of 4T1 mTNBC. This process eliminates initial tumors by effectively reducing tumor hypoxia and increasing ROS production [126, 127].

Encapsulating active, water-soluble drugs in the hydrophilic core and insoluble drugs in the hydrophobic membrane, nanosized LPs can be made of a variety of natural lipids, the most common of which are phospholipids and cholesterol. This allows for the targeted and controlled delivery of therapeutic agents, which improves the ADME (adsorption, distribution, metabolism, and excretion) process, resulting in maximum efficacy with minimal side effects. Both active and passive targeting may be achieved by targeted ligand conjugation and increased permeability and retention (EPR). Traditional LPs have a few significant flaws, however, including instability, inadequate drug loading, rapid drug release, and a short blood circulation duration. When the immune system detects LPs, macrophages will destroy them. So, at the tail end of the 1980s, scientists achieved a significant breakthrough in LP research with the introduction of stealth LPs. These were long-circulating LPs that were stabilized in the blood by PEGylation. Placing a bioactive molecule or polymer into polyethylene glycol (PEG) to increase its stability, permeability, and solubility was the original definition of PEGylation. PEGylation is now among the most advanced techniques used in the pharmaceutical industry. Scientists hypothesized that the lengthy PEG chain covering the LP surface efficiently decreases LP aggregation in plasma by preventing the adsorption of plasma protein onto the surface. This phenomenon is known as the excluded volume effect. Micelles, LPs, and polymeric NPs are just a few examples of nanocarriers that have recently had PEGylation applied to them. LPs may remain in the bloodstream for longer thanks to PEGylation, which delays their detection and clearance by the immune system. A solid tumor's intrinsically leaky vasculature and inadequate lymphatic drainage may also cause stealth LPs to passively collect in the tumour [128].

In (i) solid tumor cancer theranostics, (ii) image-guided therapies, and (iii) combination therapeutic applications, nanosized LPs are clinically validated methods for delivering several therapeutic and imaging agents to the target areas. The designed system's theranostics property may be impacted by the diagnostic and treatment choices made. However, their overall theranostics efficacy may be jeopardized if imaging and treatment probes are integrated into lipid self-assembly "LPs." However, liposomal systems have many drawbacks, including site-selective tumor targeting, particular biodistribution, premature cargo molecules leaking before reaching the target site, and their fragile nature. To address the problems mentioned above, a variety of engineering techniques have been studied,

**Table 3** Utilizing liposome as a theranostic agent in cancer

| Liposomes | Cancer | Detection agent and methods | Treatment agent | Characteristics of liposomes | Theranostic explain | References |
|---|---|---|---|---|---|---|
| Therapeutic LPs with d-alpha-tocopheryl PEG 1000 succinate mono-ester coatings | MCF-7 breast cancer (BC) cells | QDs laser scanning microscopy | Docetaxel | The population standard deviations of the non-targeted LPs (DTX-QD) and the targeting LPs (DTX-QDFA) batches were 202.3 ± 0.3 and 210.5 ± 0.6 nm, respectively, when produced using the solvent injection technique. The drug encapsulation efficiencies of DTX-QD and DTX-QDFA multi-functional LPs were 50.53 ± 0.34 and 54.18 ± 0.62%, respectively. The QDs encapsulation efficiencies of non-targeting multifunctional LPs and targeting multifunctional LPs were found to be 23.97 ± 0.41 and 22.10 ± 0.70%, respectively | Both non-targeting and folate receptor-targeting theranostic LPs were produced by using the solvent injection approach. Targeting multifunctional LPs was shown to be more effective than non-targeting LPs, suggesting great potential to improve cancer imaging and treatment | [121] |
| Theranostic nanodelivery method based on LPs for (Ru(phen)2dppz)(ClO4)2 (Lipo-Ru) | MDA-MB-231 BC | DNA binding and delivery of Ru-complexes fluorescent emission | Lipo-Ru therapy | The Ru-complex was then encapsulated using LPs composed of DPPC, cholesterol, and distearoyl phosphatidylethanolamine (DSPE)-PEG. The NPs typically have an average size of 82.53 ± 2.66 nm. Compared to empty LPs, Lipo-Ru was somewhat smaller and had a much greater ζ-potential | When incorporated into the DNA helix or the hydrophobic lipid bilayer of the delivery vehicle, this ruthenium polypyridine complex produces a strong fluorescence signal that reveals the therapeutic medicine inside tumor tissues. Upon the addition of Lipo-Ru to MDA-MB-231 BC cells, double-strand DNA breaks result, and these breaks ultimately lead to apoptosis | [123] |
| Lip-AIPH is a LP loaded with 2,2′-azobis(2-(2-imidazolin-2-yl)propane)dihydrochloride | Hypoxic tumor | Lip-AIPH Ultrasound imaging | Lip-AIPH | AIPH, lipid 1, 2-dipalmitoyl phosphatidylcholine, amphiphilic PEGylated phospholipids, and cholesterol were self-assembled to load AIPH into the LPs. TEM scans showed that the LP shell had been destroyed and that the size distribution had changed from 100 to 80 nm | As a US-activated theranostic medication, the LP exhibited enhanced US imaging and better anticancer efficacy. It could be helpful for deep tissue penetration hypoxic tumor therapy guided by US imaging | [124] |

**Table 3** (continued)

| Liposomes | Cancer | Detection agent and methods | Treatment agent | Characteristics of liposomes | Theranostic explain | References |
|---|---|---|---|---|---|---|
| Melanin@PFH@5-FU-LP | CT-26 tumor-bearing mice | 5-fluorouracil (5-FU) Ultrasound imaging | Perfluorohexane (PFH) | The thin film approach was used to create Melanin@PFH@5-FU-LPs using a previously described protocol. Without the addition of PFH, the typical dimensions of melanin@5-FU-LPs were 148.1 ± 7.5 nm. It was verified that the spherical form of the melanin@PFH@5-FU-LPs was due to the presence of an internal PFH emulsion. Within the LP, 5-FU had a loading efficiency of 56.3 ± 4.3% and melanin 57.9 ± 0.1% | Researchers suggested that the melanin@PFH@5-FU-LP, as a desirable agent, may benefit photothermal tumor treatment and ultrasound imaging | [125] |

including grafting, conjugation, encapsulation, etc. It has been shown that surface-engineered LPs have improved tumor selectivity, retention, and therapeutic efficacy in solid or cell tumors. It should be noted that many other parameters, such as repeatability, stability, smooth circulation, the toxicity of vital organs, patient compliance, etc., must be taken into account before administering liposomal theranostics medications in solid tumors or clinical models [22].

## Engineering and properties of exosome-liposome hybrid

DDS are increasingly reliant on intelligently engineered and naturally derived nanovesicles that can deliver bioactive molecules and medications into specific cells and tissues. LPs are distinguished from other varieties of self-assembled nanovesicles by their amphiphilic characteristics and lack of toxicity. Substantially releasing their contents, LPs can acquire stimulus responsiveness by modifying their surfaces. In recent years, EXOs have been increasingly utilized as intelligent delivery systems due to their capacity to diffuse through tissues and locate target cells, as well as their recognized function in cell–cell communication. Furthermore, the development of "smarter" delivery systems can be accomplished through the membrane fusion of HE-LP nanocarriers. By incorporating these systems into hydrogels derived from natural sources, one can attain controlled and sustained drug delivery [129]. EXOs are a valuable biomaterial for creating cutting-edge DDS that operate as unique nanocarriers. Researchers fused the membranes of EXOs with LPs using the freeze–thaw technique to create hybrid EXOs (HEs), which allowed them to regulate and alter the functionality of exosomal nanocarriers [130, 131]. The integration of genetic modification techniques with membrane engineering technologies is confirmed by the fusing of EXOs contained in a specific membrane protein derived from genetically modified cells with various LPs [132]. Research on how HEs are absorbed by cells has shown that changing the lipid makeup or properties of the exogenous lipids may change how the cells and the produced EXOs interact [133]. It has been demonstrated that genetic alteration methods may be combined with membrane engineering techniques. Different LPs were coupled with EXOs implanted with a specific membrane protein generated from genetically engineered cells. Changing the lipid composition or properties of the exogenous lipids may change the interactions between the produced EXOs and cells, according to research on the cellular absorption of HEs. Researchers implied that the membrane-engineering method provides a fresh way to create EXOs with well-thought-out designs that function as hybrid nanocarriers for application in cutting-edge DDS [133].

A novel drug delivery nanoparticle called MFHE is developed by merging EXOs and LPs using different membrane fusion procedures. These NPs combine the advantages of both types of DDSs. Minimal EXO immunogenicity and strong biocompatibility are added benefits of MFHEs, which already have excellent stability, a high drug loading rate, and can be easily surface-modified [24]. Research into modified EXOs has progressed to the point that they are considered essential biomaterials for the creation of cutting-edge DDSs. Researchers created a HE system by combining EXOs from mesenchymal stem cells (MSCs) with LPs that target folate. Cellular uptake tests were used to examine the efficacy of EXO nanocarriers in delivering the first-line chemotherapeutic medication PTX to tumor cells in vitro, and the goal was to enhance their drug loading capacity and target modification. The therapeutic effectiveness of HEs loaded with PTX (ELP) was also evaluated in vivo investigations utilizing a CT26 tumor-bearing animal model. Research on cellular absorption found that ELP was more effective than other methods in delivering drugs to tumor cells in laboratory settings. The poor drug-carrying ability of EXOs is a significant barrier to their therapeutic usage. By using HPLC, the PTX loading contents (LC) in both Exo and EL were ascertained. Researchers showed that EL's PTX carrying capacity was 2.2% LC, which was much more than Exo's capability of 1.0% LC. During four weeks at 4 °C, the surface ζ-potential and particle sizes of Exo, LP, and hybrid exosomes fusing with liposomes (EL) were measured. With almost little change to EL, the average Exo particle size jumped from 85.4 nm to 126.9 nm. In a 10% FBS medium, there was no discernible difference in the EL particle sizes. Researchers created HE vesicles that showed high stability, according to these data. After that, researchers evaluated EL's safety in a laboratory setting. After 24 h of incubation with varying doses of LP, Exo, and EL, the cell viability was measured. The positive charge of the LPs group may explain its considerable cytotoxicity at 500 μg/mL, yet at the same dose, Exo and EL demonstrated cell survival rates of over 90%. The findings of the hemolysis test were also in agreement. For 2 h, erythrocytes were incubated with different doses of Exo, LP, and EL. Significant hemolysis was seen in the sole LPs group at 500 μg/mL, but no hemolysis was observed in the Exo and EL groups. Researchers demonstrated that in comparison to LP, HE vesicles exhibited superior safety. In addition, the in vivo studies showed that ELP considerably reduced tumor development in the mouse model with CT26 tumors. Specifically, investigators investigated the tumor microenvironment for the first time after intratumoral ELP delivery. Researchers'

results showed that ELP administration increased the number of activated CD4 + and CD8 + T cells, decreased the number of regulatory T cells (Tregs), and polarized tumor-associated macrophages (TAMs) towards the M1 type. Researchers demonstrated that ELP has significant therapeutic effectiveness and suggest that it may be used in cancer treatment in the future. There is great hope for the future of efficient cancer treatment tactics thanks to the creation of HEs, which provide a novel way to improve drug delivery and regulate the tumor microenvironment [134].

Several factors should be considered when choosing a membrane fusion technique, including but not limited to biological activity, operability, fusion efficiency, and drug loading efficiency. Physical and chemical techniques are the two principal classifications of membrane fusion methods. LPs are frequently laden with pharmaceuticals via freeze–thaw processes. By generating ice crystals, water-soluble compounds can be introduced into the LPs through a momentary rupture of the plasma membrane [24, 135]. In research, thermosensitive LPs (TSL) and gene-engineered EXOs were combined to create hybrid therapeutic nanovesicles that combined immunotherapy with PTT for cancer treatment. After three cycles of freeze–thaw, the researchers combined the genetically modified EXOs with heat-sensitive LPs at a ratio of 1:1 to produce EXO-LP hybrid NPs. This synthetic approach demonstrated a fusion efficiency of up to 97.4%. To accomplish both homologous targeting and an extended in vivo circulation period via CD47 blockage, CT26 cells underwent genetic transfection to produce EXOs that were overexpressed in CD47 and fused with TSL. The hybrid nanovesicles that were made were dubbed hGLV. Next, researchers created the I/R@hGLV loading mixture, which included the photothermal agent ICG and the immunological adjuvant R837. The in vitro cellular cytotoxicity and photothermal impact of this mixture were assessed. In addition, the expression of DAMPs, such as ATP, HMGB1, and CRT, was measured to ascertain the ICD produced by PTT. Scientists also investigated the maturation of DCs, the anticancer efficaciousness in vivo, the biodistribution of hGLV in mice models carrying CT26 tumors, and the macrophage-mediated phagocytosis of tumor cells after treatment with hGLV. Investigators' research suggests that hybrid nanovesicles that target CD47 immune checkpoint inhibition may have promise for drug delivery in the treatment of cancer [136]. Membrane fusion is an endogenous process that is facilitated by the physicochemical constituents of vesicles. HEs are generated via electrostatic or hydrophobic interactions, wherein the vesicle contents remain undisturbed, and the lipid bilayer remains intact. By incubating HEK293FT cell-derived EXOs with CRISPR/Cas9-expressing LPs at 37 °C for 12 h, Lin et al. generated HEs. Researchers introduced a novel concept for the efficient and secure delivery of the CRISPR-Cas9 system. This process causes minimal harm to vesicles and pharmaceuticals. However, fusion efficiency is comparatively modest [24, 137].

Klaus Arnold and colleagues demonstrated thirty years ago that the PEG's ability to promote cell–cell fusion was not caused by solubilization, cross-linking, surface absorption, or any other of these processes. Rather, PEG operated only via volume exclusion, causing an osmotic force to press membranes together in a dehydrated area. A variety of physical measures and the use of detergents based on PEG that integrate into membranes, together with this straightforward discovery, led to the development of numerous significant fields of study. One such field is the use of PEG to contact membranes to thoroughly explore the function of various lipids and fusion proteins in membrane fusion [138]. Adjuvant-functional LPs are employed to transport biomolecules, including proteins, which are frequently susceptible to the demanding conditions encountered during liposomal preparation procedures. Without requiring an additional technique for size reduction, the objective of the present investigation is to prepare polymer-grafted HLs via the aqueous heat method. LPs were synthesized by combining two distinct lipids possessing adjuvant properties—dimethyldioctadecylammonium (DDA) and D-(+)-trehalose 6,6′-dibehenate (TDB)—with the amphiphilic block copolymer poly(2-(dimethylamino)ethyl methacrylate-b-poly(lauryl methacrylate) (PLMA-b-PDMAEMA)—to achieve this objective. To facilitate comparison, PAMAM dendrimer generation 4 (PAMAM G4) was also employed. Preliminary investigations were conducted utilizing differential scanning calorimetry (DSC). Utilizing light scattering and cryo-TEM, the physicochemical properties and morphological attributes of the prepared HLs were assessed. Following that, in vitro investigations into nanotoxicity were conducted. Protein loading experiments were conducted using bovine serum albumin to assess the efficiency of their encapsulation. Based on the findings, the incorporation of PDMAEMA-b-PLMA into the lipid bilayer was effective, resulting in enhanced morphological and physicochemical properties as well as the capacity to transport greater quantities of protein cargoes than pure DDA: TDB LPs, all while maintaining the biocompatibility profile unaffected. In conclusion, protein delivery via polymer-grafted HLs can be accomplished via the aqueous heat method without the need for additional size reduction procedures [139].

The process of simultaneously extruding LPs and EXOs under physical pressure via membrane holes of a regulated size to create mixed vesicles is known as the

membrane extrusion technique. The benefit of membrane extrusion over freeze–thaw and incubation techniques is a more consistent particle size for the hybrid vesicles. To treat pulmonary fibrosis, Sun et al. created hybrid nanovesicles using fibroblast-derived EXOs and clodronate-loaded (CLD) LPs. After combining L-929 fibroblast-derived EXOs with a synthetic LPs solution at a protein equivalent ratio of 1:5, the mixture was vortexed, sonicated, and repeatedly extruded (10 times) through 400 and 200 nm polycarbonate ester films. EXO hybridized LPs were successfully formed as a consequence of this [24, 140]. An alternative research group implemented comparable methodologies in the preparation of HEs. LP and EXO solutions were combined in a multitude of volumetric proportions. Following this, the solutions were thoroughly dissolved by typically vortexing and sonicating the mixtures for 2–3 min at a maximum amplitude of 20–33% using a sonicator. Subsequently, extrusion was performed on the mixtures through pore diameters of 400 nm, 200 nm, or 100 nm [141, 142] (Fig. 4).

HE characterization approaches are comparable to those of EXOs and LPs in general. However, there needs to be more reliable methods for estimating fusion efficiency, necessitating more study in this area. More experimental work is needed to fully understand the biophysical process that causes the lipids to fuse and maintain their equilibrium state. To further advance the area of HEs, it would be fascinating to study how entropic factors, lipidic interactions, additives, and physical characteristics affect the stability and effectiveness of fused HEs. A deeper understanding of the complicated biological system of HEs might be achieved by extensive experimental research in vitro and animal models. Overall, many obstacles need to be overcome before HEs can be used in clinical settings. These include optimizing the LP: EXO ratio and cargo loading methods, developing characterization techniques, producing on a large scale, ensuring quality, and addressing concerns about storage stability. Despite the small number of papers exploring HEs, this notion has great promise for ushering in a "cancer-overcoming era" due to its immense potential. HE characterization approaches are comparable to those of EXOs and LPs in general. However, there needs to be more reliable methods for estimating fusion efficiency, necessitating more study in this area. More experimental work is needed to fully understand the biophysical process that causes the lipids to fuse and maintain their equilibrium state. To further advance the area of HEs, it would be fascinating to study how entropic factors, lipidic interactions, additives, and physical characteristics affect the stability and effectiveness of fused HEs. A deeper understanding of the complicated biological system of HEs might be achieved by extensive experimental research in vitro and in animal models. Overall, many obstacles need to be overcome before HEs can be used in clinical settings. These include optimizing the LP:EXO ratio and cargo loading methods, developing characterization techniques, producing on a large scale, ensuring quality, and addressing concerns about storage stability. Despite the small number of papers exploring HEs, this notion has great promise for ushering in a "cancer-overcoming era" due to its immense potential [143].

#### Characterization of hybrid EVs-liposomes

Because of EVs' high biocompatibility, quick endocytosis, and minimal immunogenicity, miRNAs are delivered effectively without causing detectable cytotoxicity [145]. It has been shown that loading drugs into LPs is a straightforward process, resulting in excellent EE (sometimes exceeding 90%) and drug loading capacity (up to 10–20%). LPs and other synthetic vectors are linked to cost-effective manufacturing, replicability, adaptable design, and durability. LPs have restricted targeting capabilities, mostly being delivered to the liver. Some LPs lack stability due to not being PEGylated and have poor endosomal escape, which hinders their clinical use. Transferring these features to electric vehicles by fusion with EV/LPs or other synthetic objects is of great interest. Hybrids are anticipated to use the inherent characteristics of electric vehicles, including resistance to opsonization, enhanced ability to traverse biological barriers, unique targeting capabilities, improved ability to escape endosomes, and compatibility with living tissues. Hybrids may potentially benefit from both the synthetic vector qualities, such as high EE and loading capacity, as well as the natural extracellular vesicle properties, such as organ- or cell-type targeting abilities, improved cargo protection, and enhanced endosomal escape [144].

To regulate and extend the discharge of EVs, LPs were fused with EVs via a modification in their physical interaction with the bioink. Hybrid EV-LP nanovesicles (hELNVs) were encapsulated within hydrogels composed of gelatin to produce bioinks capable of delivering microRNAs to the target site in a sustained and controlled fashion. The modulation of cellular gene expression within a three-dimensional bioprinted framework was accomplished by employing the hELs-loaded bioink as a precursor to generate constructs with superior shape fidelity and high cell viability [146]. Martijn et al. prepared and assessed EV–HLs NPs (hybrids) as an alternative delivery system that combines the characteristics of EVs and LPs. Hybrids are demonstrated to be spherical particles that encapsulate siRNA, incorporate EV-surface producers, and deliver siRNA to various cell types in a functional manner. In contrast to LPs, the functional characteristics of hybrids, including gene silencing efficacy, cellular

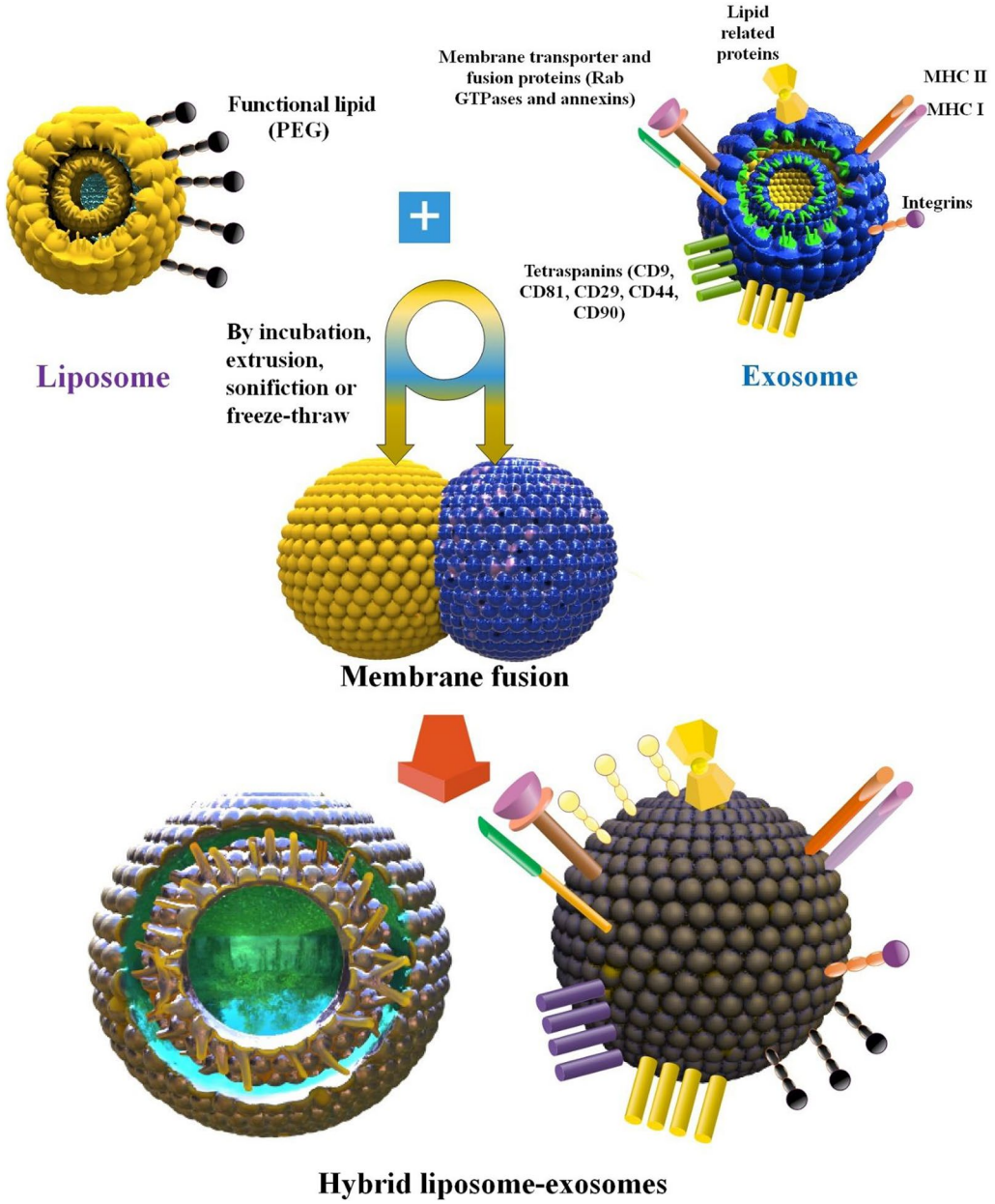


**Fig. 4** Diagram illustrating the technique used to create the EXO-HLs [133]. Methods for producing EV-HLs via incubation, with or without electrostatic interaction. Straightforward incubation; Electrostatic interactions involving LPs sensitive to pH Interactions between cations and electrostatic lipids [144]

uptake, and toxicity, differ among recipient cell types. Furthermore, functional characteristics associated with cardiac progenitor cell (CPC) derived EVs, including endothelial signaling activation and migration, are maintained in hybrids generated using CPC-derived EVs. Hybrid DDS, which incorporate the advantages of biological and synthetic DDS, may function as therapeutic carriers of siRNA in the future. The inaccessibility of siRNA molecules to the site of action restricts the therapeutic application of RNA interference. This study assesses the efficacy of EV–HLs NPs as a vehicle for siRNA drug delivery. The results demonstrate that these hybrid NPs not only deliver siRNA but also retain crucial biological functions that are typically associated with EVs [147].

Rayamajhi et al. postulate in a separate investigation that sEVs derived from immune cells can imitate immune cells to target malignancy. Various techniques for isolating sEVs, however, resulted in low yields and functional

property loss. To address this issue, researchers engineered vesicles smaller than 200 nm in diameter that resemble EXOs by hybridizing sEVs with synthetic LPs; these vesicles are designated HEs. To accomplish this, synthetic LPs were hybridized with sEVs from rodent macrophages to engineer HE. The fluorescence-based experiment validated the efficacy of the hybridization procedure, which produced HE measuring 177 ± 21 nm in diameter. Blot techniques for primary protein analysis identify the presence of EV marker proteins CD81, CD63, and CD9. In support of researchers hypothesis, differential cellular interaction of HE was observed when it was treated with normal and malignant cells. Additionally, DOX in water solubility was inserted into HE. The enhanced toxicity of drug-loaded HE towards cancer cells and its pH-sensitive drug release under acidic conditions facilitated drug delivery to acidic cancer environments. The engineered HE appears to be a promising platform for tumor-targeted drug delivery, according to these findings [148].

The amalgamation of EVs and synthetic vectors is appealing due to its capacity to preserve the topology, payload, and EV. In contrast to techniques that induce vesicular shape destruction, fusion is hypothesized to protect the properties of EVs. However, more than a definitive demonstration supporting this assertion is needed. Fusion might be sufficiently induced by a mere incubation of LPs with EVs. However, this approach is relatively sluggish, and transmembrane time-dependent release may result in LP drug escape. Lin et al. suggested employing this approach to generate plasmid-loaded hybrids by fusing LPs with HEK293FT-derived EVs for 12 h at 37 °C in the presence of surrounding plasmids encoding the Cas9 protein and a sgRNA. The researchers assert that the plasmid was encapsulated within the hybrids, an accomplishment that seemed challenging to accomplish in terms of topology. They were subsequently utilized to transfect cells that were challenging to transfect, including MSCs. The consideration of temperature is critical when employing this method due to its direct influence on the kinetics of fusion [137, 144, 149].

The exceptional ability of milk EXOs (mExos) to pass through epithelial barriers has made them a promising carrier for the oral delivery of peptide and protein medicines. However, there are still specific issues that arise from their inherent properties, such as the fact that they aren't very good at loading drugs, they can't penetrate mucus very well, and they lose proteins quickly. To address the drawbacks of mExos and maximize its use in oral peptide administration, researchers created a hybrid vesicle called mExos@DSPE-Hyd-PMPC, which combines functionalized LPs with natural mExos. The modification of mExos@DSPE-Hyd-PMPC's surface properties was accomplished by taking advantage of the jejunum's pH microenvironment via the introduction of a pH-sensitive hydrazone link between the phospholipids and the very hydrophilic zwitterionic polymer. Hybrid vesicles showed a 2.4-fold improvement in semaglutide (SET) EE compared to normal mExos. Within the jejunal lumen, the hydrophilic and neutrally charged surfaces of mExos@DSPE-Hyd-PMPC demonstrated enhanced protein retention and effective mucus barrier traversal. The hybrid vesicle's positively charged surfaces and highly retained membrane proteins allowed it to traverse the apical, intracellular transport successfully, as well as basolateral exocytosis barriers upon arrival at the surface of jejunal epithelial cells. An oral bioavailability of 8.7 percent was achieved by the hybrid vesicle's self-adaptive surface characteristics, which significantly improved the pharmacological therapeutic effects. With any luck, this research will help us get over the sequential absorption hurdles that come with oral peptide administration and make use of all the benefits that natural mExos have to offer [150].

The inherent immune-modulating capabilities and better biocompatibilities of immune-cell-derived membranes have made them a promising new delivery modality in cancer immunotherapy. Combinatorial pharmacological activities in activating antitumor immunity can be enhanced by integrating extra parental cell membranes or synthetic lipid vesicles into cellular vesicles. Researchers' findings shed light on the potential of hybrid cellular vesicles as flexible delivery vehicles for cancer immunotherapy. Scientists created a hybrid vesicle that is generated from macrophages and membranes; this vesicle may carry immunotherapeutic medicines and can shape the polarization of tumor-associated macrophages, making it useful in cancer immunotherapy. The technology integrates DOXand manganese-loaded LPs coupled with CXCR4-binding peptides with vesicles generated from M1 macrophage membranes. The CXCR4-binding peptide in the hybrid nanovesicles allowed them to target macrophages, and this boosted their polarization to the antitumoral M1 phenotype, which is defined by the production of proinflammatory cytokines. The CXCR4-expressing tumor cells induced potent cancer cytotoxicity, ICD of tumor cells, and STING activation by the hybrid vesicles loaded with manganese and DOX. Manganese and DOX, when administered together, accelerated dendritic cell development, which in turn inhibited tumor growth. The hybrid vesicles loaded with manganese and DOX demonstrated intense tumor-suppressing action at modest dosages in murine models of CT26 colon carcinoma and 4T1 BC when administered intravenously without causing any systemic side effects. An abscessive effect was also elicited by the local injection

of hybrid nanovesicles in a bilateral 4T1 tumor model. A novel strategy for combinatorial immunotherapy may be possible thanks to a biomimetic manganese/DOX hybrid nanovesicle platform that researchers have shown to be successful in cancer immunotherapy when customized to the tumor microenvironment [151].

Clinical translation of LPs for cancer therapies is hindered by immunotoxicity despite the many benefits of LPs. At now, this is being circumvented by endogenous payload-carrying EXOs, which resemble LPs structurally. Many studies have used bovine milk as a source to extract EVs/EXOs, and the current endeavor to do so from colostrum and milk has been revolutionary. Improved medication effectiveness, decreased or eliminated immunotoxicity, fewer adverse effects, and reversal of multidrug resistance are further benefits of milk EVs. HE, which combines the best features of LPs and EXOs, is a relatively new notion that scientists are working to improve. The ability to load many kinds of molecules—peptides, siRNA, hydrophilic or hydrophobic medicines, etc.—into HE is a crucial feature of these nanovesicles. Both systemic and local delivery of HE have been documented in the literature. HE administered intravenously provides better drug delivery than LPs because they remain in circulation for longer and are not readily removed by the MPS or reticuloendothelial system (RES) [143].

#### Characterization of hybrid liposome-nanoparticle

Researchers have outlined the structure of TSL-NP hybrids capable of controlling drug release based on external heat stimulation [45]. The engineering of these hybrid systems was accomplished through the effective integration of silver, iron oxide, and AuNPs into the lipid bilayer of lysolipid-containing thermosensitive liposomes (LTSL) [152]. Using cryo-EM and AFM to analyze the structure of LTSL-NPs hybrids, it was determined that the incorporation of metallic NPs into the lipid membranes did not affect the loading or retention of DOX [153]. In response to external heating, the presence of metallic NPs in the lipid bilayer enhanced bilayer retention and provided an NP concentration-dependent modulation of drug release. In summary, LTSL-NPs hybrids, which are constructed from LTSL LPs, offer a flexible and encouraging substrate that may additionally exploit the attributes of the incorporated NPs to facilitate multifunctional theranostic endeavors [154].

Moreover, LP–NPs hybrid constructs offer tremendous potential for combinatory therapeutic–imaging modalities in the engineering of nanoscale delivery systems [155]. Furthermore, nanotechnology laboratories are currently engaged in the development of numerous novel materials, which frequently necessitate the implementation of methodologies aimed at improving their compatibility with the in vitro and in vivo biological environments [156].

LPs are biocompatible with NPs due to their structure, and they offer a diverse, clinically established platform for additional pharmacological effectiveness augmentation [157]. LPs have been combined with silica, polystyrene NPs, QDs, small iron oxide NPs, and LPs for a range of uses [158]. Integration of diverse functional biopolymers has emerged as an appealing technique to address the limitations of the use of LPs [159]. Bioactive substances, such as vitamins, carotenoids, phenolics, peptides, and others, can be encapsulated, protected, and released under controlled conditions using biopolymers and phospholipid bilayers. This has important implications for functional foods, cosmetics, and pharmaceuticals [160]. The main problems, possibilities, and potential advances for future research are also mentioned [161]. HL/metal NPs that are promising have a lot of potential uses in biology. One challenge during synthesis is the poor yield of the targeted hybrid and lack of selectivity. By deliberately adding a reducing agent, Lee et al. produced a customized LP that allowed metal NPs to develop within the LP and form a stable LP/metal NP combination. Researchers produced seven LP/monometallic and more complex LP/bimetallic hybrids. The surface plasmon resonance bands of the NPs in the visible and NIR spectrum may be controlled by varying their size and metal composition. In comparison to AuNPs without the LP, their LP/Au NPs show improved colloidal stability in physiologically relevant fluids and greater endocytosis efficiency because of the presence of an outer lipid bilayer. Taking advantage of its improved physicochemical properties, researchers used this hybrid for surface-enhanced Raman spectroscopy-based intracellular imaging of living cells. Researchers believe that their method significantly improves the performance of metal NPs in in vivo applications [162].

With a focus on (1) controlled drug release from TSL brought on by NIR irradiation and (2) the photothermal impact of the Au nanoshell-like structures while absorbing laser light, Koga et al. created AuNP-coated LPs /DOX (GCL/DOX) for combination therapy. GCL/DOX was created using thiol-group-spiked LPs with glutathione bound to AuNPs under reducing conditions. The amount of HAuCl4 injected caused the absorption peak of GCL to shift from 636 to 795 nm, which corresponded to the absorption of NIR laser light (660 nm) by GCL/DOX. Within 1 min (> 80%) after NIR laser irradiation, the bulk of the encapsulated medicine was released from GCL/DOX. When compared to monotherapy (photothermal effect alone or free-DOX treatment alone), GCL/DOX demonstrated a synergistic effect in A549 cells. Thus, GCL is an effective LP carrier, and its therapeutic

method shows promise for cancer treatment when paired with NIR laser irradiation [163].

In one work, for instance, scientists devised a microfluidic approach for directing the self-assembly of LP – hydrogel hybrid NPs that are temperature sensitive. A wide range of NPs with extremely monodisperse size distributions and structural features that are important to the controlled release and targeted administration of encapsulated medicinal drugs are created by the researchers' technique. The convective-diffusive mixing of two miscible NPs precursor solutions (a DPPC:cholesterol: dicetylphosphate (DCP) phospholipid formulation in isopropanol and a photopolymerizable N-isopropyl acrylamide combination in aqueous buffer) was managed by researchers adopting microfluidic hydrodynamic focusing. The purpose was to produce nanoscale lipid vesicles that enclosed hydrogel precursors. Off-chip collection of these precursor NPs is followed by bulk UV irradiation to polymerize the NPs' interiors into hydrogel cores. The NPs size distributions were studied by applying asymmetric flow field-flow fractionation in combination with multiangle laser light scattering. The diameter range of the NPs was regulated by microfluidic mixing settings and ranged from ≈ 150 to ≈ 300 nm. The polydispersity of the NPs was calculated to range between ≈ 3% and ≈ 5% (relative standard deviation). TEM then verified the hybrid NPs' spherical form and core – shell composition. For healthcare and life science applications, this technique may be expanded to the guided self-assembly of other analogous cross-linked hybrid NPs systems with tailored size/structure – function correlations [164].

Recently, researchers generated HLs through the ultrasonication of vesicular and micellar molecules in a buffer solution. By altering the composition and proportions of their constituents, it is possible to regulate the temperature at which these LPs undergo phase transitions and their other physical characteristics, including size, shape, and membrane fluidity. High or perfect enantioselective catalysis was achieved in the reaction field of HLs, which consists of vesicular and micellar molecules, including the active tripeptide, to distinguish the L-form substrate from the D-form by varying the ionic strength, species of molecules, and composition of LPs. HLs exhibit efficacy in impeding the proliferation of diverse malignant cells both in vitro and in vivo, as demonstrated by an animal model of carcinoma, in addition to their potential utility in drug delivery. Experiments involving normal animals have additionally shown the safety of HLs, and they are currently being utilized in a clinical study [165].

To produce hybrid nanosystems containing magnetic NPs, these NPs must be synthesized before they are combined with lipid nanosystems. It is possible to create magnetic NPs using chemical, biological, and physical methods. The most common physical methods include thermal breakdown (thermolytic), photochemical processes, laser ablation, microwave irradiation, sonochemical reactions, UV radiation, and radical-induced techniques. On the other hand, the chemical approach includes several methods, such as organic solvents, coprecipitation, supercritical fluid, and inorganic matrix support. Conversely, the biological approach makes use of reactor sources or precursors made of fungus, bacteria, algae, and plants. The most common MLs are those with metallic NPs attached to the aqueous interior because of the thickness restriction of the lipid bilayer. Because of this, it is more challenging to put metal NPs into the membrane than into the aqueous core [166]. Through thermal breakdown, Choi et al. generated oleic acid-coated magnetic NPs (~ 6 nm) and placed them into the lipid bilayer (~ 3.4 nm thick) of LPs (DPPC: Dioleoyl-3-trimethylammonium propane). Chloroform was used as a solvent to guide the production of MLs, which improved the NPs' insertion efficiency into the lipid bilayer. The MLs were altered to actively target SK-Br3 (HER2-positive) and Hela (FRα-positive) cancer cells by adding folate or an anti-HER2 antibody. It was used to utilize magnetism to separate the cancer cells. The technique of entrainment of the metal NPs to the lipid membrane using chloroform demonstrated efficacy by changing the color of the hydration buffer from red to yellowish when compared to the traditional approach of hydrating the lipid film. The NPs were stable after they were incorporated into the 94 nm LPs. Because HER2 receptor antibodies target the cell surface of SK-Br3, an isolation efficiency of 75% was achieved, compared to a recovery efficiency of 9% for HeLa cells. When folate was added to the MLS, Hela cells showed high separation efficiency. The existence of differently functionalized MLs on the surface of cells expressing specific receptors is confirmed by confocal microscopy data. Antibody-conjugated MLs effectively transported ATTO590 oligonucleotide into the SKBr3 cells' nucleus. Since the size and quantity of encapsulated NPs affect the effectiveness of the produced magnetic field, the entrapment efficiency may have been assessed and compared in both approaches despite the capacity to encapsulate bigger NPs. The authors' study showed how the MLs' characteristics combined with changes for active targeting might be utilized to regulate cellular uptake by magnetic guiding [167].

### Hybrid liposomes in cancer detection

A combination of vesicular and micellar molecules in buffer solutions may be ultrasonically sonicated to create HLs, which are nano-sized liposomal particles [168]. DOX and Magnevist, MRI contrast agents with a mean diameter of 120–130 nm and restricted size distribution, are examples of nano HLs that were developed [169]. Compared to physiological pH (pH 7.4), DOX release from the proposed formulation was enhanced at acidic pH (pH 5.5 and 6.8). By covering the outside of the nano HL with HACE, the cytotoxicity caused by the blank plain LP was reduced [121]. The interaction between HA and the CD44 receptor enhanced the cellular uptake of DOX from the nano-HL in comparison to the conventional LP. The in vivo contrast-enhancing effects of nano-HL demonstrated its potential utility as a tumor-targeting MRI probe in the context of cancer diagnosis [170].

Scientists created HLs that are easily made by sonicating a combination of micellar and vesicular molecules in a buffer solution. One may manipulate the physical characteristics of HL, including its size, shape, and membrane fluidity, by adjusting its compositional ratio and components. Researchers have seen the following intriguing outcomes of using HL for chemotherapy and cancer diagnosis: (1) The homogenous and stable structure of HL, which is made up of 80 nm-diameter polyoxyethylene-dodecyl ether (C 12 (EO) n) and L-α-dimyristoylphosphatidylcholine (DMPC), was discovered. (2) In vitro experiments revealed that HL had notable growth-inhibiting properties on a variety of tumor cell types. (3) Apoptosis caused by HL was achieved, and the mechanism by which HL induces apoptosis was elucidated. (4) It was found that there was a strong association between HL's membrane fluidity and its ability to suppress tumor cells. (5) Using a mouse model of carcinoma, significantly longer lifetimes and a notable decrease in tumor volume were found after HL therapy in vivo with no adverse effects. (6) In clinical applications, individuals with lymphoma treated with HL had a significant decrease in neoplasm and an extended survival period without experiencing any adverse effects after the bioethics committee's clearance. Additionally, (7) HL was shown to have specific accumulation and growth inhibitory effects on human tumor cells while having no impact whatsoever on normal cells [171].

A separate investigation demonstrated that HLs can be generated through the straightforward process of sonicating a solution containing vesicular and micellar molecules suspended in a buffer. The objective of this research endeavor was to clarify the therapeutic properties and diagnostic capability of HLs in an orthotopic graft mouse model of CRC utilizing HCT116 cells to develop HLs as theranostic agents. HLs demonstrated therapeutic effects in the absence of a chemotherapeutic agent by impeding the proliferation of HCT116 CRC cells in vitro, potentially via upregulation of apoptosis. A mouse model of CRC developed in which intravenous HLs were administered also exhibited a significant decrease in the relative cecum weight. The histological examination of the cecal sections revealed a reduction in tumor size, which was validated by HE staining. The induction of apoptosis in HCT116 cells was confirmed by TUNEL staining in the CRC orthotopic graft mouse model. The accumulation of HLs encapsulating a fluorescent probe (ICG) was observed in HCT116 cells in the in vivo CRC model after intravenous administration for HL detection and diagnosis. According to these results, HLs can accumulate for an extended period in tumor cells located in the cecum of the orthotopic graft mouse model of CRC, thereby impeding the proliferation of HCT116 cells [172].

Erythrocyte membrane alteration offers a novel method for better drug delivery and biological applications. Red blood cell (RBC) membranes are doped with synthetic lipid molecules of various classes (PC, PS, PG) and saturation levels (14:0, 16:0–18:1) to create hybrid erythrocyte LPs. Phosphatidylcholine lipids may be added to modify the lipid orientation and membrane thickness. Phosphatidylserine and phosphatidylglycerol may be added to the hybrid membranes to change their charge and to label them fluorescently. Texas-red DHPE can also be used. It is shown that tiny compounds may be encapsulated into these HLs using fluorescein-tagged dextran as an example [173].

A critical topic of research in the realm of biomedicine is the treatment of triple-negative breast cancer (TNBC), a high-risk cancer. Immuno-sonodynamic therapy (iSDT), a therapeutic strategy that combines immunological checkpoint blockage with sonodynamic treatment (SDT), has been proposed to achieve improved anticancer results. Researchers used a cell membrane-camouflaged nanoliposome (Bio-Lipo-CB) containing the PD-1 inhibitor BMS202 and chlorin e6 (Ce6). The cell membrane was effectively encapsulated in LPs, as shown by TEM and SDS-PAGE experiments, and Bio-Lipo-CB accumulated preferentially in 4T1 cells. As shown by its increased ROS generation and enhanced cell death rate, Bio-Lipo-CB-SDT demonstrated significant cytotoxicity when compared to Bio-Lipo-CB alone. Additionally, Bio-Lipo-CB-SDT therapy, HMGB1 and ATP release to extracellular space, and calreticulin (CRT) extraversion to the cell membrane all suggested ICD. Furthermore, two hours after injection, Bio-Lipo-CB may concentrate at the tumor site, according to an in vivo fluorescence imaging test. The in vivo anticancer experiment further confirmed the effectiveness of Bio-Lipo-CB-SDT analysis against tumors and demonstrated that Bio-Lipo-CB-SDT

triggered ICD. The body weight primarily showed the safety of this combination approach and him staining of normal organs. Researchers showed the feasibility of synergistic tumor therapies based on SDT and checkpoint blockade immunotherapy in TNBC using bionic nanoplatforms [174].

Lee et al. aimed to optimize the specificity of their NPs to specific targets to improve their capacity to enter the tumor and boost immunotherapy using ketoconazole (KTZ), BMS-202, and ICG-induced photothermal treatment (PTT) for anticancer purposes. Lee created LPs by incorporating hydrophobic medications BMS-202 and KTZ inside a lipid bilayer and hydrophilic drug ICG within the LPs using a thin film creation procedure. During the technique, the cell membranes of specific cancer cells were fused to enhance penetration and targeting. The NPs were tested both in laboratory settings and in living organisms to verify their effectiveness against cancer. Several investigations have shown the characteristics of BMS-202/ICG/KTZ-loaded HLs. The in vitro and in vivo investigations demonstrated the practical improvement of the targeting capability of the NPs by fusing them with the cell membranes of specific cancer cells to boost their capacity to reach and enter the target cells. Furthermore, while the drug by itself did not exhibit notable toxicity to 4T1 cancer cells in the MTT assay, LPs containing both KTZ and BMS-202 demonstrated a substantial impact on inhibiting secondary tumors in animal trials compared to LPs with just one drug, validating the efficacy of the improved immunotherapy [175].

Exosomal miRNAs may be useful as biomarkers for cancer surveillance, according to several lines of evidence. The in situ detection of low quantities of exosomal miRNAs without damaging the EXO structure is still a vital necessity. The current work has created a unique and sensitive in situ detection technique for exosomal miR-1246 by combining the CRISPR/Cas13a system with the production of hybrids between cationic LPs and EXOs. CRISPR/Cas13a, CRISPR RNA (crRNA), and RNA reporter probes were put onto the LPs. Exosomal miR-1246 triggered CRISPR/Cas13a to cleave the reporter probes and electrostatic interactions between LPs and EXOs produced LP–HE. A quantifiable response to exosomal miR-1246 was shown by the obtained fluorescence signal, which had a linear relationship to the logarithm of MCF-7 exosome concentrations. The regression equation, using a detection limit of $3\times10^2$ particles per mL, is $y=5021\log C-9976$ ($R2=0.9985$). This approach has the potential to differentiate between the early and late stages of BC patients in addition to detecting serum exosomal miR-1246. This approach may be used in exosomal miRNA analysis in the future [176] (Table 4).

One of the main obstacles to the widespread use of Surface Enhanced Raman Scattering (SERS) in ultrasensitive diagnostics and imaging is the difficulty in preparing the SERS tags. These tags are usually metallic NPs that have been functionalized with Raman-active molecules (RRs). The production of these tags often involves complex synthetic approaches, and they need better colloidal stability and reproducibility. A straightforward platform for the self-assembly of clusters of AuNPs on lipid vesicles was developed by researchers and named LipoGold Tags. Because of the stronger electromagnetic field, the Raman signals of RRs embedded in lipid bilayers are much higher. Researchers provided strong structural characterization, and researchers controlled the amounts of RRs and lipid vesicles to maximize SERS amplification. By adding biomolecular probes, such as antibodies, to LipoGold Tags, researchers have shown how versatile these tags are. Many functionalization techniques may be used, depending on the specificities of the target cells or tissues and the needs for targeting. Electrostatic interactions, click chemistry, antibody conjugations, and ligand-receptor bonds are all examples of such processes. It is possible to add reactive lipids into the vesicle production process systematically, and most of these methods make use of the chemical groups that LPs expose to the external environment. In order to do this, the liposomal membrane was supplemented with a pegylated phospholipid DOPE-PEG, which has a reactive carboxylic acid moiety (1,2-dioleoyl-sn-glycero-3-phosphoethanolamine-N-(carboxypolyethylene glycol)−2000). Peptide linkages with antibodies are formed when the carboxylic acid moieties are activated. Although there were no discernible signals when antibodies weren't present, the Raman intensity of the MBA peak at 1577 $cm^{-1}$ increased as the concentration of PEG molecules—and, by extension, the antibodies attached to the liposomal surface—increased. When no PEG molecules (and thus no antibodies) were present, this proved that the SERS probes were not non-specifically attached to the substrate. Such findings lend credence to the idea that SERS-based tags might be helpful to probes for the quantitative identification of analytes in liquid samples. Exhibiting LipoGold Tags as a breakthrough in the manufacture of SERS probes, researchers were able to identify intracellular GM1 changes as proof of concept effectively, differentiating healthy donors from patients with infantile GM1 gangliosidosis [177].

## Hybrid liposomes in cancer treatment

Researchers investigate the role of cancer stem cells (CSCs), which are alternatively referred to as tumor-initiating cells, in tumor progression, metastasis, and drug resistance. Hypoxosome-bound liposomal particles (HLs) are readily synthesized via ultrasonication of

**Table 4** Hybrid liposome in cancer detection

| Liposomes | Cancer | Detection agent and methods | Characteristics of hybrid liposomes | Explain | References |
|---|---|---|---|---|---|
| Hybrid liposomes (HLs) are composed of vesicular and micellar molecules | Colorectal cancer (CRC) | HLs encapsulating a fluorescent probe (ICG)<br>Fluorescence imaging | A combination of 90% DMPC and 10% polyoxyethylene (25% dodecyl ether) was sonicated to produce HLs. While DMPC LPs had a hydrodynamic diameter (*dhy*) of 200–300 nm, HLs had a dhy of less than 100 nm. The DMPC LPs fell apart. Retinal endothelial system evasion is possible for HLs smaller than 100 nm | After intravenous treatment, the accumulation of HLs encapsulating a fluorescent probe (ICG) was shown in HCT116 cells in the in vivo CRC model, facilitating the identification and detection of HLs | [172] |
| Cell membrane-camouflaged nanoliposome (Bio-Lipo-CB) | Triple-negative breast cancer (TNBC) | A fluorescence imaging test conducted in vivo revealed that Bio-Lipo-CB | The thin-layer evaporation technique was used to manufacture Bio-Lipo-CB. Ce6 had an EE of 60.0 in Bio-Lipo-CB, whereas BMS202 had an efficiency of 71.2%. Around 150 nm was the size of the Bio-Lipo-CB. Compared to Lipo-CB, which had a particle size of around 90 nm, this was 1.6 times bigger. Compared to Lipo-CB, whose $\zeta$-potential is −24.06 mV, Bio-Lipo-CB has a much lower value of −3.47 mV | The in vivo anticancer experiment further proved the effectiveness of the Bio-Lipo-CB-SDT study against tumors and also showed that Bio-Lipo-CB-SDT produced ICD | [174] |
| LP–exosome (EXO) hybrids | breast cancer (BC) | A unique and sensitive in situ detection technique for exosomal miR-1246 by combining the CRISPR/Cas13a system with the production of hybrids between cationic LPs and EXOs | As opposed to the spherical shape of EXOs and LPs, signs of LP-HE included bridging membranes and large vesicles. The size of the EXOs and LPs in the combination increased to around 350 nm, which is larger than either component alone and suggests the formation of hybrids | In addition to identifying serum exosomal miR-1246, this method may be used to distinguish between individuals with BC who are in the early or late stages of the disease. In the future, exosomal miRNA analysis may use this methodology | [176] |

a buffer solution containing a mixture of vesicular and micellar molecules. The inhibitory effects of HL on the proliferation of CSC subpopulations in HepG2 liver cancer cells were investigated in vitro. Sonication was used to produce HLs consisting of 10 mol% polyoxyethylene (23) dodecyl ether and 90 mol% DMPC. The viability of cells was assessed using the trypan blue exclusion assay. Flow cytometry was utilized to identify CSCs in liver cancer cells based on the presence of the cell surface marker proteins EpCAM and CD133. To conduct a soft agar colony formation assay, HL-pretreated HepG2 cells were utilized. HLs inhibited the proliferation of liver cancer cells in a selective manner while leaving normal hepatocytes unaffected. To the contrary, HepG2 cell growth was dose-dependently reduced in the concentration range of 50–200 μM when HLs were treated. In contrast, Hc cells were unaffected by HLs at the same concentrations. These findings suggest that, within the concentration range of 50–200 μM, HLs reduced the development of HepG2 cells while not affecting normal hepatocytes. HepG2 cells were additionally subjected to apoptosis by HLs via activation of caspase-3. Significantly diminished was the CD133 + /EpCAM + CSC subpopulation of liver cancer cells that were treated with HLs. HLs also considerably reduced the quantity of colony-forming cells. Ultimately, the integration and accumulation of HLs into the cell membranes of CSCs were verified through the utilization of a fluorescently labeled lipid (NBDPC). A substantial and dose-dependent accumulation of HL/NBDPC into the CSCs, specifically EpCAM(+) cells, was observed. Based on these findings, HLs may serve as an innovative nanomedical therapeutic agent to target CSCs in the treatment of liver cancer [178].

Investigating a logical delivery system for the integration of chemotherapy and immunotherapy to expand the therapeutic benefits of cancer immunochemotherapy remains a challenge, according to another study. For combinational immunochemotherapy, scientists created DOX-loaded biomimetic hybrid nanovesicles (DOX@LINV) by fusing synthetic LPs with tumor-derived nanovesicles (TNVs). Through TEM, LPs and liposomal vesicles (LINVs) showed the distinctive liposomal morphology of a spherical vesicular structure. Researchers showed that the size of LINVs was around 166.4 ± 1.9 nm (PDI, 0.118 ± 0.023), which is in agreement with the TEM data. TNVs and LPs had sizes of 228.70 ± 1.1 nm (PDI, 0.238 ± 0.014) and 146.5 ± 2.9 nm (PDI, 0.161 ± 0.009), respectively. EPR is a property of nanoscale LINVs that may help them accumulate substantially within tumors. In addition, LINVs had superior size homogeneity compared to TNVs, as seen by the lowered PDI. One probable reason might be that the penetration of the lipid membrane caused the LINV surface protein corona to be diluted and the aggregation caused by protein–protein interactions to be reduced. The insertion of TNV membrane lipids (− 25.9 ± 2.9 mV) likely caused the ζ-potential of LINVs to be lower (− 19.7 ± 1.4 mV) than that of LPs (− 14.1 ± 1.5 mV). 34 Keeping an eye on the particle size for two weeks was another way that the colloidal stability of LPs, TNVs, and LINVs was assessed. There was no change in the size of LPs and LINVs for two weeks in physiologically relevant solutions, but the particle size of TNVs fluctuated between 228 and 268 nm. To increase the immunogenicity of a tumor, DOX@LINV with homologous targeting capability could deliver DOX to tumor tissue and induce an efficient ICD response. Concurrently, dendritic cells were stimulated, and the tumor antigens and endogenous danger signals that were preserved in DOX@LINV elicited an antigen-specific T-cell immune response. DOX@LINV exhibited a distinct antitumor effect against 4T1 BC, Lewis lung cancer, and murine melanoma using effector immune cell infiltration and enhancement of the immunosuppressive tumor microenvironment. In addition, the antitumor efficacy was enhanced by the combination of DOX@LINV and an immune checkpoint inhibitor, resulting in 33.3% of the mice remaining tumor-free. As a result, for effective immunochemotherapy, the hybrid LINV is a promising drug delivery platform with an enhanced antitumor immune response [179].

By ultrasonically treating a buffer solution containing a mixture of vesicular and micellar molecules, HLs can be generated. By altering the composition, one can modify the physical characteristics of these LPs, such as their size, membrane fluidity, phase transition temperature, and hydrophobicity. It has been reported that HLs composed of DMPC and polyoxyethylene (10) dodecyl ether inhibit the growth of human promyelocytic leukemia (HL-60) cells in the absence of pharmaceutical intervention. Scientists tested HLs with varying amounts of ethylene oxide (n = 4, 10, 23, etc.) and DMPC on the proliferation of HL-60 cells. DMPC LPs had an IC50 value higher than 1 mM. Based on these findings, the best HLs to limit HL-60 cell growth should be DMPC and 10 mol% C 12(EO) 10. Additionally, electron imaging confirmed that these HLs contained homogeneous vesicles. The HLs induced apoptosis in HL-60 cells, as confirmed by fluorescence microscopy and flow cytometry analysis after the microphysiometer-detailed fusion and accumulation of HLs. The researchers elucidated the pathways by which HLs induce apoptosis. In other words, HLs aggregated and fused across the membranes of tumor cells, and the apoptotic signal reached the nucleus after traveling first through mitochondria, caspase-9, and caspase-3, then through Fas, caspase-8, and caspase-3. Human tumor cells may be induced to undergo apoptosis by HLs, which

also exert significant inhibitory effects on tumor cell proliferation [165].

Systemic toxicity restricts the application of PTX-based chemotherapy, which remains the primary method for treating lung cancer used by researchers. EXOs derived from chimeric antigen receptor-T (CAR-T) cells are regarded as prospective carriers for PTX due to the presence of cytotoxic granules (granzyme B and perforin) and tumor-targeted CARs. Histotoxic properties and a limited capacity for drug loading are, nevertheless, impediments to the use of EXOs in the treatment of extrahepatic cancer. A novel nanovesicle for immunochemotherapy of lung cancer, referred to as Lip-CExo@PTX, was developed through the fusion of EXOs produced by bispecific CAR-T cells that specifically target mesothelin (MSLN) and programmed death ligand-1 (PD-L1) with LPs designed for the lung. More than ninety-five percent of intravenously administered Lip-CExo@PTX accumulated in lung tissue due to the LPs' propensity to target the lungs. Furthermore, the anti-MSLN single-chain variable fragment (scFv) was utilized to deliver PTX and cytotoxic granules contained within Lip-CExo@PTX into MSLN-positive lesions. Significantly, the anti-PD-L1 scFv attached to Lip-CExo@PTX inhibited PD-L1 on the tumors, thereby promoting PTX-induced ICD and preventing T cell exhaustion. In addition, Lip-CExo@PTX extended the survival of rodents harboring tumors in a CT-26 model of metastatic lung cancer. Consequently, Lip-CExo@PTX may enhance the antitumor effects of PTX by sequentially targeting delivery to tumor cells, thereby offering a promising immunochemotherapeutic strategy for lung cancer [180].

In a study, the agents promoting drug transport and tissue penetration were shown to be cancer-associated fibroblasts (CAFs), a noteworthy subpopulation of stromal cells inside the tumor microenvironment (TME). Thus, it is feasible that therapeutic drugs might be more effectively absorbed and accumulated, improving therapeutic outcomes by effectively blocking CAFs from crossing the physical barrier. Using a matrix metalloproteinase (MMP)-triggered dual-targeting hybrid micelle-in-LP system (RPM@NLQ), quercetin (Que) and PTX were sequentially administered for fibrotic TME remodeling and chemotherapeutic potentiation, respectively. Specifically, antifibrotic Que and small-sized RGD-modified micelles encapsulating PTX (RPM) were co-encapsulated using MMP-sensitive LPs. The asparagine-glycine-arginine (NGR) peptide (NL) was added to improve the LPs' targeting capabilities even further. After being injected intravenously, the RPM@NLQ was first gathered precisely at the tumor location, guided by the NGR peptide. Que and RPM were then released in reaction to the TME's intense MMP expression. After that, by downregulating Wnt16 expression, Que was kept in the stroma to reduce fibrosis and the stromal barrier in CAFs dramatically; this resulted in a significant rise in RPM for deeper tumors. RPM could target and eradicate BC cells that are present locally. As a consequence, both in vitro and in vivo studies have shown excellent anticancer effectiveness; these qualities include prolonged blood circulation, increased penetration, and selective cascade targeting of tumor cells and tissue. In conclusion, as-designed sequential delivery methods for chemotherapy potentiation and fibrotic TME remodeling may provide a viable adjuvant treatment approach for CAF-rich malignancies like BC [181].

Novel strategies are discovered in response to the aggressiveness of melanoma and the dearth of effective therapies, according to another study. A novel hybrid molecule (HM) with dual-acting properties was recently synthesized by combining triazine and an analog of ρ-tyrosine. HM was engineered to undergo specific activation by tyrosinase, an enzyme that is implicated in the biosynthesis of melanin and is upregulated in melanoma. Researchers have chosen LPs because they are a safe and effective lipid-based technology that may increase the therapeutic efficacy by improving the stability of loaded HM in the circulation, which in turn promotes preferential targeting to cancer locations. The hydrophobic chemical HM was effectively loaded into LPs derived from Egg Lecithin (EPC) by means of the dehydration-rehydration technique. HM exhibited significantly greater antiproliferative activity against numerous cancer cell lines than temozolomide (TMZ), a triazine drug currently under clinical investigation that functions via DNA alkylation. A 2.8-fold decrease in the cell proliferation index indicated that HM caused a cell cycle arrest in B16-F10 cells in phase G0/G1. Additionally, HM caused a concentration-dependent reduction in tyrosinase activity and an increase in caspase 3/7 activity relative to the control cells. HM was incorporated into long blood circulation LPs coated with polyethylene glycol (PEG) to allow passive targeting of tumor locations in order to maximize its therapeutic effectiveness in vivo. A375 cells had the lowest IC50 values for HM (40–60 μM), but B16-F10 and MNT-1 cells had IC50 values ranging from 46 to 65 μM and 62–>75 μM, respectively. Conversely, TMZ showed limited cytotoxic capabilities, as cell survival exceeded 80% at all time points at the highest tested dose of 75 μM. Lastly, HM and TMZ showed IC50 values in HaCaT cells that ranged from 44 to 60 μM and > 75 μM, respectively. EPC: DSPE-PEG LPs, referred to as LIP HM henceforth, had a mean hydrodynamic size of around 100 nm, were homogenous (PDI < 0.1), showed a high HM loading (> 33 nmol/μmol of lipid), and had an integration efficiency (I.E.) of almost 100%. According to the lipid

composition utilized, a practically neutral ζ-potential was produced. The murine melanoma cell line B16-F10 was used to investigate the antiproliferative action of HM-loaded LPs further. After 72 h of incubation, Free HM's IC50 value was 45.1 μM. HM's cytotoxicity was reduced when it was encapsulated in LPs; for every lipid composition examined, the IC50 was more than 75 μM. The stability of HM LPs in biological fluids was exceptional. Its safety for systemic administration was established in preclinical research, and a murine subcutaneous melanoma model exhibited a substantial inhibitory effect on tumor progression. In a murine melanoma model with metastasis, mice administered LIP HM exhibited a significantly reduced number of lung metastases in comparison to the positive control group (TMZ), demonstrating a superior antitumor effect. Biodistribution studies demonstrated the capacity of 111-in-labeled LIP HM to passively target tumor sites; this corresponds with the substantial therapeutic effect observed in two experimental murine melanoma models [182].

This work demonstrates that LPs, a popular DDS, nonetheless have several drawbacks, including inadequate target organ deposition and dominating liver clearance. Researchers created a new LP-and-RBC combination DDS to address the shortcomings of LPs by modifying tumor accumulation and prolonging the liposomal DDS's blood circulation life. LPs were carried by RBCs, an excellent natural carrier DDS, to prevent them from passing through the bloodstream quickly. Researchers showed that the contact between LPs and RBCs did not change the properties of RBCs; instead, LPs may either fuse with the RBCs' membrane or absorb into their surface by simply changing the interaction period at 37 °C. 1,2-dipalmitoyl-sn-glycero-3-phosphocholine (DPPC) LPs attached to the surface of RBCs demonstrated a lung targeting effect through the RBC-hitchhiking approach and decreased clearance in the liver in the in vivo antitumor therapeutic efficacy study. Based on the results of the efficiency test, the optimal ratio of 2 l.mol LPs to $3\times10^8$ RBCs was found to achieve the maximum drug loading quantity. Incubating Lipo-DPPC and Lipo-DOPE with RBCs for 1 h resulted in a combination efficiency of 30.67 ± 6 2.05% and 29.80 ± 6 7.32%, respectively. Incubating the two substances with RBCs for 4 h yielded 73.71 ± 6 2.23% and 73.95 ± 1.40%, respectively. In contrast, DPPC LPs fused with RBCs had more extended blood circulation for up to 48 h and no enrichment in any organ. Additionally, since 1,2-dioleoyl-Sn-glycero-3-phosphoethanolamine (DOPE), a pH-sensitive phospholipid, might react to the low pH tumor microenvironment and subsequently accumulate in the tumor, 20% of the DPPC LPs were substituted with DOPE. Comparing the DOPE attached/fusion RBCs to the standard liposomal DDS, which exhibited around 0.7% tumor accumulation and partial enrichment in the lung, the latter demonstrated 5–8% tumor accumulation. Consequently, RBC–LP composite DDS may enhance blood circulation and liposomal tumor accumulation, demonstrating the therapeutic application potential of autologous RBCs for anticancer treatment [183].

sEVs derived from cancer may be a promising DDS that selectively targets cancer cells on account of their distinct characteristics, including native homing ability, biological barrier traversal capability, and minimal immune response, according to another study. Nevertheless, their current applicability is restricted due to safety concerns arising from the oncogenic cargoes they contain. Scholars suggested employing an electroporation-based methodology to isolate endogenous cargoes from sEVs derived from cancer and provided evidence that these cargoes retained their ability to hominate. These sEVs and LPs were fused via membrane fusion to produce hybrid particles that possessed the advantages of both sEVs and LPs. Researchers in a study achieved optimal ratios of LPs to sEVs and explored three distinct fusing procedures for hybrid particle preparations: incubation, sonication, and freeze–thaw. Membrane fusion between LPs and sEVs allowed for the fabrication of hybrid particles. The LPs containing DPPC, dodecanyl PE, and PEG 6000 were also produced via a conventional thin-film hydration and sonication pathway. Researchers suggested that the PEG in LPs may make it easier for them to fuse with sEVs. To further enhance the targeting capability of the hybrid particles, modifications were made to the anti-EGFR monoclonal antibodies. Compared to the hybrid particles without alteration, the hybrid particles treated with mAb had a much higher cellular absorption efficiency, indicating that the hybrid particles had better targeting capacity. The engineered hybrid particles exhibited enhanced drug loading capabilities, surpassing those of LPs by 33.75 and sEVs by 43.88%, respectively. Hybrid particles, when measured by NTA, had a slightly larger diameter (139.3 ± 7.1 nm) than individual LPs or sEVs. The spherical form of the hybrid particles was reminiscent of both LPs and sEVs. Furthermore, they demonstrated a 52.23% improvement in targeting ability compared to the unmodified hybrid particles. The efficacy of this delivery system was improved, as evidenced by treatment efficiency gains of > 90% and cell migration inhibition rates of 91.58 and 79.26%, respectively, for the miR-21 inhibitor and gemcitabine [184].

According to different research, melanoma is one of the most severe types of skin cancer and results from the malignant transformation of melanocytes. Researchers created a new hybrid nanosystem that combined magnetic targeting and therapeutic methods to treat cancer.

Therefore, the researchers created long-circulating, pH-sensitive LPs that loaded iron oxide NPs (IONPs) and the lethal metallodrug dichloro(1,10-phenanthroline) Cu (II) (Cuphen). DLS and TEM were used to characterize the synthesized IONPs. The dehydration rehydration process was used to generate lipid-based nanoformulations, which were then extruded to reduce and homogenize the mean size. The dehydration-rehydration process was used to create LPs with the following lipid composition: DMPC:CHEMS:DSPE-PEG (57:38:5). These LPs exhibit pH-sensitive characteristics. The mean size and incorporation characteristics of LPs were described. High loadings of cuphen were achieved, and the parameters of cuphen integration were marginally lowered in the presence of IONPs. Following the association with LPs, the antiproliferative qualities of cuphen were retained, and IONPs (at 2 mg/mL) did not affect the cellular growth of human and murine melanoma cell lines. Cuphen LPs' physicochemical characteristics were studied in relation to the presence or absence of IONPs in nanoformulations made of Cuphen. To get the highest possible loading of IONPs, researchers examined the effects of two distinct liposomal formulations, LP A and LP B, which had diameters of around 200 nm and 300 nm, respectively. The inclusion of IONPs changed the Cuphen incorporation characteristics in all the created nanoformulations, which decreased the loading capacity and increased the mean size. Compared to Cuphen LPs, which had a loading capacity of 26 nmol/μmol, LP A showed a loading capacity of 22 nmol/μmol when using IONPs. The wavelength increased from 127 to 162 nm for LP A and 237 to 277 nm for LP B. Despite the lack of an iron content measurement in the proposed formulations, the findings show that IONPs are actually linked to LPs. Furthermore, the PDI was less than 0.2 for all of the nanoformulations that were tested, which proved that the formulations were monodispersed. Additionally, the created nanoformulations showed magnetic characteristics. Their lack of hemolytic activity showed the study formulations' safety for parenteral administration. In conclusion, it was possible to effectively build a lipid-based nanosystem that loaded the cytotoxic metallodrug Cuphen and exhibited magnetic characteristics. Based on these first findings, parenteral administration of the synthesized IONPs is safe. Furthermore, they showed magnetic qualities when co-associated with Cuphen LPs and did not impede the metallodrug's cytotoxic effect. Additional studies using a syngeneic murine melanoma model have to be conducted to verify the efficacy of this unique hybrid nanosystem and the possible therapeutic enhancement of Cuphen LPs [185].

The fundamental constituents of the nano-assembly consist of Au nanorods that are enveloped in a mesoporous silica shell, which provides an exceptional surface for loading drugs and encapsulating DOX. To augment the photothermal capability of the nano-assembly, IR 780 dye was incorporated into a thermo-sensitive LP. Subsequently, the LP encased the core nano-assembly, and folic acid and GE-11 peptide were conjugated onto its surface to yield the ultimate nano-assembly ((GM@Dox) LI)-PF. ((GM@Dox) LI)-PF employs a dual targeting strategy, which enhances cellular uptake and nano-assembly accumulation in cancer cells that exhibit overexpression of folate and the epidermal growth factor receptor (EGFR). Photothermal-induced structural disruption of the nano-assembly can be induced by NIR irradiation, enabling the controlled and precise release of Dox at specific locations. Furthermore, chemo-photothermal therapy demonstrated an efficacy that was eleven times greater in treating cancer cells than Dox alone. The internalization of the nano-assembly was improved by the presence of the LP and the GE-11 cationic peptide, and the drug delivery mediated by the assembly ideally took place by clathrin-mediated endocytosis. Laser treatment of MRC-5 cells has been shown to have little to no harm, according to the research. No toxicity was seen in MRC-5 cells treated with (GM@Dox)LI-PF, either with or without a laser, suggesting that cell viability is close to 100%. The results show that the nano-assembly of (GM@Dox)LI-PF is safe for human cells. Based on the researchers' comprehensive analysis, it appears that the nano-assemblies promote apoptosis in cancer cells through an intrinsic mitochondrial pathway that is directly activated by chemo-photothermal therapy. Investigators presented an up-and-coming candidate that exhibits significant potential for synergistic cancer therapy [186].

HLs based on Ce6-lipid stabilized DOX, and researchers created Fe3O4 NPs for a synergistic tumor treatment that includes PDT, chemotherapy, and ferroptosis. As a component of LP backbones, synthetic Ce6-lipid has the potential to inhibit HLs' release of Ce6 and evade the drop in single oxygen efficiency that results from Ce6 aggregation. The DNA pairs might be anchored by the released DOX molecules, leading to cell death and an increase in intracellular ROS. Consequently, ferroptosis might be induced by $Fe_3O_4$ NPs releasing ferrous ions under an acidic TME and converting a high concentration of $H_2O_2$ into OH. To improve the effectiveness of lung cancer treatments, researchers have proposed a synergistic technique that regulates cellular redox homeostasis. A number of components, including Ce6-lipid and water-soluble $Fe_3O_4$, were produced in order to construct DOX and $Fe_3O_4$ HLs stabilized by Ce6-lipid. In order to carry out PDT, a certain laser may excite the as-obtained Lipo-Ce6 LPs. Thin film hydration was used to manufacture a variety of Ce6-lipid-based

(Lipo-Ce6) LPs in order to achieve the best doping ratio of Ce6-lipid. The findings of the DLS experiment reveal that, regardless of the amount of Ce6-lipid doped, Lipo-Ce6 LPs had a narrow PDI and a comparable size (about 130 nm). The DPBF probe was used to assess the singlet oxygen generation profiles of the Ce6-lipid-based LPs, since cytotoxic singlet oxygen yield is an essential component of photodynamic therapy (PDT). Next, Lipo-Ce6 LPs were prepared by loading a chemotherapeutic drug (DOX) into them using a (NH4)2SO4 gradient technique. The resulting LPs were named Lipo-Ce6@DOX. Those LPs that were loaded with DOX (Lipo-DOX) and those loaded with $Fe_3O_4$ were also examined using DLS. The measurements for Lipo@ $Fe_3O_4$ were 110.06 ± 5.2 nm and 106.6 ± 3.48 nm, respectively, and the ζ-potential were − 3.2 mV and − 9.08 mV. When compared to the control group that received PBS, the Lipo-Ce6 caused up to 36.4% more early apoptosis. Because $Fe_3O_4$ is primarily a ferroptosis inducer, PDT and DOX-induced apoptosis may have gained substantial therapeutic effectiveness after treatment with Lipo-Ce6@$Fe_3O_4$-DOX under the same irradiation circumstances, as the addition of DOX/$Fe_3O_4$ further enhanced cell death. With a combined action of light-induced photodynamic therapy (PDT) and chemo/ferroptosis (dark), the HLs + 650 nm light group significantly inhibited tumor development. It is worth mentioning that the mice did not see any notable changes in body weight while being treated [187].

It was examined whether miR497 and triptolide (TP) used in tandem may further overcome ovarian cancer's (OC) chemoresistance by cooperatively decreasing the mTOR signaling pathway. To co-deliver miR497 and TP, bioinspired hybrid NPs were created by fusing cRGD-modified LPs (miR497/TP-HENPs) with CD47-expressing tumor EXOs. Researchers measured 125 ± 6 nm for the hybrid nanoparticles' particle size. Using fluorescence resonance energy transfer (FRET), researchers assessed how well EXOs and LPs fused. A reduction in the peak emission of rhodamine B (RB) at λem = 595 nm occurred following fusing, in contrast to an enhanced peak emission of FITC at λem = 525 nm. Due to the increasing distance between the fluorescent dyes FITC and RB, the FRET effect was diminished, suggesting that the EXO content was introduced into the LP lipid bilayer. The in vitro findings showed that the NPs were effectively absorbed by the tumor cells, leading to a significant increase in tumor cell death. Because their PDI was always less than 0.2 and their particle size stayed about 125 nm, researchers discovered that HENPs were more stable in blood circulation than EXOs and LPs. The stability of HENPs was much higher than that of EXOs. The toxicity of HENPs to OC cells, L929 fibroblasts, and murine macrophage RAW 264.7 cells was shown to be minimal, according to in vitro studies. Furthermore, for TP, the hybrid nanoparticles exhibited an EE% of 78 ± 3%, whereas, for miR497, it was 72 ± 5%. The intracellular disassembly of miR497/TP-HENPs occurred in an acidic environment, releasing the Cy5-miRNC and TP of HENPs at a faster rate at a pH of 5.5 compared to 7.4 since CaP is pH-sensitive. Likewise, the hybrid NPs demonstrated significant anticancer efficacy in vivo and were efficiently concentrated in the tumor regions, all without causing any adverse consequences. Mechanistically, they increased the production of ROS, stimulated the dephosphorylation of the overactive PI3K/AKT/mTOR signaling pathway, and increased the polarization of macrophages from M2 to M1 macrophages [141] (Fig. 5; Table 5).

Scientists studied the anticancer effects of ExoSpHL-DOX in Balb/c female mice with 4T1 breast tumours and the toxicological profiles of EXOs fused with long-circulating and pH-sensitive LPs carrying DOX in healthy mice. After a single intravenous injection of ExoSpHL-DOX, the acute toxicity was assessed by measuring the animals' mortality and morbidity as well as by performing hematological, biochemical, and histological studies. Researchers found that compared to free DOX, the ExoSpHL-DOX therapy was safer. The fact that ExoSpHL-DOX exhibited no nephrotoxicity even when administered with the maximum dosage of DOX suggests that the hybrid nanosystem has the potential to modify DOX distribution and mitigate kidney injury. When compared to the placebo group, ExoSpHL-DOX demonstrated anticancer efficacy. The number of metastatic foci in the lungs was also decreased by the hybrid nanocarrier of tumor-derived EXOs fused with long-circulating and pH-sensitive LPs. Scientists proved that ExoSpHL-DOX had less toxicity than free DOX, demonstrating that EXO-HLs nanocarriers may transport more significant amounts of DOX with less toxicity and less harm to organs and tissues. When comparing the two treatments, the ExoSpHL-DOX therapy had a more substantial antitumor impact than the control. Moreover, regardless of whether the EXO-HLs nanocarrier contained DOX or not, ExoSpHL-DOX decreased the amount of lung metastatic foci. With its ability to decrease toxicity and limit metastasis, particularly in the lungs, researchers suggested that ExoSpHL-DOX might be a nanocarrier that has great promise for the treatment of BC [188].

## Hybrid liposomes as theragnostic agent in cancer

The selection of therapeutics and diagnostics may have an impact on the theranostic properties of the system under development. Nevertheless, the integration of imaging and therapeutic probes into lipid self-assembly "LPs" could potentially undermine their overall theranostics performance [22]. According to an

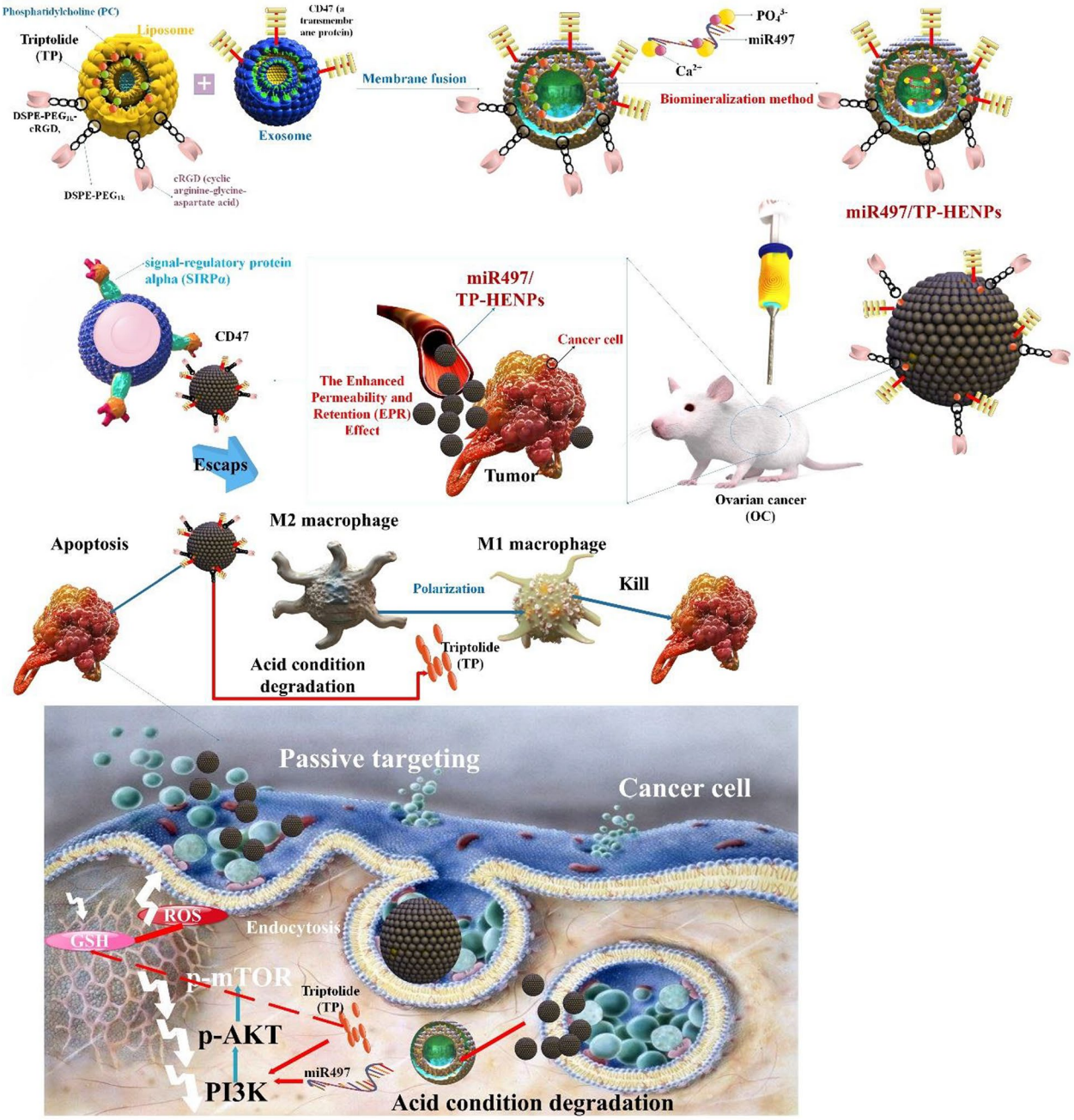


**Fig. 5** This graphic shows the creation of miR497/TP-HENPs and their mode of action. Membrane fusion and biomineralization were used to create TP-HENPs and miR497/TP, respectively. First, phosphatidylcholine (PC), encapsulated TP, DSPE-PEG1k-cRGD, and cholesterol were assembled to produce LPs. After that, EXOs and LPs were united together by membrane fusion. In the end, CaP causes miR497 to adsorb onto NPs surfaces. The following describes the ways that miR497/TP-HENPs functioned in OC cells: The enhanced permeability and retention (EPR) effect was produced by the nanoscale size of the nanoplatforms; EXO homing targeting and cRGD further improved the targeting efficiency of NPs; CD47 on the EXO surface prevented NPs clearance by the MPS system; miR497 and TP synergistically inhibited the PI3K/AKT/mTOR pathway; TP stimulated ROS production; and TP modulated [141]

investigation, photothermal therapy (PTT) is a newly developed cancer treatment technique since it can easily be used with other therapeutic approaches and treats tumors locally. To increase effectiveness, a tumor ablation guided by imaging will make it easier to administer the therapy. By inserting ICG into a hybrid lipid and

**Table 5** Hybrid liposome in cancer treatment

| Liposomes | Cancer | Treatment agent | Characteristics of hybrid liposomes | Explain | References |
|---|---|---|---|---|---|
| Hypoxosome-bound liposomal particles (HLs) | HepG2 liver cancer cells | Doxorubicin hydrochloride (DOX) | Paired with 10 mol of polyoxyethylene(23) dodecyl ether and 90 mol of DMPC. HepG2 cell growth was selectively inhibited by HLs at concentrations between 50 and 200 εM, although normal hepatocytes were unaffected | Using a fluorescently labeled lipid (NBDPC), the integration and accumulation of HLs into the cell membranes of CSCs were confirmed. It was shown that HL/NBDPC significantly and dose-dependently accumulated inside the CSCs, most especially the EpCAM(+) cells. These results suggest that HLs might be a novel nanomedical therapeutic agent to target CSCs in liver cancer therapy | [178] |
| LINV or fusing synthetic LPs with tumor-derived nanovesicles (TNVs) | 4T1 BC, lung cancer, melanoma | DOX | A simple extrusion process was used to efficiently fuse TNVs with LPs, resulting in the fabrication of LINVs. Using the solvent evaporation approach, a lipid film was produced with a molar ratio of 4:1:4 of DOPC, mPEG2000-DSPE, and cholesterol. The length of the LINVs was about 166.4 ± 1.9 nm, with a PDI of 0.118 ± 0.023. A ζ-potential of LINVs of −19.7 ± 1.4 mV was observed | By delivering DOX to tumor tissue and successfully inducing an immune-stimulating cell death response, DOX@LINV may increase a tumor's immunogenicity due to its potential for homologous targeting. Simultaneously, DOX@LINV's intrinsic danger signals and retained tumor antigens stimulated dendritic cells and initiated an antigen-specific T-cell immune response | [179] |
| Cancer cell HLs | Lung cancer | SCExo@PTX | The production of lung-targeted LPs included the solvent evaporation of DOTAP and DLin-MC3-DMA. The hybrid nanovesicles (Lip-CExo) were produced by thin-film hydration and extrusion through a 0.2 μm polycarbonate film for both the LPs and the MSLN/PD-L1 CAR-T Exos solution. The findings showed that the encapsulation efficacy of LPs was about 93.6% and that of Lip-CExos was approximately 78.6% at a PTX concentration of 400 μg/mL. Compared to CAR-T Exos's EE of 36.7%, this was much superior. It is important to note that PTX loading had no discernible effect on Lip-CExo's ζ-potential | In a CT-26 model of metastatic lung cancer, Lip-CExo@PTX increased the survival rate of animals with tumors. Therefore, by progressively directing distribution to tumor cells, Lip-CExo@PTX may augment the anti-cancer effects of PTX, providing a potential immunochemotherapeutic method for lung cancer | [180] |

**Table 5** (continued)

| Liposomes | Cancer | Treatment agent | Characteristics of hybrid liposomes | Explain | References |
|---|---|---|---|---|---|
| Hybrid micelle-in-LP system | BC | Quercetin (Que) and paclitaxel (PTX) | As anticipated, the average particle size of RPM was 18.2 nm, while the size of RPM@NLQ was 103.1 nm, confirming the aforementioned criteria. Additionally, the double-layer structure of RPM@NLQ and the uniform spheres of RPM and RPM@NLQ shown by TEM were further validated. RPM and RPM@NLQ had ζ-potential of −3 and 11.1 mV, respectively. Interestingly, RPM@NLQ's EE capacity was 92.30% for Que and 96.64% for PTX | Cancer-associated fibroblasts (CAFs) are a notable subset of stromal cells inside the tumor microenvironment (TME) that have been implicated in drug transport and tissue penetration. By successfully preventing CAFs from passing through the physical barrier, medicinal medications may be absorbed and stored more efficiently, enhancing therapeutic effects | [181] |
| LP-and-red blood cell (RBC) combination | Lung tumor | PTX | The conventional thin-film method was used to create LPs. For their study, researchers created two types of LPs: those containing 1,2-dipalmitoyl-sn-glycero-3-phosphocholine (DPPC) and those containing 1,2-dioleoyl-Sn-glycero-3-phosphoethanolamine (DOPE), which are pH-sensitive. Lipo-DPPC and Lipo-DOPE, which are 146.1 ± 9.03 and 163.7 ± 5.25 nm, respectively, and have thin size distributions. The SEM images revealed that the LPs had a naturally concave form, much like the control RBCs. At a sodium chloride concentration of 0.510 ± 0.002%, the RBCs control discharged 50% of its hemoglobin, in contrast to the RBCs-LPs, which released the same amount of hemoglobin at the same salt concentration | In contrast to the normal liposomal DDS, which showed 5–8% tumor accumulation and partial enrichment in the lung, the DOPE attached/fusion RBCs showed around 0.7% tumor accumulation. Thus, RBC–LP composite DDS may improve liposomal tumor accumulation and blood circulation, indicating the potential therapeutic use of autologous RBCs in the treatment of cancer | [183] |

**Table 5** (continued)

| Liposomes | Cancer | Treatment agent | Characteristics of hybrid liposomes | Explain | References |
|---|---|---|---|---|---|
| These sEVs and LPs were fused via membrane fusion to produce hybrid particles | BC | miR-21 inhibitor | The LPs that included DPPC: Dodecanyl PE: PEG 6000 were made by sonication after a traditional thin-film hydration method. The hybrid particles' diameter (139.3 ± 7.1 nm) was marginally greater than that of individual LPs or sEVs when measured with NTA. The hybrid particles' spherical shape was similar to that of sEVs and LPs. The engineered cancer sEV-derived modified hybrid nanoparticles showed improved drug loading ability (33.75 and 43.88% higher than LPs and sEVs, respectively), treatment efficacy (91.58 and 79.26% cell migration inhibition rate for miR-21 inhibitor and GEM, respectively), and enhanced targeting ability (52.23% higher than unmodified hybrid particles) | Treatment efficiency improvements of > 90% and cell migration inhibition rates of 91.58 and 79.26%, respectively, for the miR-21 inhibitor and gemcitabine demonstrate the enhanced effectiveness of this delivery strategy | [184] |

1,2-dimyristoyl-sn-glycero-3-phosphoethanolamine–diethylene triamine pentacetate acid–gadopentetate dimeglumine (DMPE-DTPA-Gd) combination, a particular kind of multifunctional HL is produced. In aqueous conditions, the HL demonstrated a restricted size distribution and great structural stability. MRI revealed that after tail vein injection, HL efficiently accumulated in the mice's subcutaneous CT-26 tumor. Furthermore, PTT may successfully ablate a tumor while being guided by an MRI. Therefore, theranostic nanoplatform loaded with MRI-visible PTT agents shows promise for efficient cancer therapy [189].

In another study, researchers explored theranostic LPs' in vitro evaluation, characterization, and preparation. It is well known that L–QD hybrid vesicles have a lot of promise as cell imaging nanoconstructs. Liposomal-topotecan (L-TPT) helps achieve this goal by prolonging the time that TPT accumulates in tumors and protecting against systemic clearance. Hydrophobic CdSe/ZnS QD and TPT were found in the inner core of LPs and the bilayer membrane, respectively. DLS, ζ-potential measurements, and fluorescence/absorption spectroscopy were used to ascertain the vesicle size, charge, and spectroscopic characteristics of the LPs. Moreover, the discharge of the substance was investigated at both neutral and acidic pH levels. One of the most used techniques for determining drug release from NPs, the dialysis method, was used to examine the in vitro drug release profile of L-QD-TPT. The study was performed at 37 °C under the circumstances of a tumor microenvironment (pH 5.6) and normal human tissue (pH 7.4). Compared to neutral circumstances, the acidic environment resulted in a higher release of TPT. After a little first burst in the first four hours, the medication was administered at a reduced rate throughout the next 32 h. TPT release rates were 39% at pH 7.4 and 45% at pH 5.6 after 32 h. The TPT's greater solubility with lowering pH due to protonation is responsible for the higher release rate at an acidic pH. Flow cytometry and fluorescence microscopy were utilized to determine the intracellular distribution and cellular assimilation of the TPT-loaded L–QD formulation. Using the 3-(4,5-Dimethylthiazol-2-yl)−2,5-diphenyltetrazolium bromide (MTT) assay, the cytotoxicity of the formulations on HeLa cells was evaluated in vitro. QD-micelles showed almost no toxicity in the concentration range of 0–25 μg/mL in HeLa and A549 cell lines exposed for up to 24 h when CdSe/ZnS QDs were encapsulated in phospholipid micelles based on phosphoethanolamine (polyethylene glycol). In contrast, L–TPT and L–QD–TPT clearly showed toxic effects on HeLa cells when compared to free TPT for 24 h. The reason for this is that the cells were able to absorb L-TPT and L-QD-TPT more efficiently, and the concentration of TPT released from LPs is somewhat higher than that of free TPT. The findings showed that the TPT-loaded L-QD hybrid has good physicochemical properties and shows potential as a multipurpose delivery system that may concurrently deliver therapeutic and diagnostic chemicals [190].

Researchers clarified the therapeutic effects of HLs made of polyoxyethylene dodecyl ether ($C_{12}(EO)_{25}$) and L-α-dimyristylphosphatidylcholine (DMPC) and the capacity of an HL-containing fluorescent probe to identify cancer in orthotopic graft model mice of BC (MDA-MB-453). Researchers used the sonication process to create an HL made up of 90 mol% DMPC and 10 mol% $C_{12}(EO)_{25}$. HL's anti-tumor properties were studied in vivo using mice that received orthotopic MDA-MB-453 cell grafts. Regarding HL's potential as a BC treatment, it caused apoptosis and slowed the development of MDA-MB-453 cells. In orthotopic transplant model mice with BC, the relative tumour weight was considerably decreased by intravenous administration of HL. This effect was caused by the induction of apoptosis, as the TUNEL assay showed. MDA-MB-453 cells exhibited a greater accumulation of HL carrying a fluorescent probe (ICG) in terms of BC detection, but normal breast cells did not exhibit any accumulation of HL/ICG. Increased HL/ICG accumulation was seen in the tumours of orthotopic transplant model mice for BC. HL and HL/ICG may be interesting options for theranostic targets due to their therapeutic effects and ability to detect illness in orthotopic graft model mice of BC (MDA-MB-453). Researchers showed that HL had a hydrodynamic diameter (*dhy*) of less than 100 nm and a restricted, isolated dispersion. For over a month, HL stayed stable. However, after 14 days, DMPC LPs became unstable and precipitated. DMPC LPs reduced MDA-MB-453 cell growth with an IC50 of 413 μM. In contrast, the IC50 value of 169 μM for HL-treated MDA-MB-453 cells was almost one-third that of DMPC LPs. HL markedly inhibited the proliferation of MDA-MB-453 cells. The apoptotic DNA rate in MDA-MB-453 cells increased dose-dependently to 72% after HL treatment. However, the rate of apoptotic DNA in MDA-MB-453 cells treated with DMPC LPs was 4%. In contrast, there was less ICG accumulation in the tumors of the BC orthotopic graft model mice 24 h after the injection of DMPC/ICG and C12(EO)25/ICG. The green fluorescence of ICG from the BC orthotopic graft model mice disappeared 24 h after they were injected with ICG alone. In BC orthotopic transplant model mice, HL may accumulate in tumour cells on the mammary gland over an extended period [191].

Researchers identified the EGFR as a prominent target for the treatment of CRCs and programs death ligand-1

(PD-L1) as a desirable target for CRC immunotherapy. Researchers record how liposomal nanohybrid cerasomes with porphyrin are made. These centrosomes are conjugated with MRI contrast DOTA-Gd and IRDye800CW and decorated with cetuximab, an anti-EGFR antibody. Gd-DSPE-DOTA, DSPE-IRDyeCW800, DSPE-PEG-EGFR, and cerasome-forming lipids were dissolved in DMSO in a molar ratio of 70:25:0.1:5. The ethanol injection technique was used to create porphyrin-loaded cerasomes that were cetuximab-targeted (EGFR-CPIG). The porphyrin encapsulation effectiveness of both EGFR-CPIG and IgG-CPIG surpassed 86% without a discernible difference, and both showed a negative ζ-potential (around 40 mV), which mainly was obtained from the cerasome siloxane framework. TEM showed that both kinds of porphyrin-loaded cerasomes were uniformly spherical, with a size range ranging from 80 to 100 nm. Researchers demonstrate that this was in line with the DLS measurement, which showed that both particles had a narrow size distribution and were about 90 nm in size. They serve as a tool for both in vivo tumor identification and PDT. Moreover, PD-L1 was added as an adjuvant treatment. An assessment was conducted on the combination anticancer activity of PDT and PD-L1 immunotherapy. EGFR-targeted NPs enabled targeted imaging to see tumors. In comparison to PD-L1 immunotherapy and simultaneous but nontargeted NPs administration with laser irradiation, concurrent EGFR-targeted PDT, and PD-L1 immunotherapy were more effective against tumor development. EGFR-targeted NPs, therefore, have shown significant promise as a dual-modality imaging-guided precision PDT in conjunction with immunotherapy. According to researchers' findings, the EGFR-CPIG group's relative signal increase at 24 h was almost 1.71 times greater. According to the results, EGFR-CPIG's active and specific tumor-targeting impact seems to have raised the MRI signal intensity at the tumor location when compared to the IgG control. For use in tumor treatment, NPs with minimal toxicity and high effectiveness are often favored. Researchers assessed systemic toxicity dynamically across a 21-day treatment period using mouse body weight as an indicator. Mice in the various treatment groups showed no signs of aberrant behavior or significant body weight reduction. Additionally, there was no visible tissue damage or harmful consequences on the kidney, liver, spleen, heart, or lung. Overall, researchers implied that the EGFR-CPIG NPs have the potential for clinical use in addition to having high biocompatibility [192].

Researchers explored the easy production and use of a targeted, dual therapeutic Au nanorods-LP (GNR-LP) nanohybrid for chemotherapy and imaging-guided PTT. Researchers created the nanohybrid using the film hydration and sonication procedure. GNR-LP nanohybrids were partially formed by the self-assembly of lipid bilayers, including surface-modified GNRs and a combination of dipalmitoylphosphatidylcholine (DPPC) and 1, 2-stearoyl-sn—glycerol-3-phosphocholine (DSPC). The dual therapeutic GNR-LP nanohybrid is made up of LPs loaded with DOX and supported by GNR. PEGylated folic acid (PEG-FA) was added to the GNR-LP nanohybrid surface in order to further target the overexpressing folate receptors in cancer cells. The FTIR spectra confirmed the GNR-LP nanohybrid's surface functionalization with PEG-FA. In addition to acting as a photothermal agent and improving drug release in the intracellular environment of cancer cells, GNRs provide LPs mechanical strength since they are decorated on both the inside and the outside of bilayer surfaces. The created nanohybrid shows an outstanding response for synergistic chemophotothermal treatment when compared to either chemotherapy or PTT alone. The NIR response, efficient cell uptake, disintegration of the GNR-LP nanohybrid, and the combined therapeutic effects of photothermal and chemotherapy on BC cells MDA-MB-231 are investigated in order to improve the development of a biocompatible nanomaterial-based multifunctional cancer theranostic agent. The kinetics of drug release within and outside of cells were investigated by researchers using pH 7.4, 5, 4, 2, and 2 with NIR irradiation, respectively. At a pH of 7.4, which is neutral, researchers observed very little drug release (~4%). However, more than half of the drug was released in the late endosomal conditions (pH 2) and the cancer cell interior environment (pH 4, 5) due to the nanohybrid's breakdown in the cancer-mimicked environment. 24-h tests revealed this. Nanorods detach from liposomal nanoparticles, and lipid self-assembly destabilizes at high protonation strengths at low pH (pH 2 to 5). This leads to the dissolution of the nanohybrid and the observed improved drug release ability in the cancer cell interior. Fluorescence microscopy of cancer cells treated with nanohybrids and loaded with DOX further confirmed the enhanced drug release. In addition, researchers found that at pH 2, when the NIR-exposed drug-loaded nanohybrid completely disintegrated, there was about 100% drug release within 12 h of kinetic time. The incorporation of DOX into a PEG-FA GNR-LP nanohybrid (200 μg/mL) and its capacity to target and localize inside cells were confirmed by incubating 100 μL of the hybrid with MDA-MB 231 [193].

Another study unveiled that mesoporous silica NPs (MSNs) have been extensively investigated as a prospective flexible drug-delivery platform due to their manifold advantages. At present, gadolinium (Gd) doped MSNs, which serve as a T1 MRI contrast agent, symbolize an innovative theranostic nanocomposite that has garnered

considerable scientific attention. However, concerns regarding MSN dispersibility and medication leakage persist. Given these circumstances, researchers constructed a triple-modal imaging-guided nanoplatform that is activated by NIR irradiation. To achieve this, they conjugated DOX@Gd-doped MSNs with ICG-loaded TSL, which they referred to as DOX@GdMSNs-ICG-TSLs. On this platform, ICG may augment the efficacy of photodynamic and photothermal therapies. Meanwhile, photoacoustic imaging (PAI) and NIR fluorescence imaging (NIRFI) may be enabled. In conjunction with Gd's MRI capability, NIRFI and PAI from ICG were thus effectively utilized for triple-modal imaging. To mitigate DOX leakage and improve cellular absorption, the coating of DOX@GdMSNs with folic acid-modified TSL was investigated. ICG-TSLs could rupture and discharge DOX if they are subjected to NIR light, which induces thermal generation in ICG. Given these circumstances, the multifunctional nanocomposite appeared to be a promising theranostic nanoplatform with the potential to revolutionize cancer therapy. Due to the nanocomposite's outstanding photothermal performance, scientists have been studying its impact on in vivo PTT. Injecting DOX@GdMSNs-ICG-TSLs and various control formulations intravenously into 4T1 tumor-bearing mice was followed by irradiation of the tumor locations using an 808 nm laser at a power density of 1.5 W/cm2. Using an infrared camera, researchers took full-body thermal pictures in real-time. When comparing the thermal images that were taken, it was found that the temperature at the tumor site in the group that was treated with DOX@GdMSNs-ICG-TSLs rose significantly, reaching a maximum of 55 °C within 4 min. The nanocomposite's capacity to rapidly increase temperature, in comparison to other groups, showed that it might contribute to the PTT effect and destroy tumor cells. A more consistent and upward trend in body weight was seen in the DOX@GdMSNs-ICG-TSLs + NIR treatment group compared to the PBS, DOX@GdMSNs, and ICG-TSLs + NIR groups. The percentage survival curves show that researchers ideal therapy achieved an acceptable survival rate. Additional evidence includes images of both the control group and tumor-bearing mice treated with DOX@GdMSNs-ICG-TSLs + NIR. The mice who were given DOX@GdMSNs-ICG-TSLs + NIR showed apparent tumor ablation when compared to the PBS group, confirming the impressive anti-tumor impact. The main organs, including the heart, liver, spleen, lungs, and kidneys, were not significantly affected by the DOX@GdMSNs-ICG-TSLs + NIR treatment group as compared to the control group. While DOX@GdMSNs-ICG-TSLs had a favorable anti-tumor impact in tumor tissue sections, there was noticeable widespread tumor necrosis and a reduction in intercellular space [194].

Here, scientists assessed whether liposomal DOX and Au nanoshell (NS)-based PTT may enhance colon cancer survival in a rodent model. First, tumor-bearing animals underwent NS-based PTT. The optimal injection time after PTT was then determined by tracking the accumulation of radiolabeled LPs inside the tumor by injecting them at various timepoints. Additionally, following PTT, the distribution of LPs inside the tumor was observed using fluorescent LPs. Lastly, Researchers mixed PTT and DOX-loaded LPs and tracked tumor development and survival to see how the treatment plan affected the mice. Liposomal accumulation in the tumor was greatly enhanced by PTT, but only when the LPs were administered right after following the treatment. The majority of the LPs accumulation occurred in locations close to the ablated zones. The mice showed improved survival and a slowing in tumor development when PTT and liposomal DOX were administered together [195].

Researchers detailed the invention of a multifunctional light/magnetic HT-triggered DDS utilizing thermo-sensitive MLs modified with methotrexate (MTX) (MTX-MagTSLs). In this system, magnetic NPs (MNPs) modified with oleic acid and MTX may be utilized for both biological and magnetic targeting. Cy5.5, a lipophilic fluorescent dye, and MNPs are encapsulated within the bilayer of LPs during this time. Utilizing an alternating magnetic field (AMF) enables the discharge of DOX and produces a dual-imaging effect that validates the accumulation of MTX-MagTSLs within the tumor area. The results demonstrated that MTX-MagTSLs exhibited a significant ability to selectively target HeLa cells and animals harboring HeLa tumors in vitro and in vivo. Moreover, when combined with local precise NIR laser irradiation (808 nm) (DUAL-mode), the heating effect of MTX-MagTSLs was 4.2 times amplified compared to AMF or laser stimulation alone, allowing the phase change temperature (Tm) of MTX-MagTSLs to be reached in 5 min. As a consequence, the delivery of Dox to the tumor site was considerably improved, and cancer synergetic theranostics became more precise. Researchers showed that there was a 44% release of dox from MTX-MagTSLs in PBS at 37 °C but an 83% release at 45 °C after 24 h. The free Dox, on the other hand, released its full potency after only one hour and reached a concentration of around 97% in PBS after twenty-four hours. According to SAR data, researchers indicated that a considerable improvement in Dox release could be achieved by applying AMF and laser simultaneously. Researchers also demonstrated that the temperature could be regulated to control the Dox release from MTX-MagTSLs. Both the free Dox and MTX-MagTSLs groups

had their maximum Dox plasma concentration just after injection. Still, after intravenous administration, the free Dox group had a substantially faster decline in concentration than the MTX-MagTSLs group, according to the pharmacokinetics study. The findings might be attributed to the remarkable stability of the long-circulating TSLs that were generated at room temperature. These TSLs will also serve as a benchmark for the in vivo treatment cycle that animals undergo two days later [196].

An investigation used the combination of superparamagnetic iron oxide NPs (SPIO NPs) and PTX to develop a tumor-targeted, pH-responsive theranostic LP modified with the peptide $H_7K(R_2)_2$, including PTX and SPIO-SSL-H7K(R2)2. Researchers showed that the polydispersity of PTX/SPIO-SSL-$H_7K(R_2)_2$ was 0.197 ± 0.015, and the particle size was 168.30 ± 2.80 nm. The PTX/SPIO-SSL-$H_7K(R_2)_2$ compound has a ζ-potential of − 10.50 ± 0.44 mV. In PTX/SPIO-SSL-H7K(R2)2, the PTX entrapment efficiency was more than 90%. The targeting ligand employed was $H_7K(R_2)_2$, the MRI agent was SPIO NPs, and the anticancer drug was PTX. The PTX/SPIO-SSL-$H_7K(R_2)_2$ was produced using a thin-film hydration method. The characteristics of PTX/SPIO-SSL-$H_7K(R_2)_2$ were evaluated. Analyzed comprehensively in both laboratory settings and living organisms, the impact, imaging capabilities, and effectiveness against tumors of PTX/SPIO-SSL-$H_7K(R_2)_2$ were studied using human BC MDA-MB-231 cell types. Researchers tested PTX-SSL, PTX/SPIO-SSL, and PTX/SPIO-SSL-$H_7K(R_2)_2$ in buffer solutions with a pH of 6.8 and 7.4 to see how much PTX they released in vitro. Both the 6.8- and 7.4-pH buffer solutions showed almost comparable amounts of released PTX from PTX/SPIO-SSL-$H_7K(R_2)_2$. The outcomes for PTX-SSL and PTX/SPIO-SSL were comparable. The in vivo targeting impact of DiR LPs modified with $H_7K(R_2)_2$ was tested in mice carrying the MDA-MB-231 tumor. Where fluorescent DiR is located in tumors of MDA-MB-231 mice. Compared to animals treated with DiR/SPIO-SSL, those treated with DiR/SPIO-$H_7K(R_2)_2$ had a higher DiR fluorescence signal at the tumor location across all periods of observation. Their results from live MRI, lab flow cytometry, and live imaging confirmed the pH-sensitive characteristic of $H_7K(R_2)_2$ in the MDA-MB-231 cell line both in living organisms and in a controlled environment. The theranostic effect of PTX/SPIO-SSL- $H_7K(R_2)_2$ was confirmed in the MDA-MB-231 tumor-bearing animal by in vivo MRI and in vivo anticancer activity results [197].

Photothermal therapy (PTT), an emerging anti-cancer therapeutic approach that utilizes laser irradiation to generate HT for ablating cancer cells, was investigated. It has been reported that Au-coated liposomes (AL) are an efficacious PTT agent with excellent biocompatibility and excretory properties. Nonetheless, Au components that are exposed to LPs can induce instability in vivo and impede subsequent functionalization. Researchers synthesized a theranostic dual-layered nanomaterial through the process of the liposomal layer to Au-coated liposomes (LAL) attachment, PEG attachment, and radiolabeling. LAL is capable of being imaged in vivo when it is functionalized with PEG, and radioisotope labeling is utilized to enhance its in vivo stability. Researchers revealed that the average ± standard deviation diameters of AL and LAL, as measured by TEM, were 61.02 ± 29.22 nm and 72.84 ± 22.49 nm, respectively (n = 20). Investigators measured three times in PBS and the hydrodynamic diameters of AL and LAL using DLS. All three measurements were quite close to each other, and the hydrodynamic size of the LAL was 67.32 ± 22.65 nm. Each of the three separate experiments yielded different results for the hydrodynamic size of AL: 109.5 ± 52.92 nm, 73.44 ± 41.24 nm, and 49.38 ± 26.95 nm, respectively. The fact that AL showed a reduced ζ-potential of − 23.7 mV suggests that the Au coating was influential on the LP since bare Au NPs typically have a low ζ-potential of 20 to 40 mV. The ζ-potential was raised to − 17.3 mV due to the PEG moiety of the outer liposomal layer as AL extended across an additional liposomal layer. Functionalized LAL exhibits stability under physiological conditions, and in vivo PET imaging demonstrates that $_{64}$Cu-LAL, which is labeled with $_{64}$Cu, possesses adequate blood circulation and an effective tumor targeting capability of 16.4%ID $g^{-1}$. Additionally, in the orthotopic BC mouse model, LAL injected intravenously exhibits superior tumor targeting, temperature elevation in vivo, and PTT effect in comparison to AL. The rate at which LAL inhibited tumor growth was 3.9 times that of AL. On account of its notable stability, capacity for in vivo imaging, and efficacy in targeting tumors, LAL exhibits potential as a theranostic PTT agent [198] (Fig. 6).

EXO-HLs-based vehicles (ELVs) have enormous potential as carriers of cancer treatments. Still, there aren't many efficient theranostic probes that can recognize the lipid bilayer membrane of these vehicles, allowing researchers to follow their biodistribution and provide potent therapy precisely. In a study, lipophilic NIR-II cyanine dyes with muscle donor strength are designed and synthesized to label the lipid bilayer membrane of ELV for NIR-II fluorescence image-guided and targeted NIR-II PTT of subcutaneous glioblastoma. This approach capitalizes on the inherent deep penetration and high effectiveness of photothermal treatment and fluorescence imaging in the second NIR window (NIR-II). Even though the diameters of NIR-C12-L and NIR-C12-EL were 138 and 145 nm, respectively, the PDI value for NIR-C12-EL is lower than that of NIR-C12-L and EXO

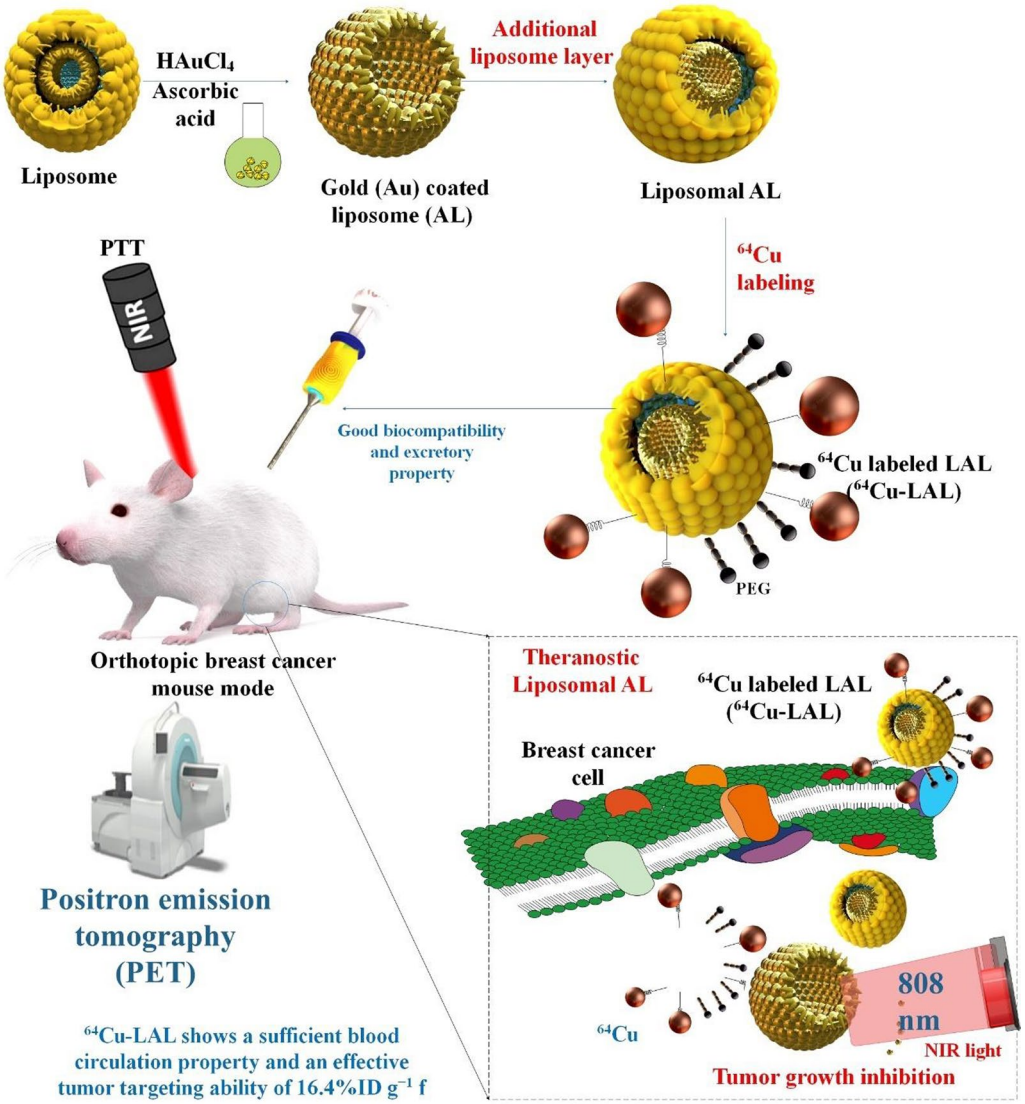


**Fig. 6** Diagram illustrating the experimental protocol for $_{64}$Cu-labeled LAL ($_{64}$Cu-LAL) for in vivo imaging and LAL for photothermal treatment (PTT) [198]

due to the membrane's repeated extrusion. Furthermore, the NIR-C12-EL sample showed ζ-potential, which is in the middle of the NIR-C12-L and EXOs, and suggests that the two particle types successfully fused. Lipid films are hydrated and subsequently extruded to produce the produced extracellular vesicles (ELV) with NIR-C12 labeling, cyclic arginyl glycyl aspartic acid decoration, liposomal PEGylation, and biological EXO activity. Because of its excellent NIR-II photoconversion efficiency (62.28 r), biocompatibility, light-harvesting capabilities, and targeting capacity to identify and ablate tumours, NIR-C12-EL has a lengthy half-life in mice treated with it and continuously exposed to 1064 nm laser irradiation. Researchers provided information on the creation of lipophilic NIR fluorescent probes for use in labeling ELVs and theranostic nanoplatforms for targeted glioblastoma treatment [199].

As a result of the advancements and benefits of MRI nano-contrast agents (CAs), there has been a proliferation of theranostic NPs based on MRI. As a biosafe nanocarrier, LPs have been utilized in phase III cancer treatment trials. The present investigation utilized LPs as nanocarriers to co-encapsulate PTX, an anticancer drug, and MRI nano-contrast agent poly(ethylene glycol)-grafted manganese oxide (PEG-MnO) to create an innovative theranostic nanocomplex. Researchers used the thin film hydration approach to create blank LPs, LP-PEG-MnO nanocomplexes, and LP-PEG-MnO-PTX nanocomplexes. Then,

the membranes were extruded. The first step was the preparation of PEG-MnO NPs. Both the blank LPs and the LP-PEG-MnO nanocomplex, as shown in the TEM, were round and had an average size of 120.89 nm and 133.87 nm, respectively. The presence of black pigmentation inside the LP-PEG-MnO nanocomplex core, as contrasted with the white LPs, signified the effective encapsulation of PEG-MnO NPs. The nanoprobe AS1411-LP-PEG-MnO-PTX, which underwent additional modification with the AS1411 Apt, demonstrated promise as a concurrent MRI diagnostic and therapeutic agent for renal carcinoma in vitro and in vivo. In contrast to PEG-MnO nano-CA, LP-PEG-MnO, and AS1411-LP-PEG-MnO demonstrated an extended retention duration in the tumor region and a more pronounced enhancement of MR contrast within the tumor. Researchers shown that with a half-life of 333.35 min—5.6 times that of PEG-MnO NPs (59.76 min)—LP-PEG-MnO nano complexes were more effective in accumulating in tumor tissue to increase MRI sensitivity. The presence of LPs and PEG coatings may account for such an extended circulation duration. In addition to increasing the contrast enhancement in the tumor, encapsulating PEG-MnO NPs into LPs might prolong their retention period. The addition of the AS1411 Apt enhances this impact even more, which is excellent news for their potential use in tumor imaging. More significantly, the tumor growth inhibition effect and the MRI effect were both improved with the addition of the AS1411 Apt, demonstrating its potential as a theranostic nanoprobe for renal carcinoma [200].

To enhance cancer cell targeting and dual fluorescence imaging, Jang et al. devised mesoporous silica core/shell magnetic NPs encased in lipid polymers (Lipo(MNP@m-$SiO_2$)) and supplemented with the hydrophilic organic pigment Texas red (TR). The targeting efficiency of the novel system was assessed through the application of Her2/neu antibodies onto Lipo(TR)(MNP@m-$SiO_2$(FITC)) surfaces. Despite the fact that the 200-nm LPs were somewhat more giant after incorporating the dye-labeled MNPs, it is very improbable that this process would significantly alter the fundamental structure of the LPs. Surface charges of − 14 mV for MNP@ m-$SiO_2$, − 50 mV for LPs, and − 49 mV for Lipo(MNP@m-$SiO_2$) were recorded, respectively. Even at high concentrations, normal 3T3 fibroblast and SKBR-3 BC cells were not adversely affected by Lipo(MNP@m-$SiO_2$) after 24 h of exposure; this indicates that the material is biocompatible. The biocompatibility of Lipo(MNP@m-$SiO_2$) was shown when no acute cytotoxicity was seen, even when administered a high metal dosage of 60 μM. The nanohybrid magnetic-liposomal system did not target BC cells after six hours at 37 °C; however, this was remedied when the temperature was decreased to 4 °C. This demonstrates that cellular internalization is influenced by both temperature and duration. The findings provided support for the application of Lipo(MNP@m-$SiO_2$) as a precise DDS in patients with Her2/neu BC. However, additional research is required to examine its behavior in living organisms and monitor the efficacy of its therapy [201] (Table 6).

## Advances and disadvantages of theranostics hybrid liposome in cancers

Nanoscale vesicles have emerged as a multifunctional medium for the conveyance of diverse categories of diagnostic and anticancer agents [203]. Vesicular carriers, such as polymersomes, LPs, and peptide-based vesicles, have shown encouraging properties that might lead to advances in nanomedicine [204]. LPs have garnered considerable interest thus far for a variety of biomedical applications; nevertheless, their morphological stability remains inadequate [205]. However, even with the quick advancements in the creation and use of innovative therapeutic nano agents, a significant obstacle remains the regulated distribution of drugs via these nanocarriers inside intricate biological systems [206].

Furthermore, several additional significant challenges, such as morphological instability in blood circulation, inadequate drug loading, and off-target drug release, impede their in vivo therapeutic effectiveness [207]. LPs offer superior pharmacokinetics and biodistribution of theranostic drugs in comparison to numerous alternative carriers due to their high agent loading efficiency, high stability in biological environments, and adjustable release kinetics facilitated by biocompatibility and responsiveness to stimuli [208]. Nanoscale DDS, including LPs, have been utilized extensively in the treatment of cancer. Chemotherapy has benefited from their ease of surface functionalization, targeted delivery, and ability to stabilize drugs in vivo [209].

Nevertheless, the indicated systems and existing therapeutic methodologies for cancer are beset by significant constraints that impede their practical implementation [210]. The previous constraints might be mitigated through the implementation of combinatorial hybrid systems [211]. By using this strategy, hybrid vesicular systems may combine the advantages of numerous carriers into a single structure, resulting in a higher therapeutic index and better clinical outcomes [212]. Vesicular and micellar molecules, which make up HLs, may be easily synthesized by sonicating the molecules in a buffer solution without introducing any organic solvents [172]. Liposomal delivery methods have gained significant acceptance due to their ability to alter the pharmacokinetics of numerous medications, especially in the context of cancer-targeted therapy [213]. Regardless of the various approaches used or whether targeted or active distribution was the goal, these nanohybrid systems provide

**Table 6** Theranostic hybrid liposome in cancer detection and treatment

| Hybrid liposomes | Cancer | Detection agent | Treatment agent | Characteristics of hybrid liposomes | Theranostic explain | References |
|---|---|---|---|---|---|---|
| Liposome–quantum dot (L–QD) hybrid vesicles | HeLa cells | L–QD hybrid | Liposomal-topotecan (L-TPT) | Researchers selected cholesterol and distearoylphosphatidylcholine (DSPC) in a 7:3 ratio. The plain LPs had an average size of around 132 nm. The size of the LP increased by about 6 nm after the trapping of QDs in the lipid bilayer. The encapsulation of TPT into L-QD had no impact on the size. In addition, researchers evaluated the LPs for their storage stability. No notable variations in size distribution, ζ-potential, or PDI were seen at 4 °C throughout the two months | The physicochemical features of the TPT-loaded L-QD hybrid are good, and it shows potential as a multifunctional delivery vehicle that may concurrently transport therapeutic and diagnostic chemicals | [190] |
| Polyoxyethylene dodecyl ether (C12(EO)25) and L-α-dimyristylphosphatidylcholine (DMPC), as well as the capacity of an HL-containing fluorescent | Breast cancer (BC) | HL containing a fluorescent probe (ICG) | Anti-HER-2 antibody (trastuzumab) targeting HER-2 | LPs that combine DMPC and Tween 20 form a hybrid. Researchers used sonication to prepare HL. A limited and single distribution was observed for the hydrodynamic diameter (*dhy*) of HL, which was less than 100 nm. For about a month, HL remained steady. While DMPC LPs were stable for up to 14 days, they eventually precipitated | HL and HL/ICG may be excellent options for theranostic targets due to their therapeutic advantages and ability to recognize (detect) illness in an orthotopic graft model mice of BC (MDA-MB-453) | [191, 202] |

**Table 6** (continued)

| Hybrid liposomes | Cancer | Detection agent | Treatment agent | Characteristics of hybrid liposomes | Theranostic explain | References |
|---|---|---|---|---|---|---|
| Liposomal nanohybrid cerasomes with porphyrin | Colorectal malignancies (CRCs) | IRDye800CW and MRI contrast DOTA-Gd | Cetuximab, an anti-EGFR antibody | Gd-DSPE-DOTA, DSPE-IRDyeCW800, DSPE-PEG-EGFR, and fearsome-forming lipids were dissolved in DMSO in a molar ratio of 70:25:0.1:5. With no discernible difference, the porphyrin encapsulation effectiveness of EGFR-CPIG and IgG-CPIG both above 86%, and negative ζ-potential of around 40 mV was clearly seen in both. The two varieties of porphyrin-loaded cerasomes were uniform in size and shape, measuring 80 to 100 nm in diameter | Because GNRs are adorned on both the inside and outside of bilayer surfaces, they not only function as a photothermal agent and enhance drug release in the intracellular milieu of cancer cells, but they also provide LPs mechanical strength | [192] |
| Au nanorods-liposome (GNR-LP) | BC cells MDA-MB-231 | Au nanorods | DOX | Lipidic film self-assembly GNR-LP nanohybrids were helped to develop by DPPC and DSPC bilayers mixed 1:9 with surface-modified GNRs. Microscopic methods were used to establish the spherical shape of the GNR-LP nanohybrid, which had an average diameter of 170 nm ± 10 nm. The hydrodynamic size was estimated to be around 160–180 nm | However, GNRs enhance drug release in the intracellular milieu of cancer cells and act as a photothermal agent. However, since they are adorned on the inside and outside of bilayer surfaces, they also provide LPs mechanical strength | [193] |

**Table 6** (continued)

| Hybrid liposomes | Cancer | Detection agent | Treatment agent | Characteristics of hybrid liposomes | Theranostic explain | References |
|---|---|---|---|---|---|---|
| MTX-MagTSLs | HeLa cells | Cy5.5, a lipophilic fluorescent dye | DOX | A thermo-sensitive magnetoliposome modified with MTX, consisting of the following components: DPPC, chlorophyll, SA, DSPE-PEG2000, and DSPE-PEG2000-MTX. A thin film dispersion approach was used to manufacture MTX-MagTSLs utilizing MNPs and TSLs. Then, Dox was encapsulated using the ammonium sulphate gradient loading method. With MTX-MagTSLs, the EE of MNPs was 87.6 ± 1.83%. Researchers showed that MTX-MagTSLs often clumped together in primitive form, with an initial size of 107.5 ± 1.19 nm and little change after one week (112.3 ± 2.19 nm), as verified by DLS. Primitive ζ-potential was also seen to be approximately 16.8 ± 1.2 mV | This method, which employs an alternating magnetic field (AMF), facilitates the release of DOX and generates a dual-imaging effect that confirms the accumulation of MTX-MagTSLs in the tumor region | [196] |
| CG-loaded TSL | BC (4T1 cells) | Indocyanine green (ICG) | DOX @ Gd doped-MSNs | On average, the DOX@GdMSNs-ICG-TSLs were around 233.8 nm in size. In double-distilled water, the PDI was 0.306. Before adding a serum, the PDI for cell-culture media was 0.291; after adding a serum, it was 0.298. With a ζ-potential of − 25.2 mV, the nanoparticle proved to be very stable | The multifunctional nanocomposite showed promise as a novel theranostic nanoplatforms that might transform the treatment of cancer | [194] |

excellent opportunities for the advancement of combinational treatment modalities [211]. The innovative nanohybrid system forges a new path as a developing drug delivery method; yet, its main drawbacks are the lack of thorough in vivo performance data, evaluations of cellular toxicity and metabolism, and cost and quality concerns [214].

In addition, the word "theranostics" has become essential to cancer research. However, creating theranostic NPs requires a thorough understanding of treatment and detection methods. This expertise comprises comprehension of a range of topics, including toxicity, biocompatibility, and biodegradability of these materials, pharmacokinetics, and pharmacodynamics, elimination of metabolites, compatibility of chemicals utilized, and synthesis parameters about chemicals involved. An ideal theranostic NPs should have the following characteristics: it should accumulate quickly and selectively in the sick cell, provide the optimal amount of medication efficiently, avoid damaging nearby healthy tissue, leave the body quickly, or break down into safer metabolites [215].

Compared to LNPs, both EVs and hybrid LP–EV technologies have substantial barriers to clinical use, particularly for the well-established LP category. When compared to LNPs, their primary drawbacks are low isolation yields, the need to choose the optimal parent cell type, and thorough assessments of both short- and long-term toxicity because of their complicated payloads. LNPs may still be enhanced to satisfy intricate therapeutic requirements. Therefore, more sophisticated LNPs are required, which may target molecules like peptides. It is challenging to load LNPs with all of these prerequisites, particularly when it comes to large-scale, economically viable manufacturing. In fact, LNPs have been used in a few preclinical studies for neurodegenerative diseases; however, these studies are typically stopped in their tracks before they can be published or are unable to demonstrate positive effects on the course of the disease. First and foremost, it is critical to assess their safety since, in clinical trials, they can show toxicity or adverse effects that are not shown in preclinical research. Comprehensive toxicity investigations are thus crucial. Furthermore, it is still challenging to create repeatable production procedures for EVs and LNPs. These platforms' batch-to-batch variability is another major obstacle since it may restrict their size and compliance with reasonable manufacturing procedures [216].

In order to ascertain the medical effectiveness of the hybrid DOX hydrochloride injection, this research will compare it to the reference product Caelyx®. Female patients with ovarian cancer who were slated to begin DOX treatment and whose condition worsened or returned after platinum-based chemotherapy were included in this bioequivalence trial. The trial was multicenter, open-label, balanced, randomized, two-treatment, two-period, two-sequence, single-dose, and the patients ranged in age from 18 to 75. On the first day of period-I chemotherapy, patients received an intravenous infusion of medications at a dose of 50 mg/m$^2$ over an hour, two hours after breakfast. They moved to the other arm of the cycle on day 29. PK studies were performed on both encapsulated and unencapsulated DOX using two separate, validated liquid chromatography-mass spectrometry methods. Neither the test formulations nor the reference formulations were found to have any adverse effects. The pharmacokinetics of both encapsulated and unencapsulated DOX were investigated in 50 participants. Regarding PK metrics, there was no discernible variation between the test and reference items. For encapsulated DOX, the geometric mean ratios (with a 90% confidence range) were Cmax: 92.08–116.46%, AUC0-t: 91.91–108.28%, and AUC0-∞: 93.45–110.05%. Cmax: 92.08–116.46% for DOX that is not encapsulated [217].

The current expansion in the development of NP-based cancer diagnosis, therapy, and theranostics approaches has made absorption, distribution, metabolism, and excretion (ADME) research more relevant for possible FDA approval. Nanocarriers tend to localize in the tumor via leaky tumor vascularization due to the enhanced permeability and retention (EPR) effect. The smaller (sub-200 nm) nanocarriers are great for regulating the EPR effect at the tumor while protecting healthy cells. Additionally, ligands may be grafted onto the surface of nanotransporters to target cancer cells and enhance DDS's pharmacokinetics. Many studies have been conducted on bioinspired NPs. Therapeutic carrier systems may lessen side effects and increase the efficacy of APIs. Common clinical problems with all DDS include undesired toxicity, conducive pharmacokinetics, targeted accuracy, and defective cellular absorption. API distribution to designated areas may not be possible with liposomal formulations. Surface characteristics, material composition, size, and manufacturing method may alter LP formulations' pharmacokinetic characteristics, circulation duration, and biodistribution. The temperature at which the lipid phase changes from an ordered gel phase to a liquid crystalline phase is known as the lipid phase transition temperature (TC). Numerous factors, including lipid head group, hydrocarbon length, charge distribution, and bond unsaturation, are crucial in controlling fluidity, drug release kinetics, and liposomal membrane permeability. The TC is also influenced by the degree of unsaturation; a lipid bilayer that contains lengthy, saturated hydrocarbons is often less permeable. Clearance and pharmacokinetics may also be impacted by the

liposomal formulation technique [218]. Nanocarriers known as EXOs and EXOs-HLs may be bioengineered to improve bio-camouflage, targeting specificity, and API delivery. To minimize delays in clinical approval, it is crucial to study pharmacokinetic features early on when creating EXO-based formulations for both preclinical and clinical usage. This will help anticipate tissue distribution, absorption, and elimination rate. The best way to optimize EXO uptake is the subject of several investigations. Glycoproteins on the surface of EXOs enhance their endocytosis in Caco-2 cells and rat small intestine epithelial cells in vitro and the function of clathrin-mediated endocytosis in the absorption of EXOs in PC12 cells. One possible use of bioengineered EXOs, such as EXO-HLs, is to conceal them from phagocytosis and to keep therapeutic EXOs in circulation for an extended period. The delivery technique is equally critical because it may govern the exosomal-API's transport to the target tissue and circulation throughout the body. Following cellular absorption, EXOs should be able to function in the cytosol and be free from endosome trapping or hydrolase destruction. By incorporating a pH-sensitive fusogenic peptide into tumor-derived EXOs, Morisitha et al. were able to improve the presentation of class I tumor antigens and accomplish cytosolic cargo delivery. Nanocarriers' ADME, efficacy, and toxicity may be predicted using physiologically based pharmacokinetic (PBPK) models, which should include the biochemical, physiological, and physicochemical properties of the drug as well as specific organs or tissues [219, 220].

After that, several clinical trials employing LP-based therapies have been approved to treat various ailments. The success of LP-based remedies can be attributed to the following factors: (1) ease of synthesis, (2) biocompatibility, (3) capability of loading hydrophilic and hydrophobic medications, and (4) prolonged circulation after PEG application. The LP platform has recently been enhanced with the following functionalities: (1) a lipid moiety sensitive to pH and temperature; (2) in vivo imaging probes for PET, SPECT, and optical; and (3) novel agents for photodynamic and photothermal therapies. The LP is considered a highly prospective nanoplatform in the field of theranostics due to its numerous established and recently demonstrated advantages. Thousands of NPs for imaging and therapy, excluding LPs, have been developed since the success of Doxil®. Notwithstanding the unique advantages that these NPs offer in terms of imaging and treatment, they frequently exhibited high-RES recognition, inadequate targeting efficacy, restricted in vivo stability, and toxicity. LPs continue to be considered among the most promising and practicable nanoplatforms due to their extended circulation half-life, long passive targeting efficacy, and biocompatibility. Additionally, research has demonstrated that LPs can be effectively employed to incorporate functionalities, including controlled release capabilities, pharmaceuticals, and various imaging probes. Developing more specialized controlled drug release techniques and identifying practicable solutions to prevent the accelerated blood clearance (ABC) phenomenon that occurs after repeated injections would be the subsequent stages toward developing effective theranostics based on LPs [23]. Preliminary studies indicate that the membrane-engineering approach will provide a unique means of synthesizing EXOs as hybrid nanocarriers that are logically tuned for use in advanced and targeted DDS. There is a drive to develop and improve downstream analytical methods to help identify low-copy targets in liquid biopsies. In the realm of NGS, for instance, larger panels with deeper sequencing depth have been produced. Novel methods like background correction and molecular barcoding have been developed for NGS solutions. The difficulty of stochastic detection of single-digit copy numbers will persist in patients with low-copy targets. For sample collecting and isolation, a front end that is quick and accurate is also required. Therefore, reliable next-generation liquid biopsy diagnostics may be made possible by validated sample collection and isolation kits for exoNA + cfDNA produced under cGMP production. Although liquid biopsies of circulating-Tumour-Cells (CTC) are an effective predictive tool for several cancer types and have been approved by the FDA, the practical use of this technique is still in its infancy. In conclusion, EXOs, detecting agents, and therapeutic medications may be combined in the future to create diagnostic and therapeutic integrated NPs that combine their benefits for use in precision cancer therapies as well as noninvasive diagnostics [220]. In contemporary times, researchers contend that the development of EV-biomimetics via a bottom-up approach is crucial, given that the path to clinical application is more straightforward and secure for completely synthetic, controllable products compared to the implementation of natural EVs. While the literature has provided some commendable instances of EV-biomimetics, further refinement, and optimization are required: it is critical to devise and develop a product that possesses the identical cargo transfer and targeting characteristics of natural EVs, albeit with a simplified composition and functionalization. This necessitates an ad hoc formulation and concentration tailored to the particular case study [221].

Among these considerations for polymer-modified LPs are their potential toxicity, immunogenicity, and interactions with biological systems. A well-established method to improve biocompatibility involves PEGylation, which consists in adding polymers like polyethyleneglycol (PEG) to LPs. By increasing the LP surface's

hydrophilicity, PEGylation shortens the time it takes for the MPS to eliminate the LPs from circulation. It is essential to assess the hemocompatibility of LPs because of their interactions with blood components. Analysis of hemolysis, aggregation of platelets, and adsorption of plasma proteins are all part of this. Because the PEG chains produce a steric barrier that limits direct contact with blood components, PEGylated LPs usually show reduced hemolytic activity and protein adsorption [222–224]. A game-changer in targeted colon cancer treatment, polymer-functionalized LPs show great potential to improve therapeutic results while reducing side effects. The incorporation of stimuli-responsive polymers is a crucial advancement since it allows for controlled medication release in reaction to specific physiological signals like pH, temperature, or enzyme activity. By concentrating the therapeutic chemicals at the tumor site, this tailored release approach maximizes their effectiveness and minimizes off-target repercussions. The potential of polymer-functionalized LPs to surpass the limitations of traditional treatment has been shown by encouraging results from clinical studies. One example is the EPR effect, which has been shown in the use of PEGylated LPs to promote accumulation in tumor tissues and lengthen circulation lengths. Active targeting, made possible by functionalizing LPs with ligands and antibodies, has also significantly improved the accuracy of drug delivery to cancer cells. Complex LP formulation, potential immunogenicity, and large-scale production are essential issues that need fixing. Comprehensive safety and effectiveness evidence is also required for regulatory approval procedures, which calls for thorough clinical and preclinical studies. Research into novel polymers and targeting moieties that improve the specificity and efficiency of liposomal delivery systems is an exciting area for the future of this field [222].

Making a biodegradable, thermoresponsive hydrogel filled with injectable liposomal DOX is one way to increase the effectiveness of DOX in treating BC. Researchers prepared the delivery platform by dissolving the poly (D, l-lactide-co-glycolide)-b-poly (ethylene glycol)-b-poly (D, l-lactide-co-glycolide) (PLGA-PEG-PLGA) triblock copolymer, which was produced by ring-opening polymerization a priori. Because of its biodegradability, compatibility with living organisms, and ability to release tiny hydrophobic or macromolecular medicines gradually, thermogels based on PLGA-PEG-PLGA have attracted much attention from the medical community. When researchers compared to DOX-loaded hydrogel, the Li-Gel hybrid system demonstrated a steady and extended release of DOX for up to eleven days after peritumoral injection, with less initial release. This highlights the importance of LPs in enhancing the release profile. In an orthotopic BC model, the Li-Gel hybrid system outperformed intravenous free DOX, liposomal DOX, and even peritumoral injection of DOX-loaded hydrogel in terms of antitumor efficiency while causing less side effects. This outcome was consistent with expectations about the system's biocompatibility [225, 226]. A number of anti-cancer medications are rapidly metabolized in vivo, have low availability, and are poorly soluble. A release platform with many levels and functions was developed to fix the medicines at the point of administration and postpone their release. Curcumin (Cur) loaded LPs (Cur@Lip) were found to have improved water solubility, EE, stability, cell intake, and bioactivity after being coated sequentially with positive Chitooligosaccharides (Cur@Lip-Cos) and negative phospholipids (Cur@Lip-Cos-PC). Compared to Cur@Lip-Cos-PC, Cur@Lip-Cos was able to amp up MCF-7's inhibitory impact much more. Next, the LPs were embedded in an injectable chitosan hydrogel that had been thiolated. This allowed for local immobilization and prolonged release of Cur, which successfully delayed its release and inhibited MCF-7 development. The novel and biomimetic liposomal hydrogels should inspire further drug carrier design concepts. Researchers showed that a specific sustained release effect may be achieved by slowing the release rate from the Li-Gel hybrid system (61.40% in 72 h) when the LP concentration is increased to 200 μM. Curcumin was able to significantly inhibit the progression of BC in vitro thanks to the created delivery platform [227]. Numerous in vitro and in vivo studies have shown that hydrogel systems, including LPs, have excellent chemical tunability, biodegradability, and biocompatibility. The use of these hybrid platforms to facilitate correct tissue regeneration or targeted and regulated delivery of medicinal medicines is very promising. With its many achievements and ability to overcome the shortcomings of particular platforms, the hybrid system shows great promise for the future. Their application to people, however, is currently not possible because to a lack of clinical trials. To demonstrate that LP-integrated hydrogel systems are game-changing alternatives for cancer treatment and tissue regeneration, they will need to undergo more preclinical studies to optimize and evaluate their biophysical and biochemical characteristics before extensive clinical testing [228].

A potential nanosized targeted DDS is MFHEs, which are produced via membrane fusion technology and combine the benefits of EXOs and LPs. Important challenges in delivering high-quality MFHEs include enhancing LP-EXO membrane fusion and avoiding LP-to-LP fusion. In order to increase the effectiveness of LP and EXO fusion, self-assembled single-stranded DNA nanostructures have been used to create a protective barrier

surrounding LPs. This layer prevents unwanted fusing between the LPs. To maximize their therapeutic impact, MFHEs must be developed with the ability to target recipient cells selectively. While much of the current research focuses on using EXOs' inherent targeting capabilities, surface modification of lipid membranes may potentially improve MFHE's active targeting capacity. Improving cell targeting specificity and achieving effective cell-specific uptake may be accomplished by engineering MFHEs to conjugate suitable targeting probes, such as Apts, peptides, monoclonal antibodies, and small molecules. Systemic and local administration of MFHEs are both possible at this time. Intravenous MFHEs outperform LPs in drug administration because they are more resistant to clearance by the reticuloendothelial and mononuclear phagocytic systems. Researchers showed that hydrogels might be used to regulate the release and prolong the life of locally given MFHEs. More studies are needed to fill the gaps in our understanding of MFHEs in hydrogels, whether they are natural or manufactured. To summarize, MFHEs have only entered the diagnostic and therapy arena, but preliminary findings show that they are superior to EXOs and LPs. Researchers have faith that the rapid advancement of methods for fusing and modifying membranes will lead to the creation of MFHE DDSs that are both novel and efficient. In the realm of illness therapy, MFHEs may provide crucial platforms and chances for advancements [24].

Researchers have suggested the potential enhancement of antitumor drug efficacy and apoptosis in cancer treatment through the combination of magnetic NPs and LPs. In vivo, Gogoi et al. assessed the self-controlled HT efficacy, combined chemotherapy, and biocompatibility of drug-loaded MLs comprising PTX and a biphasic suspension of $Fe_3O_4$ NPs. Despite extensive in vivo and in vitro investigation into MLs, the commencement of clinical trials has yet to occur. The magnesium ferrite ($MgFe_2O_4$) MNPs utilized by researchers were initially synthesized via chemical co-precipitation and subsequently subjected to surface modification using nanoliposome $MgFe_2O_4$@LP NPs MLs and Que-loaded MLs to generate Que-MLs. The magnetic properties and structures of uncoated and LP-coated NPs were analyzed and utilized in applications involving HT, chemotherapy/HT, and SDD. AMF analysis was performed on the self-heating temperature rise characteristics and specific absorption rate of these NPs to determine their viability as thermal agents in HT. The evaluation of the EE and drug dosage of Que revealed that the Que drug was effectively encapsulated within MLs. An investigation was conducted into the cytotoxic effects of free Que, MLs, and Que-MLs on MFC-7 cancer cells. The synthesized $MgFe_2O_4$, MLs, and Que-MLs were spherical with average sizes of 23.7, 35.5, and 329.5 nm, according to TEM analysis. The $MgFe_2O_4$ demonstrated an exceptional and efficient saturation magnetization (MS) of 40.5 emu/g, as determined by the VSM. The loading and entrapment efficiencies for quercetin were determined to be $42.3 \pm 2.2\%$ and $2.1 \pm 0.1\%$, respectively. Que-loaded MLs exhibited an in vitro Que release of 40.2% at pH 5.1 and 69.87% at pH 7.4, confirming the pH sensitivity of Que-loading. As MHT agents, the hybrid systems composed of MLs and Que-MLs demonstrate specific absorption rates (SAR) of 205 and 197 W/g, respectively. Additionally, the cytotoxicity of Que-MLs was investigated using the MCF-7 BC cell line. The results obtained from this study indicate that Que-MLs exhibit a significantly higher cytotoxicity effect in comparison to MLs and unbound Que [229]. The unique nanohybrid system creates a new route as an emerging drug delivery method; nonetheless, the primary constraints for this particular nanohybrid complex are the absence of comprehensive in vivo performance, cellular toxicity, and metabolism, in addition to budgetary and quality issues. Additional research will support this system's development and make it easier for it to be used in clinical settings [214].

## Future and landscape

Because of their versatility and multifunctionality, HLs seem to have a bright future in cancer therapy and detection. The biocompatibility of lipid bilayers and the adaptability of other substances, such as polymers, NPs, or targeting ligands, are combined in HLs. Their potential for focused treatment, diagnostics, and theranostics (combination of therapy and diagnostics) is increased by this synergy. Multiple imaging agents may be integrated into HLs to allow for the simultaneous use of various imaging modalities. Imaging modalities such as MRI, PET, or optical imaging may have their sensitivity and resolution increased by incorporating radioactive isotopes, fluorescent dyes, or MRI contrast agents into HLs. Early diagnosis is made possible by the ability of functionalized HLs to identify cancer-specific biomarkers in blood or tissues [230, 231].

Furthermore, EXOs initially functioned as a means of intercellular communication across great distances. Drug delivery using EXOs has recently exploded in popularity due to its excellent biocompatibility and active targeting capabilities. Medication efficacy may be enhanced substantially by using EXOs as a carrier. EXOs have the potential to revolutionize the medicinal business, but their complicated purification procedure and poor drug-loading efficiency make them unsuitable for usage at this time. LPs are a kind of drug delivery carrier that has been extensively studied. They are easy

to synthesize and carry drugs efficiently. In addition to retaining adequate drug loading efficiency, cell transport efficiency, and safety, researchers discovered that EXO-LP fusion NPs (EL-FNP) retained the active targeting capability of EXOs. The fusion method improves vesicle controllability and drastically decreases the need for EXOs in drug manufacturing. The EL-FNP has already been found to be useful in gene editing and cancer therapy. It is easy to imagine that EL-FNP will evolve into fully formed delivery systems as methods for separating and modifying EXOs continue to improve and as novel ways to boost EXO formation and LPs emerge. When that happens, EL-FNP will be ready to make a splash in the area of disease-targeted drug delivery, paving the way for a smooth transition from research to clinical practice [232].

There is an immediate need to develop a wide range of hybrid inorganic/organic NPs that can be combined with EXOs for diagnostic and therapeutic purposes. This might pave the way for the creation of hybrid nanoparticles for use in individualized medical treatment. This synergy offers the potential to generate theranostics on a unified platform, with advantages including increased dispersion, tailored delivery, and immune system clearance evasion. Gene delivery vehicles may be created from hybrid nanosystems by adjusting their size and surface charge. The integration of heat agents or photosensitizers into multifunctional therapeutic EXO-NP hybrid platforms might lead to a significant improvement in therapeutic efficacy. These hybrid nanoplatforms may be engineered to have targeting ability in addition to theranostic capabilities. It is anticipated that hybrid nanosystems that are compatible with living organisms and can contain larger macromolecules will be developed. Improving and optimizing the function of these hybrid nanoplatforms in vivo requires more research. To avoid inorganic or organic chemical buildup, it is essential to determine if hybrid systems are biodegradable. More efficient ways of producing these hybrid nanoplatforms may emerge as a result of recent scientific advances [233].

Since HLs overcome the drawbacks of traditional treatments, they hold great promise for the future of clinical practice. Thanks to developments in nanotechnology and bioengineering, as well as their capacity to combine diagnostic and therapeutic functions, they are positioned to be significant instruments in precision medicine. Because of their pinpoint accuracy, versatility, and lack of side effects, HLs have the potential to alter the cancer detection and treatment landscape completely. As research into nanotechnology, materials science, and bioengineering continues to progress, HLs are expected to be an essential component in the creation of tailored and coordinated cancer treatment. Several different kinds of cancer have been the subject of HLs in vitro and in vivo investigations. These studies have looked at the cytotoxicity, effectiveness, and toxicity of different hybrid LP formulations. By doing systematic investigations and meta-analyses, researchers may contribute to the future advancement of clinical trials. Extensive research has to be done into the mass manufacture of HLs. HLs have the potential to revolutionize cancer therapy, diagnostics, and theranostics; nevertheless, there is a need for more efficient, less expensive, and user-friendly ways of generating these NPs. Consequently, it is critical to develop GMP-compliant, cost-effective manufacturing methods for scalable production of HLs, to guarantee quality and performance at scale, and to enhance storage and stability for future use in cancer theranostic clinical applications.

## Conclusion

Advanced theranostic nanomedicine is a multifunctional technique that combines effective disease therapy with tissue diagnostics. A liposomal formulation is the first nanomedicine to be approved by the US FDA for clinical use. Recently, the treatment of cancer has been impacted by both promoted and hidden LPs. Because of their unique ability to encapsulate therapeutic and imaging substances that are both hydrophobic (located in their lipophilic exterior) and hydrophilic (placed in their aqueous core), LPs have found use in cancer theranostics. Lipid-coated or -encapsulated NPs have structural properties similar to those of the cell membrane. It is worthwhile to think about how this LP-NPs hybrid system can help develop novel co-delivery platforms. Functionalized LPs are more therapeutically effective than normal LPs. The versatility of surface modification and payloads improves the stability, therapeutic effectiveness, and specificity of theranostics agents. However, there are still a few key areas that need to be worked on to use them in clinical practice successfully. Additionally, EXOs and EXO-HLs may be bioengineered as nanocarriers to provide enhanced targeted specificity, bio-camouflage, and theranostics agent delivery. In conclusion, future research is expected to enable the creation of therapeutic and diagnostic integrated NPs that combine the advantages of EXOs, therapeutic medications, detection agents, and diagnostic agents for application in noninvasive diagnostics and precision cancer treatments. NPs serve as optical probes to track the systems' distribution both in vitro and in vivo when they are enclosed in LPs. They are also capable of controlling the drug's binding and release from the hybrid delivery systems. As we already said, this integrated hybrid structure has a lot of benefits. It makes the system more stable, lets you deliver both covalent and non-covalent drugs to specific targets

at the same time, and gives you more precise control over when and where drugs are released to help with drug treatment plans. More research into theranostic HL engineering, like that of the hybrid metal NP LP, could lead to the creation of EXO-LP-based personalized medicines and the early detection of certain types of cancer.

**Acknowledgements**
Research becomes more valuable when it saves a patient's life.

**Author contributions**
H.A., A.G., M.H.A., R.A.K., A.J.Z., A.S.M., Z.H.A., S.K., Writing—original draft. H.A., A.G., M.H.A., Reviewd and editng. H.A., A.G., Investigation, Validation. M.H.A., R.A.K., design original figure draft. S.K., Corresponding author. All authors read and approved the final manuscript.

**Funding**
Not applicable.

**Availability of data and material**
No datasets were generated or analysed during the current study.

## Declarations

**Ethics approval and consent to participate**
Not applicable.

**Consent for publication**
All authors consent to the publication.

**Competing interests**
The authors declare no competing interests.

**Author details**
[1]Inventor Member of International Federation of Inventors Associations, Geneva, Switzerland. [2]College of Dentistry, Alnoor University, Mosul, Iraq. [3]Ahl Al Bayt University, Kerbala, Iraq. [4]Collage of Pharmacy, National University of Science and Technology, Dhi Qar 64001, Iraq. [5]Gilgamesh Ahliya University, Baghdad, Iraq. [6]Department of Pharmacy, Al-Zahrawi University College, Karbala, Iraq. [7]Department of Clinical Pharmacy, Faculty of Pharmacy, Islamic Azad University of Medical Sciences, Tehran, Iran.

Received: 19 August 2024 Accepted: 10 December 2024
Published online: 27 January 2025

**References**

1. Bobo D, et al. Nanoparticle-based medicines: a review of FDA-approved materials and clinical trials to date. Pharm Res. 2016;33:2373–87.
2. Morgan B. Opportunities and pitfalls of cancer imaging in clinical trials. Nat Rev Clin Oncol. 2011;8(9):517–27.
3. Kievit FM, Zhang M. Cancer nanotheranostics: improving imaging and therapy by targeted delivery across biological barriers. Adv Mater. 2011;23(36):H217–47.
4. Schadendorf D, et al. Melanoma. Nat Rev Dis Primers. 2015;1(1):1–20.
5. Gao Q, et al. Gold nanoparticles in cancer theranostics. Front Bioeng Biotechnol. 2021;9: 647905.
6. Dhas N, et al. Organic quantum dots: an ultrasmall nanoplatform for cancer theranostics. J Control Release. 2022;348:798–824.
7. Li X, et al. Magnetic nanoparticles for cancer theranostics: advances and prospects. J Control Release. 2021;335:437–48.
8. Fernandes DA, et al. Multifunctional nanoparticles as theranostic agents for therapy and imaging of breast cancer. J Photochem Photobiol, B. 2021;218: 112110.
9. Kumar A, et al. Nanoscience: an overview about nanotheranostics for cancer treatment. Egypt J Basic Appl Sci. 2024;11(1):55–68.
10. Khan I, Saeed K, Khan I. Nanoparticles: properties, applications and toxicities. Arab J Chem. 2019;12(7):908–31.
11. Viswanadh MK, et al. Nanotheranostics: emerging strategies for early diagnosis and therapy of brain cancer. Nanotheranostics. 2018;2(1):70.
12. Patra JK, et al. Nano based drug delivery systems: recent developments and future prospects. J Nanobiotechnol. 2018;16(1):1–33.
13. Prasad R, et al. Liposomal nanotheranostics for multimode targeted in vivo bioimaging and near-infrared light mediated cancer therapy. Commun Biol. 2020;3(1):284.
14. Park S-M, et al. Towards clinically translatable in vivo nanodiagnostics. Nat Rev Mater. 2017;2(5):1–20.
15. Prasad R, et al. Graphene oxide supported liposomes as red emissive theranostics for phototriggered tissue visualization and tumor regression. ACS Appl Bio Mater. 2019;2(8):3312–20.
16. Muthu MS, Feng S-S. Nanopharmacology of liposomes developed for cancer therapy. Nanomedicine. 2010;5(7):1017–9.
17. Muthu MS, et al. Vitamin E TPGS coated liposomes enhanced cellular uptake and cytotoxicity of docetaxel in brain cancer cells. Int J Pharm. 2011;421(2):332–40.
18. Alexis F, et al. Factors affecting the clearance and biodistribution of polymeric nanoparticles. Mol Pharm. 2008;5(4):505–15.
19. Zahiri M, et al. Theranostic nanobubbles towards smart nanomedicines. J Control Release. 2021;339:164–94.
20. Fernandes DA. Liposomes for cancer theranostics. Pharmaceutics. 2023;15(10):2448.
21. Ghosh B, Biswas S. Polymeric micelles in cancer therapy: State of the art. J Control Release. 2021;332:127–47.
22. Kommineni N, et al. Engineered liposomes in interventional theranostics of solid tumors. ACS Biomater Sci Eng. 2023;9(8):4527–57.
23. Lee W, Im HJ. Theranostics based on liposome: looking back and forward. Nuclear Med Mol Imaging. 2019;53(4):242–6.
24. Liu A, et al. Research progress in membrane fusion-based hybrid exosomes for drug delivery systems. Front Bioeng Biotechnol. 2022;10: 939441.
25. Gupta S, et al. Neoadjuvant chemotherapy followed by radical surgery versus concomitant chemotherapy and radiotherapy in patients with stage IB2, IIA, or IIB squamous cervical cancer: a randomized controlled trial. J Clin Oncol. 2018;36(16):1548–55.
26. Li H, et al. Cancer nanomedicine: mechanisms, obstacles and strategies. Nanomedicine. 2018;13(13):1639–56.
27. Nsairat H, et al. Liposomes: structure, composition, types, and clinical applications. Heliyon. 2022;8(5): e09394.
28. Lin R, Cui H. Supramolecular nanostructures as drug carriers. Curr Opin Chem Eng. 2015;7:75–83.
29. Al-Jamal WT, Kostarelos K. Liposomes: from a clinically established drug delivery system to a nanoparticle platform for theranostic nanomedicine. Acc Chem Res. 2011;44(10):1094–104.
30. Cao Z, et al. Stable cerasomes for simultaneous drug delivery and magnetic resonance imaging. Int J Nanomed. 2014; 5103–5116.
31. Hameed S, Bhattarai P, Dai Z. Cerasomes and bicelles: Hybrid bilayered nanostructures with silica-like surface in cancer theranostics. Front Chem. 2018;6:127.
32. Okumura M, Ichihara H, Matsumoto Y. Hybrid liposomes showing enhanced accumulation in tumors as theranostic agents in the orthotopic graft model mouse of colorectal cancer. Drug Deliv. 2018;25(1):1192–9.
33. Lu M, Huang Y. Bioinspired exosome-like therapeutics and delivery nanoplatforms. Biomaterials. 2020;242: 119925.
34. Setia A, et al. Advances in hybrid vesicular-based drug delivery systems: improved biocompatibility, targeting, therapeutic efficacy and pharmacokinetics of anticancer drugs. Curr Drug Metab. 2022;23(9):757–80.
35. Kim SY, et al. Engineered hybrid vesicles and cellular internalization in mammary cancer cells. Pharmaceutics. 2024;16(4):440.
36. Fan Y, et al. Cationic liposome–hyaluronic acid hybrid nanoparticles for intranasal vaccination with subunit antigens. J Control Release. 2015;208:121–9.
37. Bhavsar D, et al. 'Nano–in–nano'hybrid liposomes increase target specificity and gene silencing efficiency in breast cancer induced SCID mice. Eur J Pharm Biopharm. 2017;119:96–106.
38. Wagner A, Vorauer-Uhl K. Liposome technology for industrial purposes. J Drug Delivery. 2011; 2011.

39. Tadokoro S, Hirashima N, Utsunomiya-Tate N. Effect of Complexin II on membrane fusion between liposomes containing mast cell SNARE proteins. Biol Pharm Bull. 2016;39(3):446–9.
40. Ahmed KS, et al. Liposome: composition, characterisation, preparation, and recent innovation in clinical applications. J Drug Target. 2019;27(7):742–61.
41. Shehata T, et al. Prolongation of residence time of liposome by surface-modification with mixture of hydrophilic polymers. Int J Pharm. 2008;359(1–2):272–9.
42. Akbarzadeh A, et al. RETRACTED ARTICLE: Preparation and in vitro evaluation of doxorubicin-loaded Fe3O4 magnetic nanoparticles modified with biocompatible copolymers. Int J Nanomed. 2012; 511–526.
43. Akbarzadeh A, et al. Liposome: classification, preparation, and applications. Nanoscale Res Lett. 2013;8:1–9.
44. Ichim CV. Revisiting immunosurveillance and immunostimulation: implications for cancer immunotherapy. J Transl Med. 2005;3(1):1–13.
45. Allen TM, Cullis PR. Liposomal drug delivery systems: from concept to clinical applications. Adv Drug Deliv Rev. 2013;65(1):36–48.
46. Zhou X, Chen Z. Preparation and performance evaluation of emulsomes as a drug delivery system for silybin. Arch Pharmacal Res. 2015;38:2193–200.
47. Alavi M, Karimi N, Safaei M. Application of various types of liposomes in drug delivery systems. Adv Pharm Bull. 2017;7(1):3.
48. Hattori Y, Hu S, Onishi H. Effects of cationic lipids in cationic liposomes and disaccharides in the freeze-drying of siRNA lipoplexes on gene silencing in cells by reverse transfection. J Liposome Res. 2020;30(3):235–45.
49. Bulbake U, et al. Liposomal formulations in clinical use: an updated review. Pharmaceutics. 2017;9(2):12.
50. Mare R, et al. Post-insertion parameters of PEG-derivatives in phosphocholine-liposomes. Int J Pharm. 2018;552(1–2):414–21.
51. Maja L, Željko K, Mateja P. Sustainable technologies for liposome preparation. J Supercritical Fluids. 2020;165: 104984.
52. Hua S, Wu SY. The use of lipid-based nanocarriers for targeted pain therapies. Front Pharmacol. 2013;4:143.
53. Kelly C, Jefferies C, Cryan S-A. Targeted liposomal drug delivery to monocytes and macrophages. J Drug Delivery. 2011; 2011.
54. Tan X, et al. Layer-by-layer self-assembled liposomes prepared using sodium alginate and chitosan: Insights into vesicle characteristics and physicochemical stability. Food Hydrocolloids. 2024;149: 109606.
55. Wang S, et al. Liposomes for tumor targeted therapy: a review. Int J Mol Sci. 2023;24(3):2643.
56. Li Y, et al. Aromatized liposomes for sustained drug delivery. Nat Commun. 2023;14(1):6659.
57. Wang K, et al. Highly sensitive and specific colorimetric detection of cancer cells via dual-aptamer target binding strategy. Biosens Bioelectron. 2015;73:1–6.
58. Hu S-W, et al. A paper-based SERS test strip for quantitative detection of Mucin-1 in whole blood. Talanta. 2018;179:9–14.
59. Hasebroock KM, Serkova NJ. Toxicity of MRI and CT contrast agents. Expert Opin Drug Metab Toxicol. 2009;5(4):403–16.
60. Sharma M, et al. Cancer treatment and toxicity outlook of nanoparticles. Environ Res. 2023; 116870.
61. Havelikar U, et al. Comprehensive insights into mechanism of nanotoxicity, assessment methods and regulatory challenges of nanomedicines. Discover Nano. 2024;19(1):165.
62. Petersen AL, et al. Liposome imaging agents in personalized medicine. Adv Drug Deliv Rev. 2012;64(13):1417–35.
63. Mukherjee A, et al. Lipid–polymer hybrid nanoparticles as a next-generation drug delivery platform: state of the art, emerging technologies, and perspectives. Int J Nanomed. 2019; 1937–1952.
64. De Leo V, et al. Liposomes containing nanoparticles: preparation and applications. Colloids Surfaces B: Biointerfaces. 2022: 112737.
65. Guilbault GG. Practical fluorescence. CRC Press; 2020.
66. Ghosh A, et al. Fluorescence lifetime correlation spectroscopy: basics and applications. Methods. 2018;140:32–9.
67. Borisova EG, Angelova LP, Pavlova EP. Endogenous and exogenous fluorescence skin cancer diagnostics for clinical applications. IEEE J Sel Top Quantum Electron. 2013;20(2):211–22.
68. Weissleder R, Pittet MJ. Imaging in the era of molecular oncology. Nature. 2008;452(7187):580–9.
69. Wang D-E, et al. Aptamer-functionalized polydiacetylene liposomes act as a fluorescent sensor for sensitive detection of MUC1 and targeted imaging of cancer cells. Sens Actuators, B Chem. 2020;309: 127778.
70. Wang G, et al. Liposomal extravasation and accumulation in tumors as studied by fluorescence microscopy and imaging depend on the fluorescent label. ACS Nano. 2021;15(7):11880–90.
71. Yang C, et al. Recent progress on the liposomes loaded with quantum dots. Rev Nanosci Nanotechnol. 2012;1(4):257–70.
72. Al-Jamal WT, et al. Functionalized-quantum-dot–liposome hybrids as multimodal nanoparticles for cancer. Small. 2008;4(9):1406–15.
73. Awad NS, et al. Ultrasound-triggered liposomes encapsulating quantum dots as safe fluorescent markers for colorectal cancer. Pharmaceutics. 2021;13(12):2073.
74. Sun C, Lee JS, Zhang M. Magnetic nanoparticles in MR imaging and drug delivery. Adv Drug Deliv Rev. 2008;60(11):1252–65.
75. Soenen SJ, et al. Magnetoliposomes as magnetic resonance imaging contrast agents. Wiley Interdiscip Rev Nanomed Nanobiotechnol. 2011;3(2):197–211.
76. Taneja SS. Imaging in the diagnosis and management of prostate cancer. Rev Urol. 2004;6(3):101.
77. Kostevšek N, et al. Magneto-liposomes as MRI contrast agents: a systematic study of different liposomal formulations. Nanomaterials. 2020;10(5):889.
78. Zhang N, et al. DNA-functionalized liposomes in vivo fusion for NIR-II/MRI guided pretargeted ferroptosis therapy of metastatic breast cancer. ACS Appl Mater Interfaces. 2022;14(18):20603–15.
79. Rizzitelli S, et al. Sonosensitive theranostic liposomes for preclinical in vivo MRI-guided visualization of doxorubicin release stimulated by pulsed low intensity non-focused ultrasound. J Control Release. 2015;202:21–30.
80. Park S-W, et al. Preclinical application of CEST MRI to detect early and regional tumor response to local brain tumor treatment. Pharmaceutics. 2024;16(1):101.
81. Cheng H-D, et al. Automated breast cancer detection and classification using ultrasound images: a survey. Pattern Recogn. 2010;43(1):299–317.
82. Deckers R, Moonen CT. Ultrasound triggered, image guided, local drug delivery. J Control Release. 2010;148(1):25–33.
83. Prabhakar A, Banerjee R. Nanobubble liposome complexes for diagnostic imaging and ultrasound-triggered drug delivery in cancers: a theranostic approach. ACS Omega. 2019;4(13):15567–80.
84. Escoffre J-M, et al. Doxorubicin liposome-loaded microbubbles for contrast imaging and ultrasound-triggered drug delivery. IEEE Trans Ultrason Ferroelectr Freq Control. 2012;60(1):78–87.
85. Liu Y, et al. A biocompatible and near-infrared liposome for in vivo ultrasound-switchable fluorescence imaging. Adv Healthc Mater. 2020;9(4):1901457.
86. Prasad R, et al. Emissive lipid nanoparticles as biophotonic contrast agent for site-selective solid tumor imaging in pre-clinical models. ACS Appl Mater Interfaces. 2024;16(40):53393–404.
87. Rahmim A, Zaidi H. PET versus SPECT: strengths, limitations and challenges. Nucl Med Commun. 2008;29(3):193–207.
88. Man F, Gawne PJ, de Rosales RT. Nuclear imaging of liposomal drug delivery systems: a critical review of radiolabelling methods and applications in nanomedicine. Adv Drug Deliv Rev. 2019;143:134–60.
89. Xing H, Hwang K, Lu Y. Recent developments of liposomes as nanocarriers for theranostic applications. Theranostics. 2016;6(9):1336.
90. Chang Y, et al. Novel water-soluble and pH-responsive anticancer drug nanocarriers: doxorubicin–PAMAM dendrimer conjugates attached to superparamagnetic iron oxide nanoparticles (IONPs). J Colloid Interface Sci. 2011;363(1):403–9.
91. Dagar S, et al. VIP grafted sterically stabilized liposomes for targeted imaging of breast cancer: in vivo studies. J Control Release. 2003;91(1–2):123–33.
92. Gao J, et al. EGFR-specific PEGylated immunoliposomes for active siRNA delivery in hepatocellular carcinoma. Biomaterials. 2012;33(1):270–82.
93. Srivatsan A, Chen X. Recent advances in nanoparticle-based nuclear imaging of cancers. Adv Cancer Res. 2014;124:83–129.
94. Tzror-Azankot C, et al. Glucose-functionalized liposomes for reducing false positives in cancer diagnosis. ACS Nano. 2020;15(1):1301–9.
95. Low HY, Yang CT. Radiolabeled liposomes for nuclear imaging probes. Molecules. 2023;28(9):3798.

96. Almeida B, et al. Recent progress in bioconjugation strategies for liposome-mediated drug delivery. Molecules. 2020;25(23):5672.
97. Belfiore L, et al. Towards clinical translation of ligand-functionalized liposomes in targeted cancer therapy: challenges and opportunities. J Control Release. 2018;277:1–13.
98. Bunker A, Magarkar A, Viitala T. Rational design of liposomal drug delivery systems, a review: combined experimental and computational studies of lipid membranes, liposomes and their PEGylation. Biochimica et Biophysica Acta (BBA) Biomembranes. 2016;1858(10):2334–52.
99. Lin C, et al. HIF1α-siRNA and gemcitabine combination-based GE-11 peptide antibody-targeted nanomedicine for enhanced therapeutic efficacy in pancreatic cancers. J Drug Target. 2019;27(7):797–805.
100. Raza F, et al. Liposome-based diagnostic and therapeutic applications for pancreatic cancer. Acta Biomater. 2023;157:1–23.
101. Birngruber T, et al. Enhanced doxorubicin delivery to the brain administered through glutathione PEGylated liposomal doxorubicin (2B3-101) as compared with generic Caelyx,®/Doxil®—a cerebral open flow microperfusion pilot study. J Pharm Sci. 2014;103(7):1945–8.
102. Badiee A, et al. The role of liposome size on the type of immune response induced in BALB/c mice against leishmaniasis: rgp63 as a model antigen. Exp Parasitol. 2012;132(4):403–9.
103. Awada A, et al. A randomized controlled phase II trial of a novel composition of paclitaxel embedded into neutral and cationic lipids targeting tumor endothelial cells in advanced triple-negative breast cancer (TNBC). Ann Oncol. 2014;25(4):824–31.
104. Alshaer W, et al. Aptamer-guided siRNA-loaded nanomedicines for systemic gene silencing in CD-44 expressing murine triple-negative breast cancer model. J Control Release. 2018;271:98–106.
105. Kiaie SH, et al. Axial pharmaceutical properties of liposome in cancer therapy: recent advances and perspectives. Int J Pharm. 2020;581: 119269.
106. Park JW. Liposome-based drug delivery in breast cancer treatment. Breast Cancer Res. 2002;4:1–5.
107. Petersen GH, et al. Meta-analysis of clinical and preclinical studies comparing the anticancer efficacy of liposomal versus conventional non-liposomal doxorubicin. J Control Release. 2016;232:255–64.
108. Liu Y, et al. Antitumor drug effect of betulinic acid mediated by polyethylene glycol modified liposomes. Mater Sci Eng, C. 2016;64:124–32.
109. He K, Tang M. Safety of novel liposomal drugs for cancer treatment: advances and prospects. Chem Biol Interact. 2018;295:13–9.
110. Xie Y, et al. A novel estrogen-targeted PEGylated liposome co-delivery oxaliplatin and paclitaxel for the treatment of ovarian cancer. Biomed Pharmacother. 2023;160: 114304.
111. Sadeghi N, et al. Hyperthermia-triggered release of hypoxic cell radiosensitizers from temperature-sensitive liposomes improves radiotherapy efficacy in vitro. Nanotechnology. 2019;30(26): 264001.
112. You J, et al. Near-infrared light-sensitive liposomes for the enhanced photothermal tumor treatment by the combination with chemotherapy. Pharm Res. 2014;31:554–65.
113. Ma J, et al. Novel core-interlayer-shell DOX/ZnPc co-loaded MSNs@ pH-sensitive CaP@ PEGylated liposome for enhanced synergetic chemo-photodynamic therapy. Pharm Res. 2018;35:1–12.
114. Greenlee JD, et al. TRAIL-conjugated liposomes that bind natural killer cells to induce colorectal cancer cell apoptosis. J Biomed Mater Res, Part A. 2024;112(1):110–20.
115. Inglut CT, et al. Immunological and toxicological considerations for the design of liposomes. Nanomaterials (Basel). 2020;10(2):190.
116. Barenholz YC. Doxil®—the first FDA-approved nano-drug: lessons learned. J Control Release. 2012;160(2):117–34.
117. Malam Y, Loizidou M, Seifalian AM. Liposomes and nanoparticles: nanosized vehicles for drug delivery in cancer. Trends Pharmacol Sci. 2009;30(11):592–9.
118. Bertrand N, et al. Cancer nanotechnology: the impact of passive and active targeting in the era of modern cancer biology. Adv Drug Deliv Rev. 2014;66:2–25.
119. Michel R, et al. Control of the stability and structure of liposomes by means of nanoparticles. Soft Matter. 2013;9(16):4167–77.
120. Min Y, et al. Recent advance of biological molecular imaging based on lanthanide-doped upconversion-luminescent nanomaterials. Nanomaterials. 2014;4(1):129–54.
121. Muthu MS, et al. Theranostic liposomes of TPGS coating for targeted co-delivery of docetaxel and quantum dots. Biomaterials. 2012;33(12):3494–501.
122. Yang C, et al. Folate receptor–targeted quantum dot liposomes as fluorescence probes. J Drug Target. 2009;17(7):502–11.
123. Shen J, et al. A liposome encapsulated ruthenium polypyridine complex as a theranostic platform for triple-negative breast cancer. Nano Lett. 2017;17(5):2913–20.
124. Lin X, et al. Ultrasound activation of liposomes for enhanced ultrasound imaging and synergistic gas and sonodynamic cancer therapy. Nanoscale Horizons. 2019;4(3):747–56.
125. Kim MA, Lee C-M. NIR-Mediated drug release and tumor theranostics using melanin-loaded liposomes. Biomater Res. 2022;26(1):22.
126. Liu L, et al. In situ photocatalyzed oxygen generation with photosynthetic bacteria to enable robust immunogenic photodynamic therapy in triple-negative breast cancer. Adv Func Mater. 2020;30(10):1910176.
127. Esfahani FN, et al. Functionalized and theranostic lipidic and tocosomal drug delivery systems: potentials and limitations in cancer photodynamic therapy. Adv Pharm Bull. 2024;14(3):524.
128. Muthu MS, Feng SS. Theranostic liposomes for cancer diagnosis and treatment: current development and pre-clinical success. 2013, Taylor & Francis. p. 151–155.
129. Elkhoury K, et al. Engineering smart targeting nanovesicles and their combination with hydrogels for controlled drug delivery. Pharmaceutics. 2020;12(9):849.
130. Jia S, et al. Emerging technologies in extracellular vesicle-based molecular diagnostics. Expert Rev Mol Diagn. 2014;14(3):307–21.
131. van der Meel R, et al. Extracellular vesicles as drug delivery systems: lessons from the liposome field. J Control Release. 2014;195:72–85.
132. Lee J, et al. Liposome-based engineering of cells to package hydrophobic compounds in membrane vesicles for tumor penetration. Nano Lett. 2015;15(5):2938–44.
133. Sato YT, et al. Engineering hybrid exosomes by membrane fusion with liposomes. Sci Rep. 2016;6(1):21933.
134. Wang X, et al. Enhanced therapeutic potential of hybrid exosomes loaded with paclitaxel for cancer therapy. Int J Mol Sci. 2024;25(7):3645.
135. Costa AP, Xu X, Burgess DJ. Freeze-anneal-thaw cycling of unilamellar liposomes: effect on encapsulation efficiency. Pharm Res. 2014;31:97–103.
136. Cheng L, et al. Gene-engineered exosomes-thermosensitive liposomes hybrid nanovesicles by the blockade of CD47 signal for combined photothermal therapy and cancer immunotherapy. Biomaterials. 2021;275: 120964.
137. Lin Y, et al. Exosome–liposome hybrid nanoparticles deliver CRISPR/Cas9 system in MSCs. Adv Sci. 2018;5(4):1700611.
138. Lentz BR. PEG as a tool to gain insight into membrane fusion. Eur Biophys J. 2007;36(4–5):315–26.
139. Pippa N, et al. Aqueous heat method for the preparation of hybrid lipid-polymer structures: from preformulation studies to protein delivery. Biomedicines. 2022;10(6):1228.
140. Sun L, et al. Clodronate-loaded liposomal and fibroblast-derived exosomal hybrid system for enhanced drug delivery to pulmonary fibrosis. Biomaterials. 2021;271: 120761.
141. Li L, et al. Exosome-liposome hybrid nanoparticle codelivery of TP and miR497 conspicuously overcomes chemoresistant ovarian cancer. J Nanobiotechnol. 2022;20(1):50.
142. Hu Y, et al. Exosome-guided bone targeted delivery of Antagomir-188 as an anabolic therapy for bone loss. Bioactive Mater. 2021;6(9):2905–13.
143. Moholkar DN, et al. Advances in lipid-based carriers for cancer therapeutics: liposomes, exosomes and hybrid exosomes. Cancer Lett. 2023;565: 216220.
144. Ducrot C, et al. Hybrid extracellular vesicles for drug delivery. Cancer Lett. 2023;558: 216107.
145. Koudelka Š, Turánek J. Liposomal paclitaxel formulations. J Control Release. 2012;163(3):322–34.

146. Elkhoury K, et al. Hybrid extracellular vesicles-liposome incorporated advanced bioink to deliver microRNA. Biofabrication. 2022;14(4): 045008.
147. Evers MJ, et al. Functional siRNA delivery by extracellular vesicle–liposome hybrid nanoparticles. Adv Healthc Mater. 2022;11(5):2101202.
148. Rayamajhi S, et al. Macrophage-derived exosome-mimetic hybrid vesicles for tumor targeted drug delivery. Acta Biomater. 2019;94:482–94.
149. Piffoux M, et al. Modification of extracellular vesicles by fusion with liposomes for the design of personalized biogenic drug delivery systems. ACS Nano. 2018;12(7):6830–42.
150. Xiao P, et al. Milk exosome-liposome hybrid vesicles with self-adapting surface properties overcome the sequential absorption barriers for oral delivery of peptides. ACS Nano. 2024;18(32):21091–111.
151. Jang Y, et al. CXCR4-targeted macrophage-derived biomimetic hybrid vesicle nanoplatform for enhanced cancer therapy through codelivery of manganese and doxorubicin. ACS Appl Mater Interfaces. 2024;16(14):17129–44.
152. Lozano N, et al. Monoclonal antibody-targeted PEGylated liposome-ICG encapsulating doxorubicin as a potential theranostic agent. Int J Pharm. 2015;482(1–2):2–10.
153. Tian B, Al-Jamal KT, Kostarelos K. Doxorubicin-loaded lipid-quantum dot hybrids: surface topography and release properties. Int J Pharm. 2011;416(2):443–7.
154. Al-Ahmady Z, et al. Engineering thermosensitive liposome-nanoparticle hybrids loaded with doxorubicin for heat-triggered drug release. Int J Pharm. 2016;514(1):133–41.
155. Aadinath W, Bhushani A, Anandharamakrishnan C. Synergistic radical scavenging potency of curcumin-in-β-cyclodextrin-in-nanomagnetoliposomes. Mater Sci Eng, C. 2016;64:293–302.
156. Alehosseini A, et al. Electrospun curcumin-loaded protein nanofiber mats as active/bioactive coatings for food packaging applications. Food Hydrocolloids. 2019;87:758–71.
157. Altin G, Gültekin-Özgüven M, Ozcelik B. Chitosan coated liposome dispersions loaded with cacao hull waste extract: effect of spray drying on physico-chemical stability and in vitro bioaccessibility. J Food Eng. 2018;223:91–8.
158. Al-Jamal WT, Kostarelos K. Liposome–nanoparticle hybrids for multimodal diagnostic and therapeutic applications. Nanomedicine. 2007;2:85–98.
159. Catalan-Latorre A, et al. Freeze-dried eudragit-hyaluronan multicompartment liposomes to improve the intestinal bioavailability of curcumin. Eur J Pharm Biopharm. 2016;107:49–55.
160. Chun J-Y, Min S-G, Jo Y-J. Production of low molecular collagen peptides-loaded liposomes using different charged lipids. Chem Phys Lipid. 2017;209:1–8.
161. Tan C, Wang J, Sun B. Biopolymer-liposome hybrid systems for controlled delivery of bioactive compounds: recent advances. Biotechnol Adv. 2021;48: 107727.
162. Lee J-H, et al. General and programmable synthesis of hybrid liposome/metal nanoparticles. Sci Adv. 2016;2(12): e1601838.
163. Koga K, Tagami T, Ozeki T. Gold nanoparticle-coated thermosensitive liposomes for the triggered release of doxorubicin, and photothermal therapy using a near-infrared laser. Colloids Surf, A. 2021;626: 127038.
164. Hong JS, et al. Microfluidic directed self-assembly of liposome– hydrogel hybrid nanoparticles. Langmuir. 2010;26(13):11581–8.
165. Matsumoto Y, et al. Novel mechanism of hybrid liposomes-induced apoptosis in human tumor cells. Int J Cancer. 2005;115(3):377–82.
166. Luiz MT, Dutra JAP, Viegas JSR. Hybrid magnetic lipid-based nanoparticles for cancer therapy. Pharmaceutics. 2023;15(3):751.
167. Choi WI, et al. Magnetoliposomes with size controllable insertion of magnetic nanoparticles for efficient targeting of cancer cells. RSC Adv. 2019;9(26):15053–60.
168. Jonker DJ, et al. Napabucasin versus placebo in refractory advanced colorectal cancer: a randomised phase 3 trial. Lancet Gastroenterol Hepatol. 2018;3(4):263–70.
169. Cho H-J, et al. Polyethylene glycol-conjugated hyaluronic acid-ceramide self-assembled nanoparticles for targeted delivery of doxorubicin. Biomaterials. 2012;33(4):1190–200.
170. Park J-H, et al. Hyaluronic acid derivative-coated nanohybrid liposomes for cancer imaging and drug delivery. J Control Release. 2014;174:98–108.
171. Ichihara H, Matsumoto Y, Ueoka R. Chemotherapy and detection of cancer using hybrid liposomes. in 2014 World Automation Congress (WAC). 2014. IEEE.
172. Okumura M, Ichihara H, Matsumoto Y. Hybrid liposomes showing enhanced accumulation in tumors as theranostic agents in the orthotopic graft model mouse of colorectal cancer. Drug Delivery. 2018;25(1):1192–9.
173. Himbert S, et al. Hybrid erythrocyte liposomes: functionalized red blood cell membranes for molecule encapsulation. Adv Biosyst. 2020;4(3):1900185.
174. Wang H, et al. Cell membrane-liposome hybrid platform for ultrasound-activated immune-sonodynamic therapy for triple-negative breast cancer. ACS Appl Nano Mater. 2023;6(18):16453–64.
175. Lee J, et al. Cancer cell membrane-decorated hybrid liposomes for treating metastatic breast cancer based on enhanced cancer immunotherapy. J Pharm Investig. 2024; 1–13.
176. Zhou X, et al. Liposome–exosome hybrids for in situ detection of exosomal miR-1246 in breast cancer. Analyst. 2024;149:403–9.
177. Cardellini J, et al. Hybrid lipid-AuNP clusters as highly efficient SERS substrates for biomedical applications. Nat Commun. 2024;15(1):7975.
178. Inamura K, et al. Inhibitory effect of hybrid liposomes on the growth of liver cancer stem cells. Biochem Biophys Res Commun. 2019;509(1):268–74.
179. Hu M, et al. Immunogenic hybrid nanovesicles of liposomes and tumor-derived nanovesicles for cancer immunochemotherapy. ACS Nano. 2021;15(2):3123–38.
180. Zhu T, et al. Sequential targeting hybrid nanovesicles composed of chimeric antigen receptor T-cell-derived exosomes and liposomes for enhanced cancer immunochemotherapy. ACS Nano. 2023;17(17):16770–86.
181. Duan H, et al. Sequential delivery of quercetin and paclitaxel for the fibrotic tumor microenvironment remodeling and chemotherapy potentiation via a dual-targeting hybrid micelle-in-liposome system. ACS Appl Mater Interfaces. 2022;14(8):10102–16.
182. Pinho JO, et al. Preclinical validation of a new hybrid molecule loaded in liposomes for melanoma management. Biomed Pharmacother. 2023;157: 114021.
183. Zhu K, et al. Hybrid liposome-erythrocyte drug delivery system for tumor therapy with enhanced targeting and blood circulation. Regenerative Biomater. 2023; rbad045.
184. Zhang W, et al. Engineered cancer-derived small extracellular vesicle-liposome hybrid delivery system for targeted treatment of breast cancer. ACS Appl Mater Interfaces. 2023;15(13):16420–33.
185. Cruz N, et al. A novel hybrid nanosystem integrating cytotoxic and magnetic properties as a tool to potentiate melanoma therapy. Nanomaterials. 2020;10(4):693.
186. Patel U, et al. Dual targeted delivery of liposomal hybrid gold nanoassembly for enhanced photothermal therapy against lung carcinomas. ACS Appl Bio Mater. 2023;6(5):1915–33.
187. Huang Y, et al. Disrupting redox homeostasis for tumor therapy based on PDT/chemo/ferroptosis therapeutic hybrid liposomes. RSC Adv. 2024;14(28):20152–62.
188. Gomes ER, et al. Investigation of the antitumor activity and toxicity of tumor-derived exosomes fused with long-circulating and pH-sensitive liposomes containing doxorubicin. Pharmaceutics. 2022;14(11):2256.
189. Zhang C, et al. Multifunctional hybrid liposome as a theranostic platform for magnetic resonance imaging guided photothermal therapy. ACS Biomater Sci Eng. 2018;4(7):2597–605.
190. Seleci M, et al. Theranostic liposome–nanoparticle hybrids for drug delivery and bioimaging. Int J Mol Sci. 2017;18(7):1415.
191. Ichihara H, et al. Theranostics with hybrid liposomes in an orthotopic graft model mice of breast cancer. Anticancer Res. 2018;38(10):5645–54.
192. Li Y, et al. EGFR-targeted liposomal nanohybrid cerasomes: theranostic function and immune checkpoint inhibition in a mouse model of colorectal cancer. Nanoscale. 2018;10(35):16738–49.
193. Chauhan DS, et al. Disintegrable NIR light triggered gold nanorods supported liposomal nanohybrids for cancer theranostics. Bioconjug Chem. 2017;29(5):1510–8.
194. Sun Q, et al. Theranostic nanoplatform: triple-modal imaging-guided synergistic cancer therapy based on liposome-conjugated mesoporous silica nanoparticles. ACS Appl Mater Interfaces. 2018;10(2):1963–75.

195. Simón M, et al. Neoadjuvant gold nanoshell-based photothermal therapy combined with liposomal doxorubicin in a mouse model of colorectal cancer. Int J Nanomed. 2023; 829–841.
196. Guo Y, et al. Light/magnetic hyperthermia triggered drug released from multi-functional thermo-sensitive magnetoliposomes for precise cancer synergetic theranostics. J Control Release. 2018;272:145–58.
197. Zheng X-C, et al. The theranostic efficiency of tumor-specific, pH-responsive, peptide-modified, liposome-containing paclitaxel and superparamagnetic iron oxide nanoparticles. Int J Nanomed. 2018: 1495–1504.
198. Jeon M, et al. Development of theranostic dual-layered Au-liposome for effective tumor targeting and photothermal therapy. J Nanobiotechnol. 2021;19:1–16.
199. Liu Y, et al. Engineering of exosome-liposome hybrid-based theranostic nanomedicines for NIR-II fluorescence imaging-guided and targeted NIR-II photothermal therapy of subcutaneous glioblastoma. Colloids Surf, B. 2025;245: 114258.
200. Li J, et al. AS1411 aptamer-modified theranostic liposomes co-encapsulating manganese oxide nano-contrast agent and paclitaxel for MRI and therapy of cancer. RSC Adv. 2019;9(60):34837–46.
201. Jang M, et al. Trastuzumab-conjugated liposome-coated fluorescent magnetic nanoparticles to target breast cancer. Korean J Radiol. 2014;15(4):411–22.
202. Merino S, et al. Mechanisms of Klebsiella pneumoniae resistance to complement-mediated killing. Infect Immun. 1992;60(6):2529–35.
203. Etheridge ML, et al. The big picture on nanomedicine: the state of investigational and approved nanomedicine products. Nanomed Nanotechnol Biol Med. 2013;9(1):1–14.
204. Alibolandi M, et al. Extensive preclinical investigation of polymersomal formulation of doxorubicin versus Doxil-mimic formulation. J Control Release. 2017;264:228–36.
205. Guo J, et al. Gold nanoparticles enlighten the future of cancer theranostics. Int J Nanomed. 2017: p. 131–6152.
206. Barbosa-Barros L, et al. Bicelles: lipid nanostructured platforms with potential dermal applications. Small. 2012;8(6):807–18.
207. Bhattarai P, Hameed S, Dai Z. Recent advances in anti-angiogenic nanomedicines for cancer therapy. Nanoscale. 2018;10(12):5393–423.
208. Papahadjopoulos D, Poste G, Schaeffer B. Fusion of mammalian cells by unilamellar lipid vesicles: influence of lipid surface charge, fluidity and cholesterol. Biochimica et Biophysica Acta (BBA) Biomembranes. 1973;323(1):23–42.
209. Siegel RL, Miller KD, Jemal A. Cancer statistics, 2018. CA Cancer J Clin. 2018;68(1):7–30.
210. Mathiyazhakan M, Wiraja C, Xu C. A concise review of gold nanoparticles-based photo-responsive liposomes for controlled drug delivery. Nano-micro letters. 2018;10:1–10.
211. Madamsetty VS, Mukherjee A, Mukherjee S. Recent trends of the bio-inspired nanoparticles in cancer theranostics. Front Pharmacol. 2019;10:1264.
212. Mohammadi M, et al. Hybrid vesicular drug delivery systems for cancer therapeutics. Adv Func Mater. 2018;28(36):1802136.
213. Thakor AS, Gambhir SS. Nanooncology: the future of cancer diagnosis and therapy. CA Cancer J Clin. 2013;63(6):395–418.
214. Alwattar JK, et al. Smart stimuli-responsive liposomal nanohybrid systems: a critical review of theranostic behavior in cancer. Pharmaceutics. 2021;13(3):355.
215. Shetty A, Chandra S. Inorganic hybrid nanoparticles in cancer theranostics: understanding their combinations for better clinical translation. Mater Today Chem. 2020;18: 100381.
216. Tsakiri M, et al. Lipidic nanoparticles, extracellular vesicles and hybrid platforms as advanced medicinal products: future therapeutic prospects for neurodegenerative diseases. Pharmaceutics. 2024;16(3):350.
217. Prakash SS, et al. Bioequivalence of a hybrid pegylated liposomal doxorubicin hydrochloride injection and Caelyx®: a single-dose, randomized, multicenter, open-label, two-period crossover study in patients with advanced ovarian cancer. Eur J Pharm Sci. 2022;176:106248.
218. Ait-Oudhia S, Mager DE, Straubinger RM. Application of pharmacokinetic and pharmacodynamic analysis to the development of liposomal formulations for oncology. Pharmaceutics. 2014;6(1):137–74.
219. Tian T, et al. Exosome uptake through clathrin-mediated endocytosis and macropinocytosis and mediating miR-21 delivery. J Biol Chem. 2014;289(32):22258–67.
220. Mukherjee A, et al. Current advances in the use of exosomes, liposomes, and bioengineered hybrid nanovesicles in cancer detection and therapy. Acta Pharmacol Sin. 2022;43(11):2759–76.
221. Rosso G, Cauda V. Biomimicking extracellular vesicles with fully artificial ones: a rational design of EV-BIOMIMETICS toward effective theranostic tools in nanomedicine. ACS Biomater Sci Eng. 2022;9:5924–32.
222. Sharma S, et al. Strategic developments in polymer-functionalized liposomes for targeted colon cancer therapy: an updated review of clinical trial data and future horizons. Biomacromol. 2024;25(9):5650–69.
223. Maghsoudnia N, et al. Application of nano-based systems for drug delivery and targeting: a review. J Nanopart Res. 2020;22:1–41.
224. Zhang Z, et al. Anti-PEG scFv corona ameliorates accelerated blood clearance phenomenon of PEGylated nanomedicines. J Control Release. 2021;330:493–501.
225. Wang P, et al. Modified PLGA–PEG–PLGA thermosensitive hydrogels with suitable thermosensitivity and properties for use in a drug delivery system. J Mater Chem B. 2017;5(8):1551–65.
226. Cao D, et al. Liposomal doxorubicin loaded PLGA-PEG-PLGA based thermogel for sustained local drug delivery for the treatment of breast cancer. Artif Cells Nanomed Biotechnol. 2019;47(1):181–91.
227. Li R, et al. Fabrication of a multi-level drug release platform with liposomes, chitooligosaccharides, phospholipids and injectable chitosan hydrogel to enhance anti-tumor effectiveness. Carbohyd Polym. 2021;269: 118322.
228. Sanati M, Yavari SA. Liposome-integrated hydrogel hybrids: promising platforms for cancer therapy and tissue regeneration. J Control Release. 2024;368:703–27.
229. Elbeltagi S, et al. Biosynthesis, characterization, magnetic hyperthermia, and in vitro toxicity evaluation of quercetin-loaded magnetoliposome lipid bilayer hybrid system on MCF-7 breast cancer. Biochimica et Biophysica Acta (BBA) General Subjects. 2024;1868(3):130543.
230. Zahednezhad F, et al. Liposomal drug delivery systems for organ-specific cancer targeting: early promises, subsequent problems, and recent breakthroughs. Expert Opin Drug Deliv. 2024;21(9):1363–84.
231. Adeyemi SA, et al. Peptide-based targeting of nanoplatforms for cancer theranostics. In: Site-specific cancer nanotheranostics. CRC Press; 2024. p. 245–74.
232. Zheng L, et al. Recent progresses of exosome–liposome fusions in drug delivery. Chin Chem Lett. 2024;35(2): 108647.
233. Soltanmohammadi F, et al. Current knowledge of hybrid nanoplatforms composed of exosomes and organic/inorganic nanoparticles for disease treatment and cell/tissue imaging. Biomed Pharmacother. 2024;178: 117248.


## Publisher's Note